Final Report

MASH TL3 EVALUATION OF MASSDOT'S REVISED CM-MTL3 BRIDGE RAIL DESIGN USING FINITE ELEMENT ANALYSIS

Prepared for: **Gill Engineering and the Massachusetts Department of Transportation**

PARS No: **X22LRFDBM1 Q11**

Contract No: **115763**

Assignment No: **4NTP**

Report No: **TR22-1228-GEA**

Prepared by: **Chuck A. Plaxico, Ph.D.,** and
Archie M. Ray
ROADSAFE LLC
P.O. BOX 312
CANTON, ME 04221

March 6, 2023

Technical Report Documentation Page

1. Report No.	2. Government Accession No.	3. Recipient's Catalog No.

4. Title and Subtitle	5. Report Date
MASH TL3 EVALUATION OF MASSDOT'S REVISED CM-MTL3 BRIDGE RAIL DESIGN USING FINITE ELEMENT ANALYSIS	**March 6, 2023**
	6. Performing Organization Code

7. Authors	8. Performing Organization Report No.
Chuck A. Plaxico and Archie M. Ray	**TR 23-0207-GEA**

9. Performing Organization Name and Address	10. Work Unit No. (TRAIS)
RoadSafe LLC **12 Main St.** **Canton, ME 04221**	11. Contract or Grant No. **115763**

12. Sponsoring Agency Name and Address	13. Type of Report and Period Covered
Gill Engineering Associates **63 Kendrick Street** **Needham, MA 02494**	**Technical Report:** **November - February 2022**
	14. Sponsoring Agency Code

15. Supplementary Notes

Prepared in cooperation with the Massachusetts Department of Transportation - Bridge Section, 10 Park Plaza, Boston, MA 02116

16. Abstract

The crash performance of the revised MassDOT CM-MTL3 combination concrete barrier with steel top rail was evaluated for the Massachusetts Department of Transportation (MassDOT). The evaluation was performed using finite element analysis (FEA) using impact conditions and evaluation procedures set forth in the AASHTO Manual for Assessing Safety Hardware (MASH) for Test Level 3 (TL3). Two critical impact cases were evaluated for Test 3-10 and Test 3-11: (1) Splice Reference Case – critical impact point for maximizing potential for snag on the rail expansion splice, and (2) Post Reference Case – critical impact point for maximizing loading and potential snag on the critical bridge rail post located immediately downstream of the rail splice and expansion joint. Based on the results of all analysis cases, the CM-MTL3 with the proposed design revisions is expected to meet all performance criteria specified in MASH for test level 3.

17. Key Words	18. Distribution Statement
CM-MTL3, Combination Rail, Concrete Barrier, Steel Top Rail, Vertical Face Barrier, MASH TL3, Finite Element Analysis, FEA	**No restrictions. This document is available to the public through the National Technical Information Service, Springfield, Virginia 22161**

19. Security Classif. (of this report)	20. Security Classif. (of this page)	21. No. of Pages	22. Price
Unclassified	**Unclassified**	**92**	

Form DOT F 1700.7 (8-72) **Reproduction of completed pages authorized**

TABLE OF CONTENTS

LIST OF FIGURES

LIST OF TABLES

LIST OF APPENDICES

CHAPTER 1 – INTRODUCTION

The purpose of this project was to evaluate the crash performance of a revised design for the MassDOT CM-MTL3 bridge rail using finite element analysis (FEA). The CM-MTL3 was shown to be MASH compliant in a previous study.[*Plaxico21b*] However, based on feedback from installers, further revisions have been proposed to facilitate installation and repair of the system. The evaluations were carried out in accordance with the AASHTO Manual for Assessing Safety Hardware (*MASH*) for test level 3 (TL-3), and the results of those evaluations are presented in the following chapters of this report.

Background

The original design (i.e., CM-TL3) was developed by researchers at Worcester Polytechnic Institute (WPI), and its crash performance was evaluated under impact and evaluation criteria specified in NCHRP Report 350 for test level 3 (TL3). [*Ray07*] The system received eligibility status for use on federally funded roadways in 2008 based on the results from that study (see Eligibility Letter B-168).

The design for the CM-TL3 was subsequently revised to improve crash performance and was evaluated under impact conditions and performance criteria recommended in MASH for TL3 using finite element analysis (FEA). [Plaxico21b] The most significant change for the modified CM-MTL3 design compared to the original CM-TL3 design was a decreased offset distance for the post. The offset distance was 5-7/8" for the CM-MTL3 compared to 7-1/4" for the original CM-TL3. Two cases were evaluated, one with an integral safety curb and another with a vertical face on the concrete barrier. The results of that study showed that the performance for both designs met MASH TL3 performance criteria; however, the damage to the system was significantly reduced and the overall performance improved for the case with the vertical barrier face. The results from that study led to a recommendation for the vertical face design to be used for the CM-MTL3 barrier.[Plaxico21b]

System Design

Based on feedback from installers, further revisions were proposed to facilitate installation and repair of the system. Drawing details for the proposed design are shown in Appendix A. The proposed design includes a 15-inch tall steel post-and-beam railing mounted onto the top of a 17-inch tall continuous reinforced concrete barrier, as illustrated in Figures 1-4. The overall height of the barrier is 32 inches measured from the top of the roadway to the top of the steel rail. The steel post-and-beam rail is composed of a HSS 8"x3"x1/4" longitudinal beam supported by HSS 5"x5"x1/4" posts which are spaced at 6 feet on centers. The longitudinal beam is welded to the posts. A 3/4-inch thick steel base plate is welded to the bottom of each post, and the base plate is fastened to the top of the curb or sidewalk using four ¾-inch diameter ASTM F1554 anchor bolts that are 12-inch long, as shown in Figure 4. Two bolts are positioned on the front side of the posts and two bolts positioned at the back of the base plate and closely aligned with the back edge of the posts. A 3/8" x 9½" x14½" anchor plate is attached at the bottom of the anchor bolts to secure the anchors and to prevent pullout during impact.

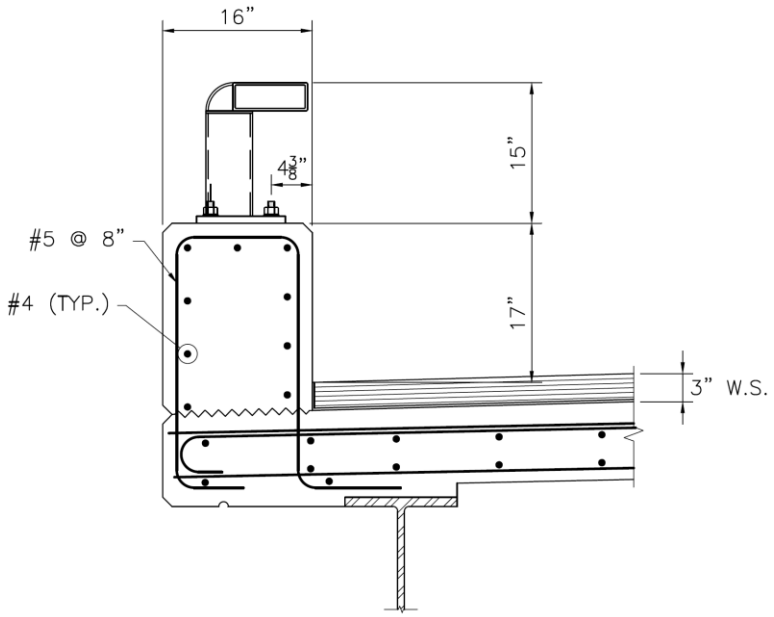

Figure 1. Section drawing for the proposed CM-MTL3.

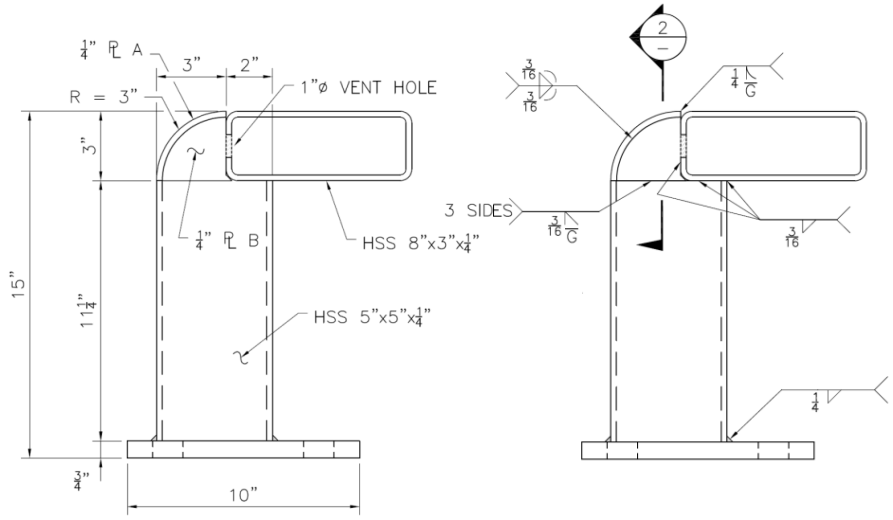

Figure 2. Section drawing and weld details for the post of the proposed CM-MTL3.

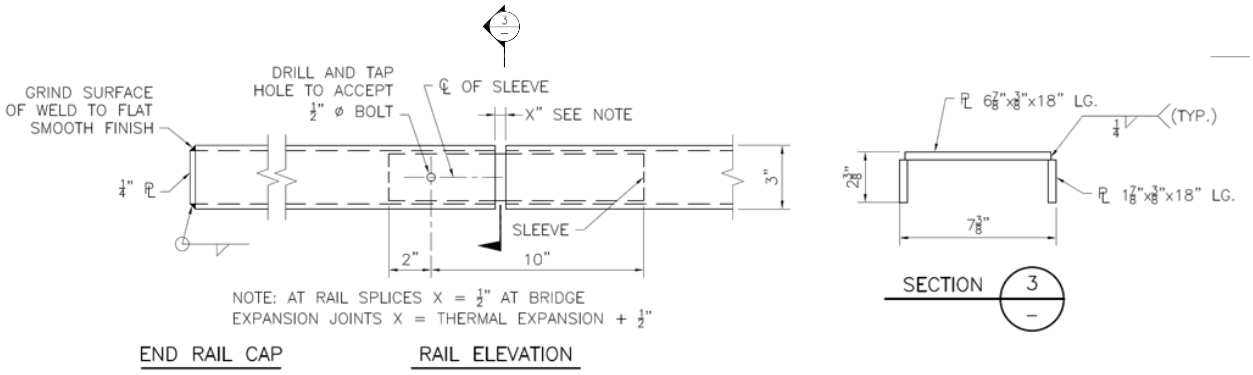

Figure 3. Splice details for the proposed CM-MTL3.

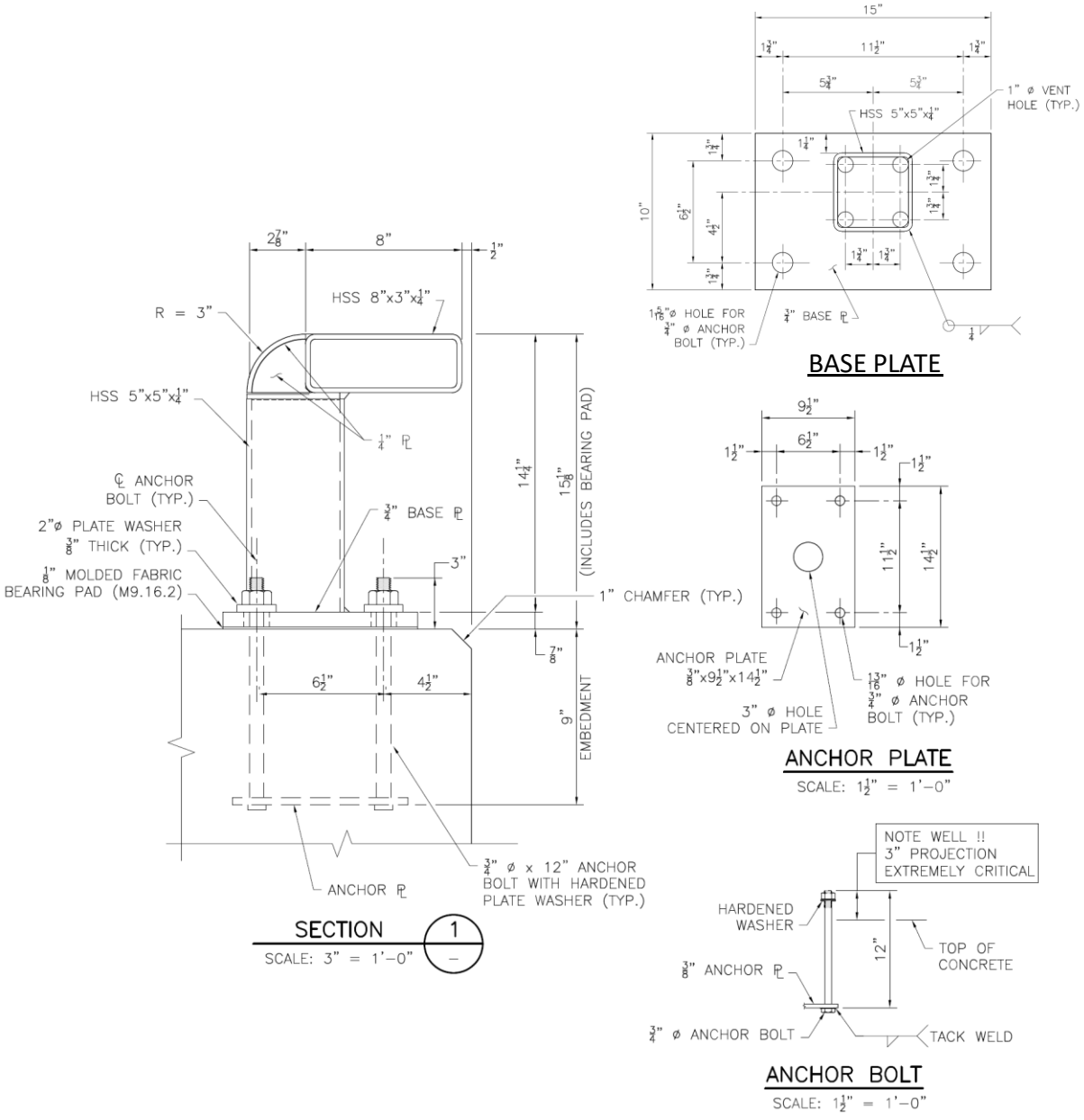

Figure 4. Section drawing and anchor details for the proposed CM-MTL3.

The most significant revisions of the proposed design involve the base plate, the splice connection, and the weld size for the plates and rail welded to the top of the post. The revised based plate is ½" longer and ½" wider than the previous MASH design, as illustrated in Figure 5. It also includes larger diameter holes (1-5/16" diameter) for mounting on the anchor bolts as well as 2" diameter plate washers under the nut for the anchor bolts. Several changes were made to the splice bar including reduced length (12" vs. 18"), thicker plates (3/8" vs. ¼"), welded connection to main rail replaced with a single bolt connection and changing from a closed section design to an open C-shape design, as illustrated in Figure 6. The proposed weld size for the plates and rail welded to the top of the post was reduced from ¼" welds to 3/16" welds.

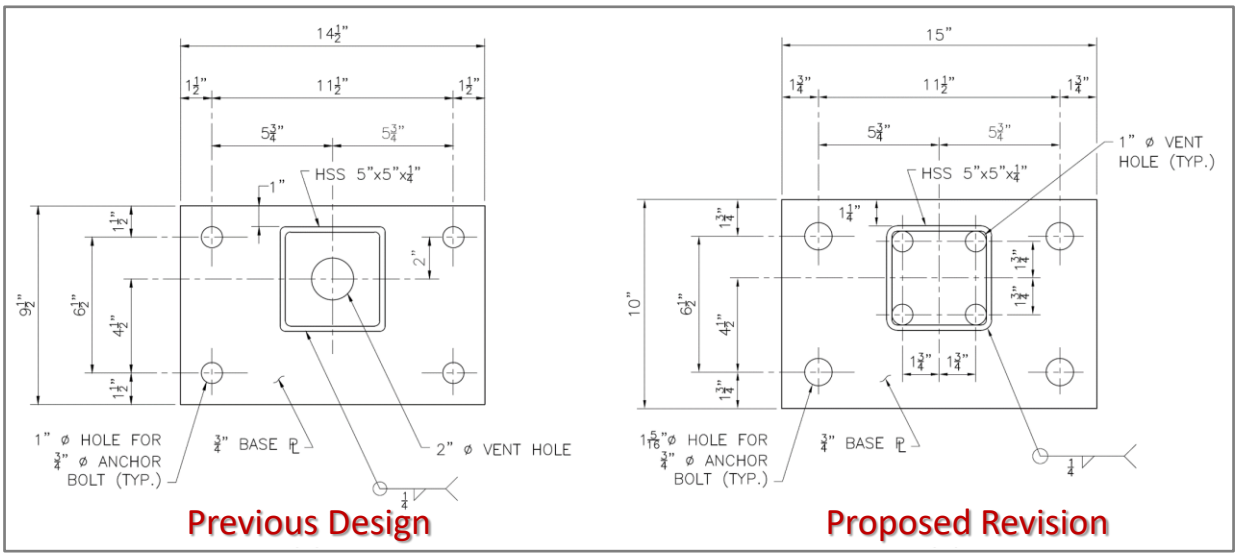

Figure 5. Proposed revisions to the base plate.

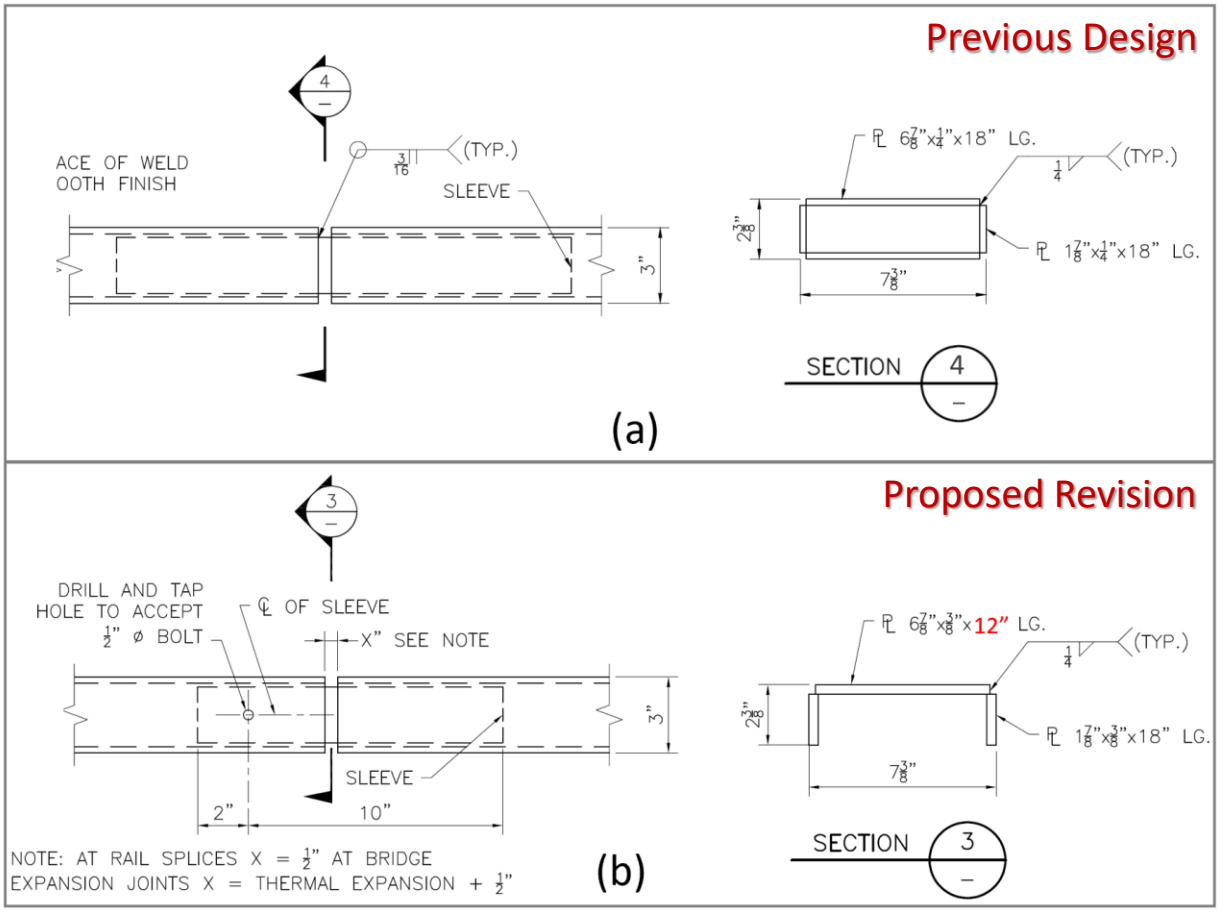

Figure 6. Proposed revisions to the splice connection.

CHAPTER 2 – OBJECTIVES AND SCOPE

The objective of this project was to use finite element analysis (FEA) computer simulation to evaluate the crash performance of a revised design for the MassDOT CM-MTL3 bridge rail under impact and evaluation procedures of *MASH* for TL3. The crash evaluations were carried out using the non-linear, dynamic, explicit finite element analysis software LS-DYNA. [*LSDYNA20*]. The assessment procedures included evaluations of structural capacity, risk of occupant injury, and vehicle stability during impact and redirection.

CHAPTER 3 – RESEARCH APPROACH AND EVALUATION CRITERIA

The basic approach for the study was to develop a finite element model of the CM-MTL3 bridge rail (see Chapter 5) and to use FEA to simulate *MASH* TL3 tests (see Chapters 6). The crash performance of the system was evaluated for structural capacity, occupant risk, vehicle stability and trajectory during impact and redirection according to the recommended procedures and criteria contained in *MASH*. The FEA model was not directly validated against full-scale testing in this study; however, the same methodologies used in the development and validation of the FEA models used in early phases of this project, which were validated against full-scale crash testing using NCHRP Report 179 procedures, were implemented here.[*Ray10;Plaxico21b*] The FEA model for HSS tube, the steel anchor plate, and the anchor rods were based on the validated models developed in Phase II for the S3-TL4 bridge rail, and the FEA model for concrete and steel reinforcement were based on the validated models developed in Phase III for the CT-TL2.[*Plaxico19; Plaxico21a*]

Table 1 shows a summary of the evaluation criteria required for test levels 1 through 4 (taken directly from *MASH*) with the specific criteria for TL3 outlined with a red box. Table 2 shows the details for each criterion. The required test conditions specified in *MASH* for test level 3 evaluation of longitudinal barrier include:

- Test 3-10 – the 1100C vehicle (2,225-lb sedan) impacting the barrier at the critical impact point at a nominal speed and angle of 62.0 mph and 25 degrees, respectively.
- Test 3-11 – the 2270P vehicle (5,000-lb ½-ton quad-cab pickup) impacting the barrier at the critical impact point at a nominal speed and angle of 62.0 mph and 25 degrees, respectively.

Table 1. (*MASH* Table 2-2A) Recommended test matrices for longitudinal barriers. [*AASHTO16*]

Test Level	Barrier Section[c]	Test No.	Vehic.	Impact Speed,[a] mph (km/h)	Impact Angle,[a] θ, deg.	Im-pact Point	Acceptable IS Range,[a] kip-ft (kJ)	Evaluation Criteria[b]
1	Length-of-Need	1-10 1-11	1100C 2270P	31 (50.0) 31 (50.0)	25 25	(c) (c)	≥13 (17.4) ≥27 (36.0)	A,D,F,H,I A,D,F,H,I
	Transition	1-20[d] 1-21	1100C 2270P	31 (50.0) 31 (50.0)	25 25	(c) (c)	≥13 (17.4) ≥27 (36.0)	A,D,F,H,I A,D,F,H,I
2	Length-of-Need	2-10 2-11	1100C 2270P	44 (70.0) 44 (70.0)	25 25	(c) (c)	≥25 (34.2) ≥52 (70.5)	A,D,F,H,I A,D,F,H,I
	Transition	2-20[d] 2-21	1100C 2270P	44 (70.0) 44 (70.0)	25 25	(c) (c)	≥25 (34.2) ≥52 (70.5)	A,D,F,H,I A,D,F,H,I
3	Length-of-Need	3-10 3-11	1100C 2270P	62 (100.0) 62 (100.0)	25 25	(c) (c)	≥51 (69.7) ≥106 (144)	A,D,F,H,I A,D,F,H,I
	Transition	3-20[d] 3-21	1100C 2270P	62 (100.0) 62 (100.0)	25 25	(c) (c)	≥51 (69.7) ≥106 (144)	A,D,F,H,I A,D,F,H,I
4	Length-of-Need	4-10 4-11 4-12	1100C 2270P 10000S	62 (100.0) 62 (100.0) 56 (90.0)	25 25 15	(c) (c) (c)	≥51 (69.7) ≥106 (144) ≥142 (193)	A,D,F,H,I A,D,F,H,I A,D,G
	Transition	4-20[d] 4-21 4-22	1100C 2270P 10000S	62 (100.0) 62 (100.0) 56 (90.0)	25 25 15	(c) (c) (c)	≥51 (69.7) ≥106 (144) ≥142 (193)	A,D,F,H,I A,D,F,H,I A,D,G

Table 2. (*MASH* Table 5-1A and 5-1B) Safety evaluation guidelines for structural adequacy and occupant risk. *[AASHTO16]*

Evaluation Factors		Evaluation Criteria
Structural Adequacy	A.	Test article should contain and redirect the vehicle or bring the vehicle to a controlled stop; the vehicle should not penetrate, underride, or override the installation although controlled lateral deflection of the test article is acceptable.
Occupant Risk	D.	Detached elements, fragments or other debris from the test article should not penetrate or show potential for penetrating the occupant compartment, or present an undue hazard to other traffic, pedestrians or personnel in a work zone. Deformations of, or intrusions into, occupant compartment should not exceed limits set forth in Section 5.2.2 and Appendix E.
	F.	The vehicle should remain upright during and after the collision. The maximum roll and pitch angles are not to exceed 75 degrees.
	H.	The longitudinal and lateral occupant impact velocity (OIV) shall not exceed 40 ft/s (12.2 m/s), with a preferred limit of 30 ft/s (9.1 m/s)
	I.	The longitudinal and lateral occupant ridedown acceleration (ORA) shall not exceed 20.49 G, with a preferred limit of 15.0 G.

Accelerometers were positioned between the front seat occupants for both the 1100C and 2270P vehicles at the center of gravity for each vehicle models. The acceleration-time histories and angular rate-time histories were collected during the impact event and were used to evaluate occupant risk metrics according to the procedures outlined in *MASH*. The acceleration data from

the analyses were collected at a frequency of 50,000 Hz and were filtered using the SAE Class 180 filter prior to input into the Test Risk Assessment Program (TRAP). [*TTI22*] The TRAP program calculates standardized occupant risk factors from vehicle crash data in accordance with *MASH* guidelines and the European Committee for Standardization (EN1317). TRAP computes important evaluation parameters including the occupant impact velocities (OIV), occupant ridedown accelerations (ORA), 50 millisecond running average acceleration, and maximum roll, pitch and yaw. Also computed in TRAP are the EN1317 occupant risk metrics which include the Theoretical Head Impact Velocity (THIV), the Post Impact Head Deceleration (PHD) and the Acceleration Severity Index (ASI). The details of these calculations are provided in *MASH.* [*AASHTO16*]

With regards to occupant risk, *MASH* lists certain limitations for passenger compartment intrusion. Specifically, it states:

"*A clear distinction should be made between: (a) penetration, in which a component of the test article actually penetrates into the occupant compartment; and (b) intrusion or deformation, in which the occupant compartment is deformed and reduced in size, but no actual penetration is observed. No penetration by any element of the test article into the occupant compartment is allowed. As for deformation or intrusion, the extent of deformation varies by area of the vehicle damaged and should be limited as follows:"*

- *"Roof ≤ 4.0 in. (102 mm).*
- *Windshield – no tear of plastic liner and maximum deformation of 3 in. (76 mm).*
- *Window – no shattering of a side window resulting from direct contact with a structural member of the test article, except for special considerations pertaining to tall, continuous barrier elements discussed below (Note: evaluation of this criteria requires the side windows to be in the up position for testing). In cases where side windows are laminated, the guidelines for windshields will apply.*
- *A- and B- pillars – no complete severing of support member and maximum resultant deformation of 5 in. (127 mm). Lateral deformation should be limited to 3 in. (76 mm).*
- *Wheel/foot well and toe pan areas ≤ 9 in. (229 mm).*
- *Side front panel (forward of A-pillar) ≤ 12 in. (305 mm).*
- *Front side door area (above seat) ≤ 9 in. (229 mm).*
- *Front side door area (below seat) ≤ 12 in. (305 mm).*
- *Floor pan and transmission tunnel areas ≤ 12 in. (305 mm)."* [*AASHTO16*]

Post-impact vehicle trajectory, although not required by *MASH*, was examined for completeness of the evaluations. *MASH* uses the concept of the "exit box" which was adopted directly from CEN standards. The width of the exit box is the lateral distance "A" in Figure 7, which is defined as 7.2 feet plus the width of the vehicle plus 16 percent of the length of the vehicle. The length of the exit box is the longitudinal distance "B" in Figure 7 which is 32 feet. All wheel tracks of the vehicle should remain within the exit box throughout distance "B". [*AASHTO16*] A graphical representation of the exit box is shown in Figure 7.

Distance for Exit Box Criterion

Vehicle Type	A ft (m)	B ft (m)
Car/Pickup	$7.2 + V_W + 0.16V_L$ $(2.2 + V_W + 0.16V_L)$	32.8 (10.0)
Other Vehicles	$14.4 + V_W + 0.16V_L$ $(4.4 + V_W + 0.16V_L)$	65.6 (20.0)

V_W = Vehicle Width
V_L = Vehicle Length

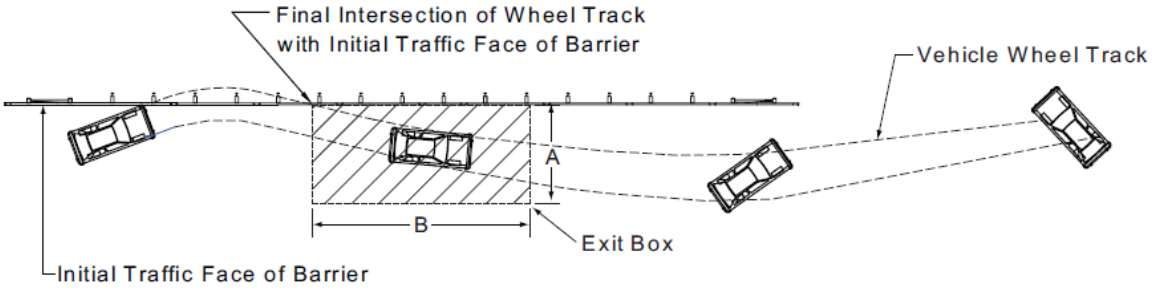

Figure 7. *MASH* exit box. [*AASHTO16*]

The exit box values were calculated based on the dimensions of the finite element analysis vehicle models that are further described in Chapter 4. Table 3 shows the vehicle widths and lengths and resulting exit box dimensions for the small car and pickup truck.

Table 3. Exit box dimensions for *MASH* tests for small car and pickup.

Test	V_w (ft)	V_L (ft)	A (ft)	B (ft)
2-10	5.5	14.1	15	32.8
2-11	6.02	16.8	15.86	32.8

CHAPTER 4 – FEA VEHICLE MODELS

The models for the 1100C and 2270P vehicles used for the *MASH* analysis cases were the YarisC_v1L model (based on a 2010 Toyota Yaris) and the Ram2018_V02u model (based on a 2018 quad-cab Dodge Ram). These vehicles closely represent the two test vehicles specified in *MASH*. [*AASHTO16*] The vehicle models were developed through the process of reverse engineering by the members of George Mason University (GMU) and were initially validated based on NCAP frontal wall impact tests through comparison with NHTSA test data. The models also include validated suspension and steering subsystems. The Dodge Ram model is relatively new and is continually being improved by GMU as well as the user community. The Yaris model has been used extensively by the research team and has routinely provided good results. [*Plaxico19; Plaxico20*] The validation reports for these vehicles can be accessed from the George Mason University's Center for Collision Safety and Analysis website. [*Marzougui12; CCSA16; CCSA18*] Additional modifications were made to the 1100C and the 2270P models in previous work by the research team, which included development of a new tire

model.[*Plaxico21a*] The steer response for the 1100C and 2270P models was also corrected in recent projects by the research team.[Carrigan22; Plaxico22]

A comparison of the physical and inertial properties of the 1100C and 2270P vehicle models with those of recent full-scale test vehicles (i.e., Test 469468-3-1 and Test 469468-3-2) is provided in Figure 8 and Figure 9, respectively.[*Bligh19*] The most notable difference for the 1100C vehicle was that the center of gravity (c.g.) was set 6.15 inches farther back in the model compared to the test vehicle, which resulted in a 17 percent difference, and the height of the model was approximately 12 percent taller than the test vehicle. For the 2270P vehicle model, except for the *bumper extension* and the *wheel-well clearance*, all other measurements were within 10 percent of those measured on the test vehicle. The longitudinal c.g. and the vertical c.g. of the 2270P model was within 4 percent and 1 percent, respectively, compared to the test vehicle. The accelerometer for both the 1100C and the 2270P models were positioned at the c.g. of the vehicle.

VEHICLE PROPERTIES AND INFORMATION

Date:	12/21/2016	Test No.:	607451-3	Vin No.:	KNADHA33A6692034
Year:	2010	Make:	Kia	Model:	Rio
Odometer:	140035	Tire Size:	35/65R14	Tire Inflation Pressure:	32 psi

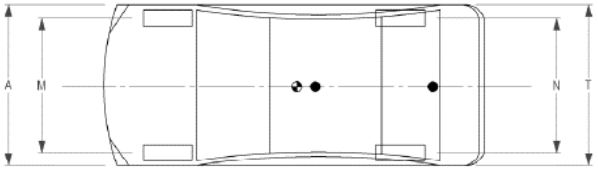

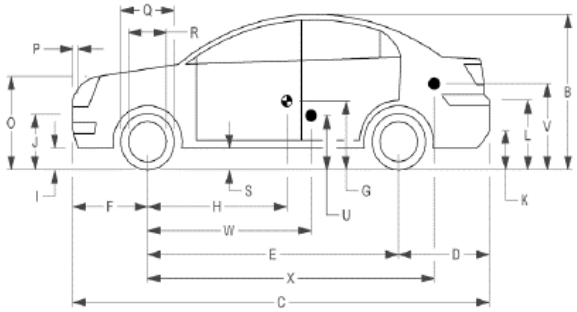

Vehicle Geometry (inches)

		Test	Model	% Error
a	Front Bumper Width:	66.38	65.67	-1.07
b	Overall Height:	51.5	57.68	11.99
c	Overall Length:	165.75	169.17	2.07
d	Rear Overhang:	34	37.09	9.08
e	Wheel Base:	98.75	99.92	1.19
f	Front Overhang:	33	32.13	-2.65
g	C.G. Height:		21.67	
h	C.G. Horz. Dist.	35.9	42.05	17.12
i	Front Bumper Bottom:	7.75	7.91	2.11
j	Front Bumper Top:	21.5	21.42	-0.38
k	Rear Bumper Bottom:	12.25	13.74	12.16
l	Rear Bumper Top:	25.25	25.20	-0.21
m	Front Track Width:	57.75	58.62	1.51
n	Rear Track Width:	57.7	57.64	-0.11
o	Hood Height:	28.25	31.73	12.33

		Test	Model	% Error
p	Bumper Extension:	4.12	3.66	-11.13
q	Front Tire Width:	22.5	22.99	2.19
r	Front Wheel Width:	15.5	15.08	-2.72
s	Bottom Door Height:	8.25	7.87	-4.56
t	Rear Bumper Width:	66.2	65.83	-0.56

Engine Type:	4 cylinder
Engine Size:	1.6 liter

Accelerometer Location (mm) - measured from front axle and ground	X	Y	Z
Test Vehicle:	35.9	0	15.8
FEA Vehicle:	41.7	0	13.0

Weights (lbs)

	Curb Test	Curb Model	Curb % Error	Gross Static Test	Gross Static Model	Gross Static % Error
$W_{front\ axle}$	1597	0	-100.00	1641	1511.2	-7.91
$W_{rear\ axle}$	921	0	-100.00	971	1097.9	13.07
W_{total}	2518	0	-100.00	2612	2609.1	-0.11

GVWR Ratings (lbs)	Test	Model	% Error
Front	1718	0	-100.00
Rear	1874	0	-100.00

Dummy Data				
Type	50th Percentile male		
Mass (lbs)	165	0	-100.00
Seat Position	Impact Side		

Other Notes:

Figure 8. Vehicle property sheet for the 1100C vehicle model compared with the test vehicle in full-scale test 469468-3-1.

VEHICLE PROPERTIES AND INFORMATION

Date:	10/8/2003	Test No.:	420020-3	Vin No.:	1D7HA18N455243883
Year:	2005	Make:	Dodge	Model:	RAM 1500 Quad-Cab
Odometer:	138200	Tire Size Front:	265/70R17	Tire Size Rear:	245/70R17

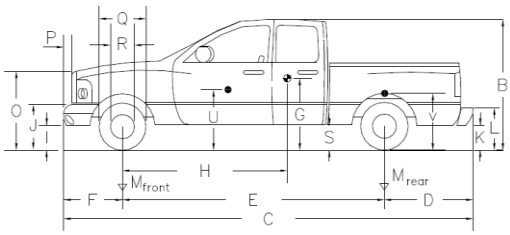

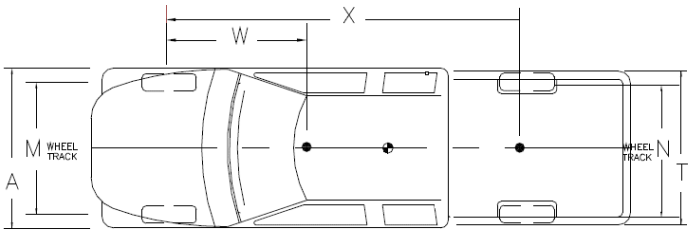

Vehicle Geometry (inches)

		Test	Model	% Error
a	Front Bumper Width:	78.50	76.02	-3.15
b	Overall Height:	74.00	75.51	2.04
c	Overall Length:	227.50	229.33	0.80
d	Rear Overhang:	44.00	48.31	9.79
e	Wheel Base:	140.50	140.20	-0.22
f	Front Overhang:	40.00	40.20	0.49
g	C.G. Height:	28.87	28.98	0.38
h	C.G. Horz. Dist.	62.40	60.11	-3.68
i	Front Bumper Bottom:	11.75	12.56	6.89
j	Front Bumper Top:	27.00	25.94	-3.91
k	Rear Bumper Bottom:	20.00	20.47	2.36
l	Rear frame Top:	30.00	31.14	3.81
m	Front Track Width:	68.50	69.49	1.44
n	Rear Track Width:	68.00	67.24	-1.11
o	Hood Height:	46.00	44.84	-2.52

		Test	Model	% Error
p	Bumper Extension:	3.00	2.6	-12.07
q	Front Tire Width:	30.50	31.8	4.17
r	Front Wheel Width:	18.00	18.4	2.36
s	Bottom of Body Height:	13.00	13.6	4.78
t	Overall Width:	77.00	79.3	2.98
u	Accelerometer Height:	27.75	27.7	-0.21
w	Accelerometer from Axle	62.40	62.4	0.00
	Wheel Center Height Front:	14.75	16.0	8.37
	Wheel Center Height Back:	14.75	16.0	8.37
	Wheel Well Clearance (F):	6.00	NA	
	Wheel Well Clearance (R):	9.25	11.9	28.54
	Frame Height (F):	12.00	12.6	4.66
	Frame Height (R):	25.50	27.0	5.76
	Engine Type:	V-8		
	Engine Size:			

Weights (lbs)

	Curb		
	Test	Model	% Error
$W_{front\ axle}$	2850	0	-100.00
$W_{rear\ axle}$	2106	0	-100.00
W_{total}	4956	0	-100.00

Accelerometer Location (inches) - measured from front axle and ground	X	Y	Z

	Gross Static		
	Test	Model	% Error
$W_{front\ axle}$	2870	2960	3.14
$W_{rear\ axle}$	2307	2221	-3.71
W_{total}	5177	5182	0.09

GVWR Ratings (lbs)

	Test	Model	% Error
Front	3700	0	-100.00
Rear	3900	0	-100.00

Dummy Data

Type	50th Percentile Male			
Mass (lbs)	165	0	-100.00
Seat Position	Impact Side		

Other Notes:

Figure 9. Vehicle property sheet for the 2270P vehicle model compared with the test vehicle in full-scale test 469468-3-2.

CHAPTER 5 – FEA MODEL DEVELOPMENT

A detailed finite element model of the proposed CM-MTL3 bridge rail design was developed, as shown in Figure 10, based on the system drawings provided by MassDOT, which are included in Appendix A. The overall FEA model included a 48-ft length of the CM-MTL3 bridge rail and a 3-ft width of the bridge deck. The basic components of the bridge rail model include:

- Eight (8) 5”x5”x1/4” posts spaced at 6-feet on centers,
- Eight (8) 10”x15”x ¾” base plates (i.e., one at each post),
- Eight (8) 9.5”x14.5”x 3/8” anchor plates (i.e., one at each post)
- Thirty-two (32) anchor bolts (i.e., four (4) at each base plate connecting the base plate to the concrete parapet),
- Two (2) HSS 8”x3”x ¼” tube rails that are 24 feet long (each) and hardware,
- One (1) splice tube weldment, 12 inches long made from 3/8-inch thick steel plate, with one ½” diameter screw fastener, and
- Concrete parapet and bridge deck with steel reinforcement.

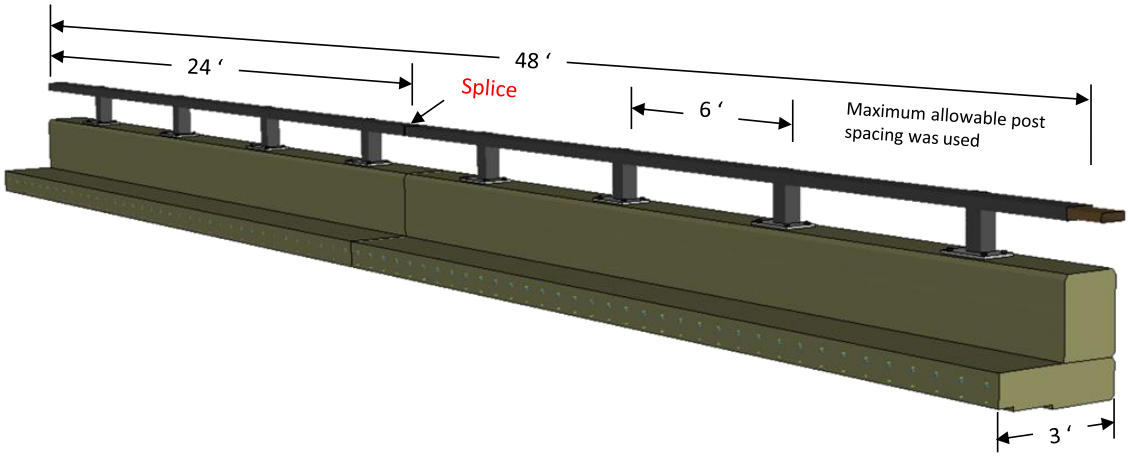

Figure 10. FEA model of the MassDOT CM-MTL3 bridge rail.

Posts

The geometry of the posts was modeled according to the detailed drawings in Appendix A. The FEA model of the post is shown in Figure 11. The material for the HSS portion of the post model conformed to ASTM A500 Grade C; the material for the top weldment portion of the post conformed to ASTM A709 Grade 50 steel. The post was modeled with thin-shell Belytschko-Tsay elements (Type 2 in LS-DYNA) with five (5) integration points through the thickness. The mesh size was modeled with a nominal element size of 5/8” x 5/8”. The weldment was modeled as *Constrained_Spotwelds in LS-DYNA with no failure, as illustrated in Figure 12. The 3/16-inch weld thickness was simulated by reducing the thickness of the elements around the top perimeter of the post to that of the weld (i.e., 3/16”). The plastic strains in these elements were monitored during the impact simulation to assess weld strength/performance. The

weld between the post and the base plate was modeled using the *Contact-Tied-Nodes-to-Surface option in LS-DYNA.

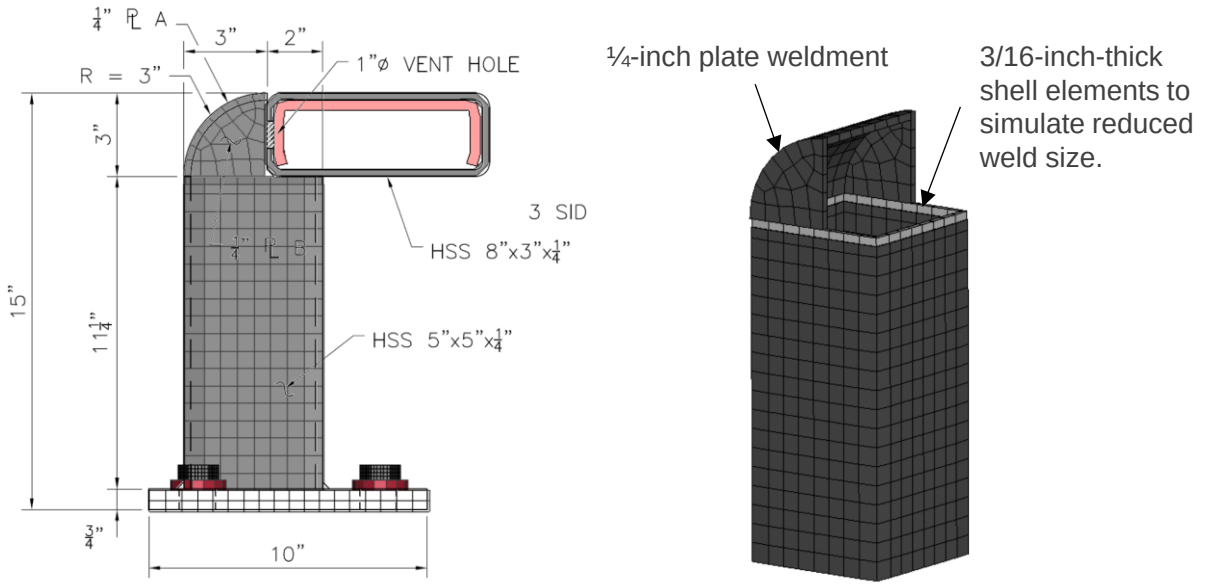

Figure 11. FEA mesh of steel bridge rail post.

Tubular Rail

The tubular rail section was modeled according to the dimensional specifications for HSS 8" x 3" x ¼". A representative portion of the rail model is shown in Figure 12. The material for the railing conformed to ASTM A500 Grade C. The tube rails were modeled with Type 2 element with five (5) integration points through the thickness. The nominal element size for the mesh is 5/8" x 5/8". The weldment of the rail to the post was modeled using *Constrained_Spotwelds option in LS-DYNA.

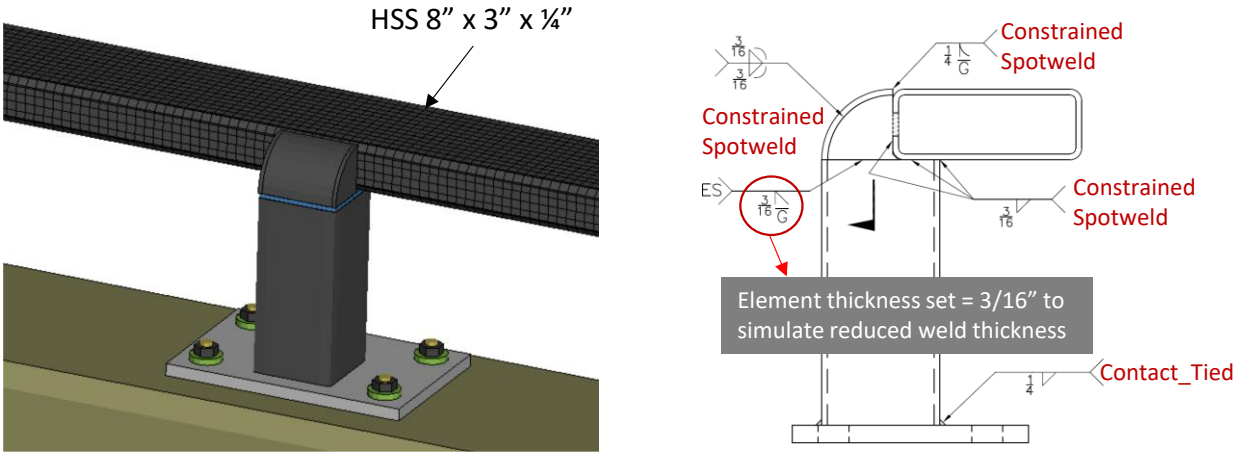

Figure 12. FEA mesh of tubular rail and weld model methodology.

The splice connection of the adjoining tube rails included a 12-inch-long c-shape weldment inserted 5.75 inches into the end of the main rail section (see Appendix A for dimension details). This end of the splice weldment was fastened to the main rail with a ½" diameter bolt. A constrained nodal rigid body was used to connect the end of the bolt to the internal splice weldment to simulate the threaded connection. The other end of the splice weldment was inserted into the adjoining main rail section and was free to slide inside the rail. A 1.5-inch gap between the adjoining main-rail sections was included to represent an expansion gap. The modeled splice connection is shown in Figure 13. The splice plates were modeled with material properties conforming to ASTM A36.

Figure 13. Model of rail splice with rail-tube shown transparent.

Base Plate and Anchor Bolts

The base plate was modeled with dimensions 15" x 10" x ¾" and with material properties conforming to ASTM A709 Grade 50. The part was meshed with Type 3 hexahedral element (fully integrated quadratic 8 node element with nodal rotations) with nominal side length of 9/16". The welded connection of the post to the base plated was modeled using *Contact_Tied option in LS-DYNA. The ¾-inch diameter anchor bolts were modeled with Type 1 beam elements in LS-DYNA. The material for the anchor bolts conformed to ASTM F1554 Grade 105, which has a minimum yield strength of 105 ksi, ultimate strength of 125 ksi, and 15 percent elongation. The nuts for the anchor rods were modeled as rigid, and a 2-inch diameter washer with thickness of 3/8" was included under the nut. The material for the washer was ASTM A36. The anchor bolts were embedded into the rigid deck, as illustrated in Figure 14. The bolts were anchored inside the deck using the *Constrained_Beam_in_Solid option in LS-DYNA. Null beams were added to the anchor plate so that its constraint to the curb/deck could also be modeled using *Constrained_Beam-in-Solid.

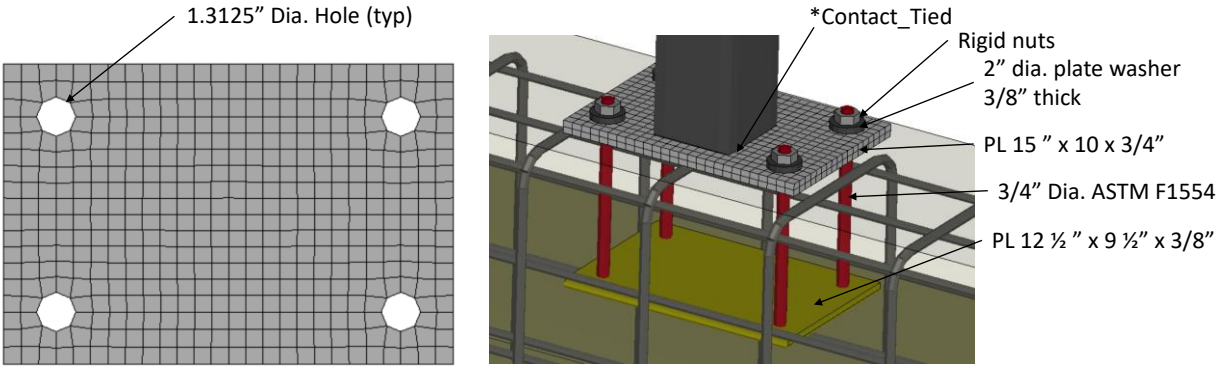

Figure 14. Transparent view of concrete showing model of base plate and anchor bolts.

Concrete Parapet and Deck

The concrete for the parapet and deck was modeled with Type 1 hexahedral elements in LS-DYNA with nominal element size of 1" x 1" x 1" in the regions where the posts are mounted, and are modeled with nominal element size of 1"x1"x1.5" elsewhere, as illustrated in Figures 15 and 16. All reinforcing bars were modeled with Type 1 beam elements with a nominal element length of 13/16 inch. The material properties for the reinforcing steel conformed to ASTM A615 Grade 60 steel.[*TFHRC15*]

The concrete material for the bridge rail and deck was modeled using two different concrete constitutive models in LS-DYNA (i.e., **Mat-RHT* and **MAT-Concrete-Damage-REL3*) with material properties based on an unconfined compressive strength of 4,000 psi (27.5 MPa), which corresponds to MassDOT's current minimum strength specification. Both material models provided essentially identical results, so only the RHT results are presented herein. Bonding of the reinforcing steel within the concrete was modeled using the **Constrained_Beam_in_Solid* option in LS-DYNA.

Fixed constraints were imposed on the boundary ends of the rebar in the deck and on the boundary face of the concrete, as indicated in Figure 15 by "+" symbols. The roadway was model as rigid using the **Rigidwall_Planar_Finite* option in LS-DYNA.

A 1.5" gap was included at the splice connection and in the concrete parapet to represent the expansion joint, as illustrated in Figure 17.

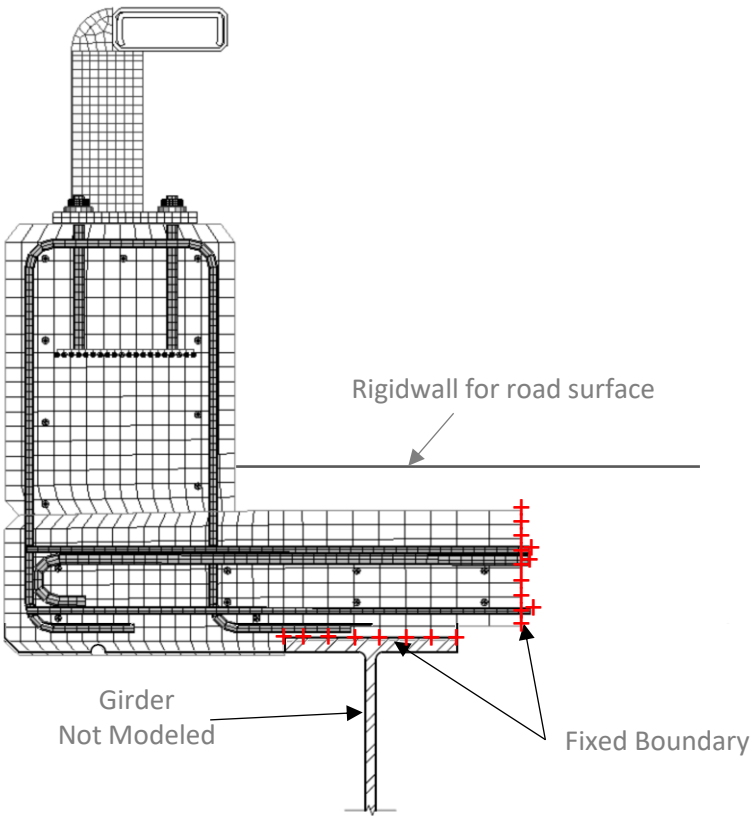

Figure 15. FEA model boundary details for the CM-MTL3.

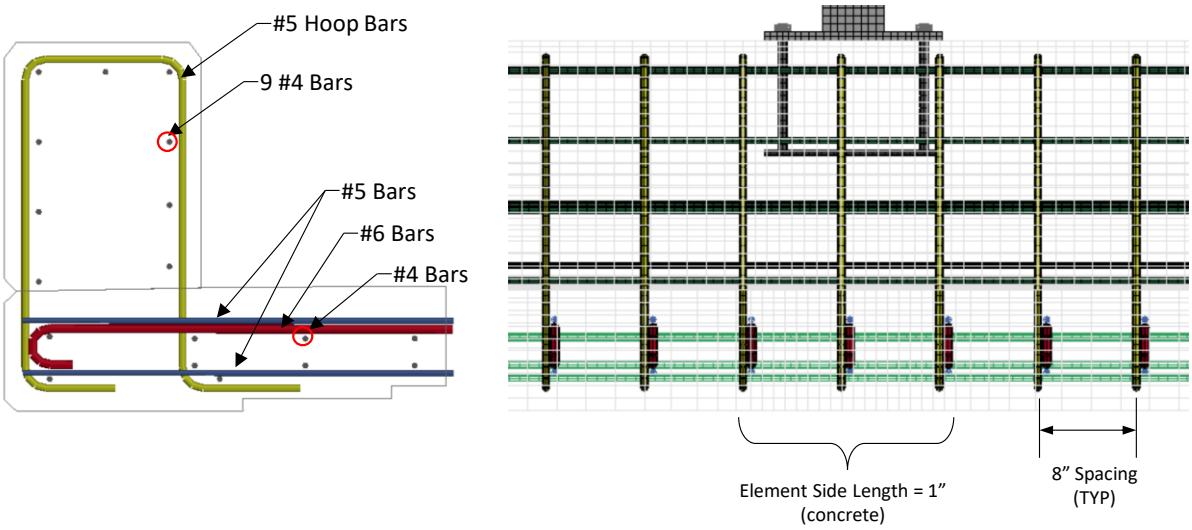

Figure 16. FEA model details for concrete barrier and deck reinforcement.

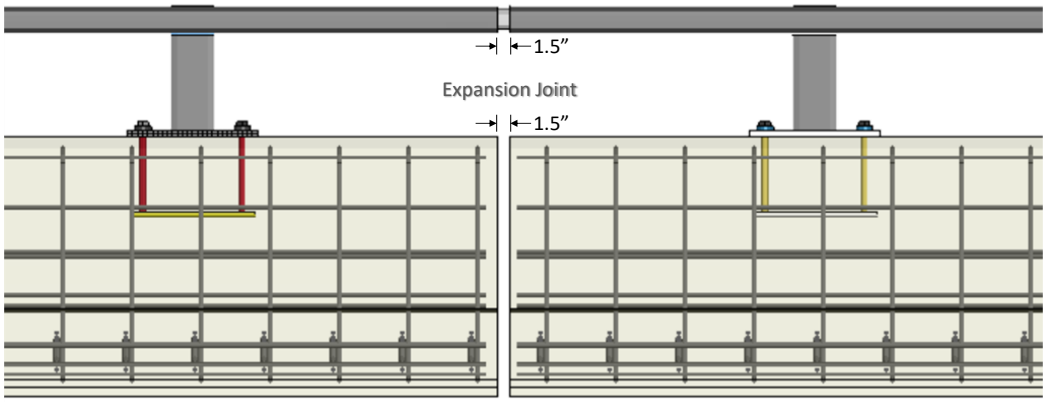

Figure 17. Expansion joint gap for the CM-MTL3.

CHAPTER 6 – *MASH* TL3 EVALUATION OF THE CM-MTL3 WITH PROPOSED DESIGN REVISIONS

FEA was used to evaluate the crash performance of the CM-MTL3 bridge rail with the proposed design revisions. The evaluations were based on structural adequacy, vehicle stability during and after redirection, and occupant risk factors using criteria specified in *MASH* for Test Level 3. The RHT concrete model in LS-DYNA was used for these analyses with parameters as described in Chapter 5. The analysis, in all cases, was performed using LS-DYNA version mpp_s_R13 revision number R13.1.0-3-g4cd30680f9. The analysis cases were conducted with a time-step of 1.0 microsecond for a period of 0.75 second of the impact event. The evaluations included:

- **Simulation of Test 3-10** with the 1100C Yaris model ballasted to 2,609 lb (1183 kg) impacting the barrier at 62.2 mph and 25 degrees.

- **Simulation of Test 3-11** with the 2270P Chevrolet Silverado model ballasted to 5,182lb (2,351 kg) impacting the railing at 62.2 mph and 25 degrees.

Test 3-10 with CIP for Expansion Splice and Critical Post

Simulation of Test 3-10 involved the 2,609-lb Yaris model impacting the bridge rail at 62.2 mph and 25 degrees. Two critical impact cases were evaluated:

- Splice Reference Case - involved impact point at 3.6 ft upstream from the center of the expansion splice on the rail to maximize the potential for snagging at the rail splice and
- Post Reference Case - involved impact point at 3.6 ft upstream of a post to maximize the potential for snagging on the critical bridge rail post (i.e., immediately downstream of rail splice). [*AASHTO16*]

The critical impact point (CIP) was selected based the *MASH* recommended CIP for rigid barrier tests (see Table 2-7 of *MASH*) to maximize potential for snagging on the rail splice or the critical post. [*AASHTO16*] The two CIP cases for Test 3-10 are illustrated in Figure 18.

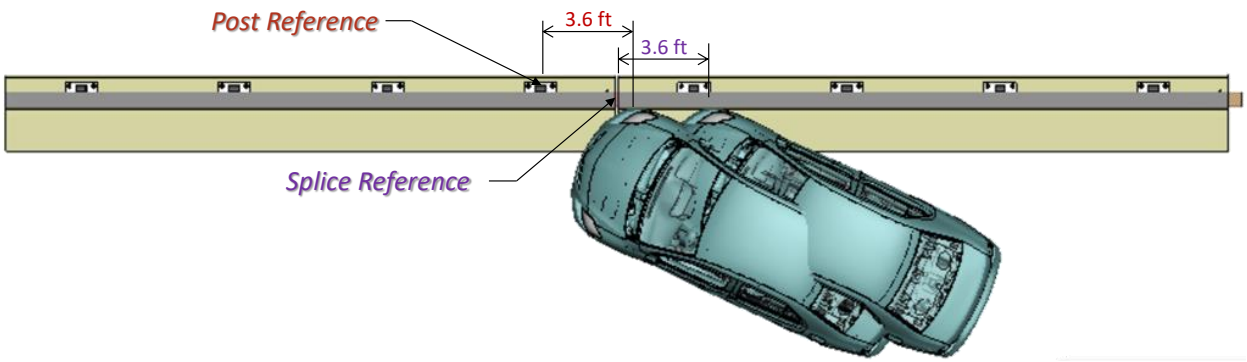

Figure 18. Critical impact points evaluated for Test 3-10.

Summary of Crash Event

CIP for Rail Splice

The 2,609-lb Yaris model struck the face of the barrier at 3.6 feet upstream of the rail expansion splice at a speed of 62.2 mph and at an impact angle of 25 degrees. The sequential views of the impact event are shown in Appendix B. Additional details regarding the sequence of key events are provided in **Error! Reference source not found.**. The following sections p rovide time-history data evaluation, occupant risk assessments, and damages sustained by the barrier and vehicle.

CIP for Critical Post

The 2,609-lb Yaris model struck the face of the barrier at 3.6 feet upstream of the critical post, which was located just downstream of the expansion joint in the deck, at a speed of 62.2 mph and at an angle of 25 degrees. The sequential views of the impact event are shown in Appendix C. Additional details regarding the sequence of key events for this analysis case are provided in Table 4. Additional details regarding time-history data evaluation, occupant risk

assessments, and damages sustained by the barrier and vehicle are included in the following sections.

Table 4. Sequence of events for Test 3-10.

	Event	Expansion Splice	Critical Post
1	Initial contact with barrier Right front fender and right front tire impacts vertical wall @ post 4	0.01 sec Impact speed = 62.2 mph Impact angle = 25 deg	0.01 sec Impact speed = 62.2 mph Impact angle = 25 deg
2	Peak 50-ms average x-acceleration	13.2 G @ 0.0081 - 0.0581 sec	13.6 G @ 0.0065 - 0.0565 sec
3	Front right tire deflates	0.025 - 0.083 sec	0.024 - 0.082 sec
4	Peak 50-ms average y-acceleration	17.6 G @ 0.0089 - 0.0589 sec	17.9 G @ 0.0087 - 0.0587 sec
5	Vehicle contacts splice - no snag	0.045 sec	0.025 sec
6	Lower right edged of windshield begins to crack	N.A.	N.A.
7	Maximum dynamic barrier deflection occurs at splice	0.92 in @ 0.05 sec	0.98 in @ 0.05 sec
8	Vehicle begins to yaw counterclockwise	≈ 0.05 sec	≈ 0.045 sec
9	Both passenger windows begin to fail	≈ 0.055 sec	≈ 0.055 sec
10	Left rear wheel leaves the ground	0.065 sec	0.065 sec
11	Maximum occupant compartment intrusion. Maximum OCI Location Maximum OCI Magnitude	0.060 sec(*) Right front toe pan 3.76 in (permanent)	0.065 sec Right front toe pan 4.12 in (permanent)
12	Occupant impact with vehicle interior	0.0678 sec OIV-x = 22.3 ft/s OIV-y = 29.9 ft/s	0.0680 sec OIV-x = 22.6 ft/s OIV-y = 29.5 ft/s
13	Maximum ORA-x	5.6 G @ 0.0678 - 0.0778 sec	4 G @ 0.0680 - 0.0780 sec
14	Vehicle contacts critical post	0.08 sec	0.05 sec
15	Left front wheel leaves the ground	0.085 sec	0.08 sec
16	Vehicle parallel with barrier	0.16 sec	0.16 sec
17	Tail slap with barrier Rear quarter panel impacts steel railing	0.17 sec Speed = 45.1 mph	0.17 sec Speed = 44.98 mph
18	Maximum ORA-y	13.9 G @ 0.1709 - 0.1809 sec	13.9 G @ 0.1705 - 0.1805 sec
19	Vehicle exits barrier (body and wheels)	0.27 sec Exit speed = 44.2 mph Exit angle = 8.2 deg	0.28 sec Exit speed = 44.0 mph Exit angle = 8.2 deg
20	Max positive roll (top of vehicle toward barrier)	≈ 9.9 deg @ 0.307 sec	≈ 9.2 deg @ 0.316 sec
21	Right rear wheel leaves the ground	0.36 sec	0.37 sec
22	Left front wheel returns to ground	0.42 sec	0.39 sec
23	Max negative pitch (front pitched downward)	≈ -6.4 deg @ 0.47 sec	≈ -6.5 deg @ 0.46 sec
24	Left rear wheel returns to ground	0.585 sec	0.57 sec
25	Right rear wheel returns to ground	0.595 sec	0.57 sec
26	Analysis Terminated	0.75 sec Speed = 41.5 mph Yaw angle = -30.9 deg (total angle) Roll angle = 2.3 deg (away from barrier) Pitch angle = -0.90 deg (rear pitched up)	0.75 sec Speed = 41.5 mph Yaw angle = -30.3 deg (total angle) Roll angle = 1.92 deg (away from barrier) Pitch angle = -1.24 deg (rear pitched up)

Time History Plots and Occupant Risk Measures

CIP for Rail Splice and Critical Post

Figures 19 through 21 show the longitudinal, transverse, and vertical acceleration-time histories, respectively, computed from the center of gravity of the vehicle; Figures Figure 22 through Figure 24 show a comparison of angular rates and angular displacements (i.e., yaw, roll, and pitch) at the center of gravity of the vehicle. Table 5 shows the results for the occupant risk calculations.

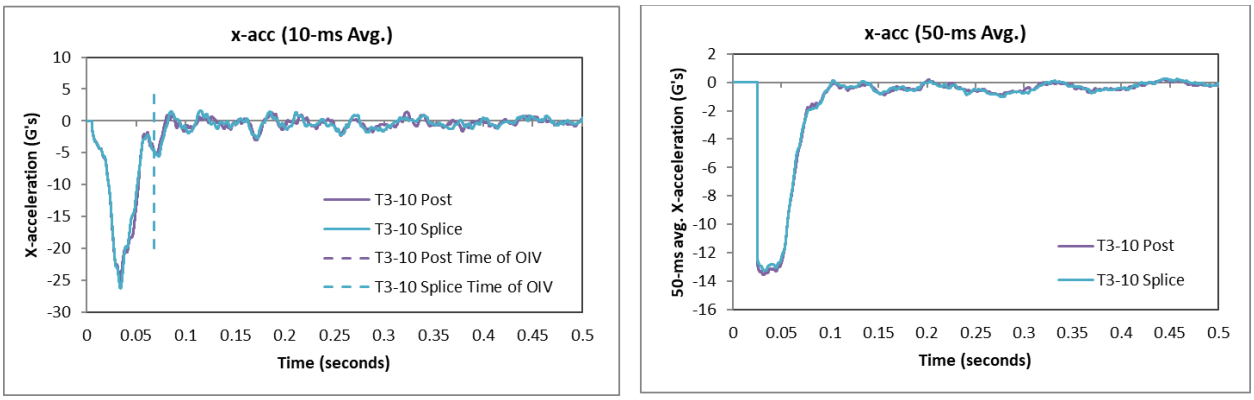

Figure 19. 10- and 50-millisecond average X-acceleration from FEA of Test 3-10.

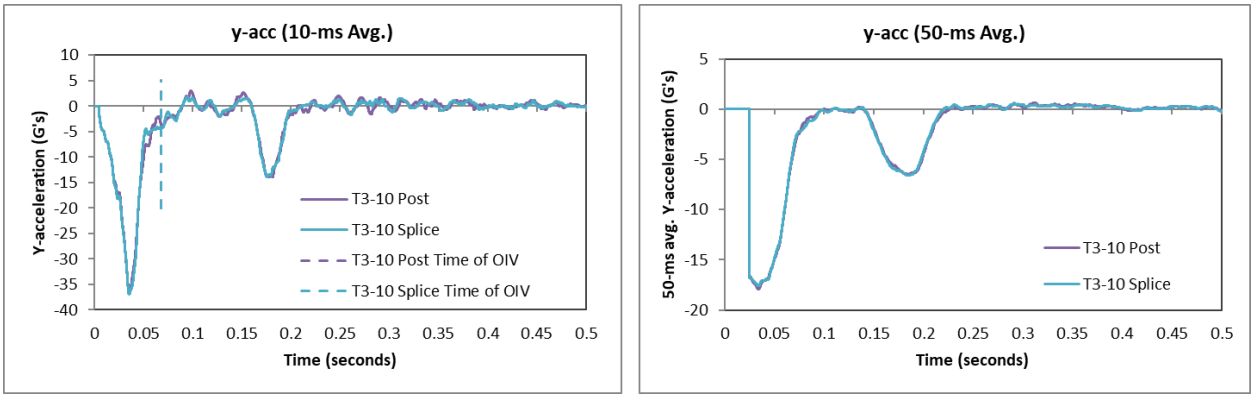

Figure 20. 10- and 50-millisecond average Y-acceleration from FEA of Test 3-10.

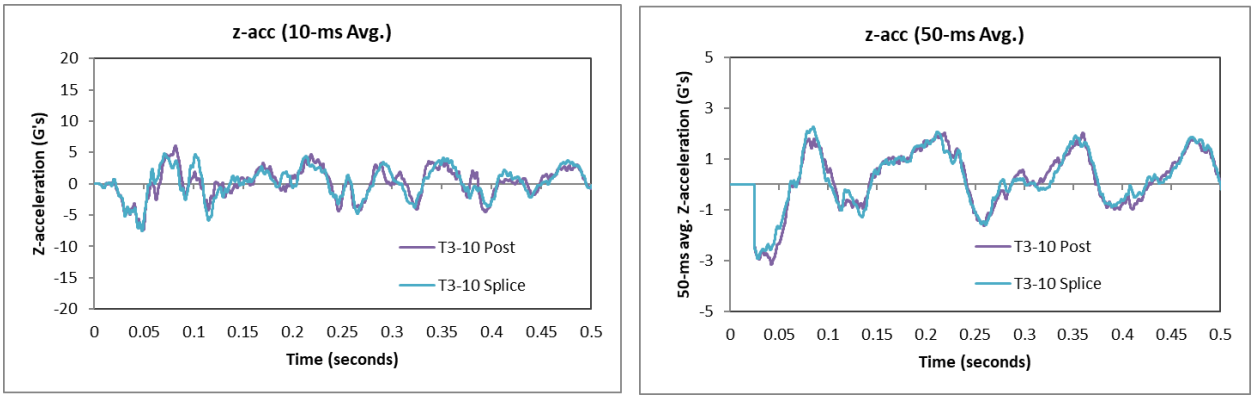

Figure 21. 10- and 50-millisecond average Z-acceleration from FEA of Test 3-10.

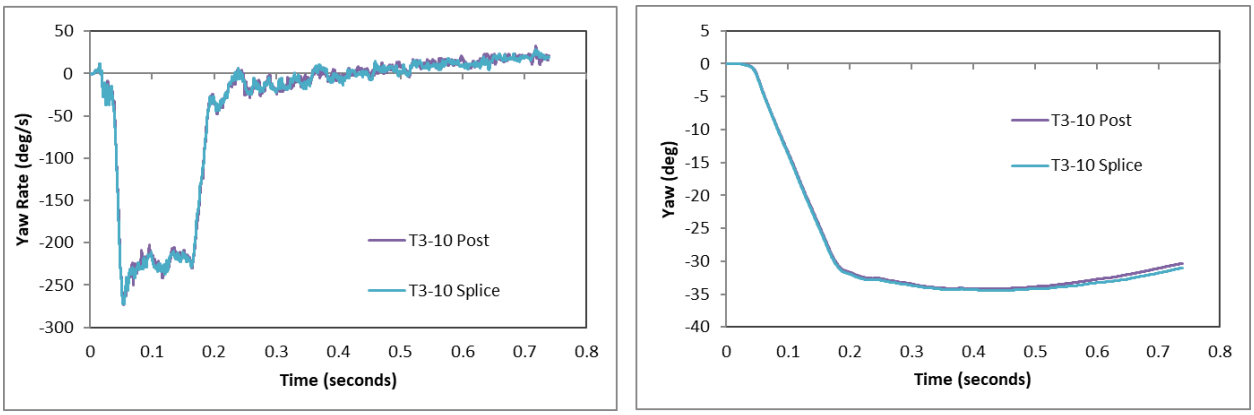

Figure 22. Yaw rate and yaw angle time-history from FEA of Test 3-10.

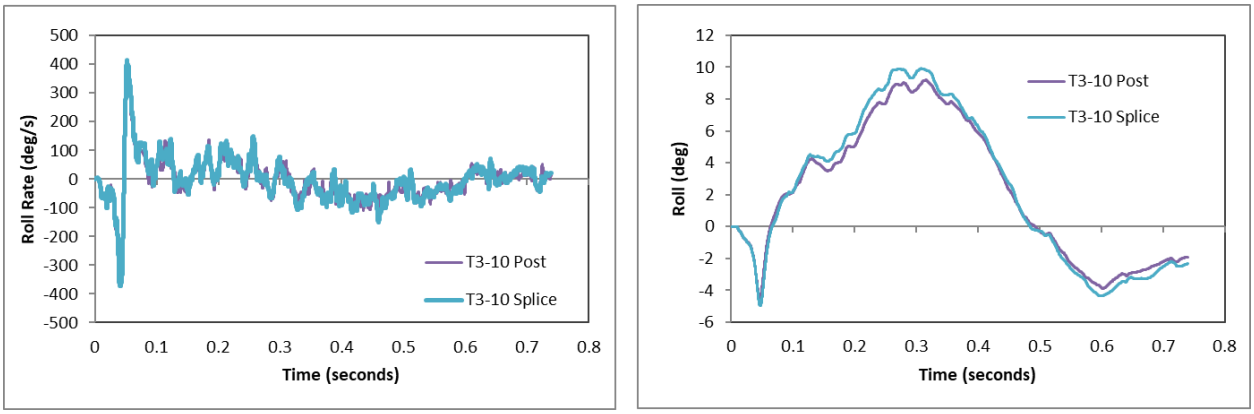

Figure 23. Roll rate and roll angle time-history from FEA of Test 3-10.

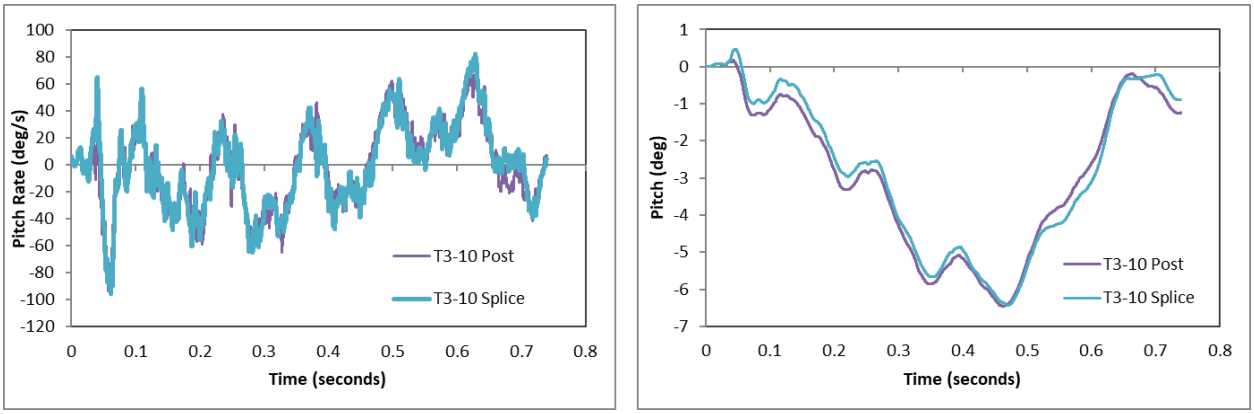

Figure 24. Pitch rate and pitch angle time-history from FEA of Test 3-10.

Table 5. Summary of MASH occupant risk metrics for Test 3-10.

Occupant Risk Factors		MASH Test 3-10	
		T3-10 Post	T3-10 Splice
Occupant Impact Velocity (ft/s)	x-direction	22.6	22.3
	y-direction	29.5	29.9
	at time	at 0.0680 seconds on right side of interior	at 0.0678 seconds on right side of interior
THIV (ft/s)		37.1 at 0.0659 seconds on right side of interior	36.7 at 0.0658 seconds on right side of interior
Ridedown Acceleration (g's)	x-direction	-4 (0.0680 - 0.0780 seconds)	-5.6 (0.0678 - 0.0778 seconds)
	y-direction	-13.9 (0.1705 - 0.1805 seconds)	-13.9 (0.1709 - 0.1809 seconds)
PHD (g's)		14 (0.1704 - 0.1804 seconds)	13.9 (0.1709 - 0.1809 seconds)
ASI		2.57 (0.0373 - 0.0873 seconds)	2.55 (0.0370 - 0.0870 seconds)
Max 50-ms moving avg. acc. (g's)	x-direction	-13.6 (0.0065 - 0.0565 seconds)	-13.2 (0.0081 - 0.0581 seconds)
	y-direction	-17.9 (0.0087 - 0.0587 seconds)	-17.6 (0.0089 - 0.0589 seconds)
	z-direction	-3.2 (0.0173 - 0.0673 seconds)	-2.9 (0.0036 - 0.0536 seconds)
Maximum Angular Disp. (deg)	Roll	9.2 (0.3163 seconds)	9.9 (0.3074 seconds)
	Pitch	-6.5 (0.4628 seconds)	-6.4 (0.4700 seconds)
	Yaw	-34.2 (0.4158 seconds)	-34.5 (0.4569 seconds)

MASH Criteria

< 30 ft/s (preferred) ✓
< 40 ft/s (limit)

< 15 G (preferred) ✓
< 20.49 G (limit)

< 75 deg ✓

The peak 10-ms running average accelerations in the longitudinal direction were approximately -26.2 G and -25.0 G for rail splice and critical post CIP cases, respectively, as shown in Figure 19. The peak lateral acceleration was approximately -37.0 G and -36.6 G for rail splice and critical post CIP cases, respectively, as shown in Figure 20. The occupant impact velocity (OIV) in the longitudinal direction was 22.3 ft/s and 22.6 ft/s for rail splice and critical post CIP cases, respectively. The OIV in the lateral direction was 29.9 ft/s and 29.5 ft/s for rail splice and critical post CIP cases, respectively. The highest occupant ridedown acceleration (ORA) in the longitudinal direction was -5.6 G and -4.0 G for rail splice and critical post CIP cases, respectively. The highest ORA in the lateral direction was -13.9 G for both cases. The maximum roll angle was 9.9 degrees and 9.2 degrees for rail splice and critical post CIP cases, respectively. The maximum pitch angle was -6.4 degrees and -6.5 degrees (rear pitching upward) for rail splice and critical post CIP cases, respectively. The OIV and ORA were within the preferred limits recommended in MASH.

Damages to the Barrier System

CIP for Rail Splice and Critical Post

Figure 25 shows the maximum deflection of the barrier with a contour plot for lateral displacement on the steel railing components. The maximum dynamic deflection was 0.92

inches and 0.98 inches for rail splice and critical post CIP cases, respectively, and occurred on the railing near the splice. The maximum deflection occurred at 0.05 seconds for both cases, during impact with the front corner of the vehicle. The maximum permanent deflection was 0.36 inches for both cases.

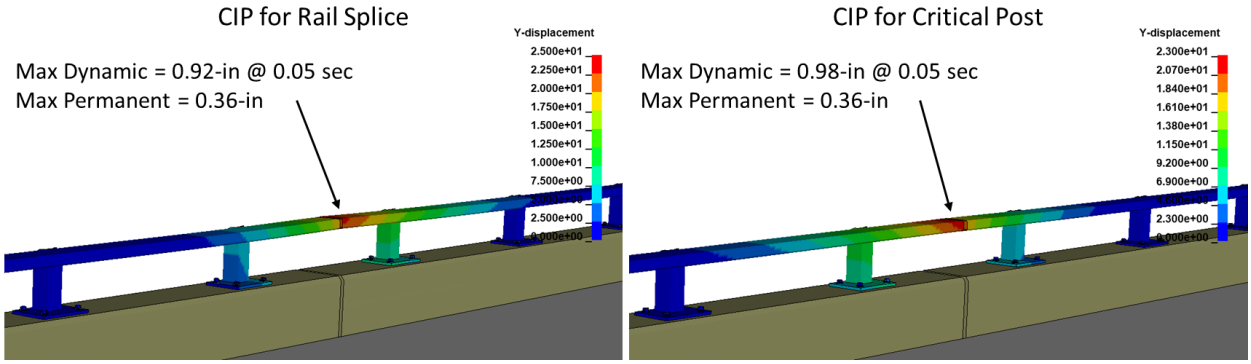

Figure 25. Contour plot of lateral displacement for Test 3-10.

Recall that one of the design revisions included an increase in diameter for the anchor-bolt hole in the base plate. This resulted in a lateral translation of the base plates that were located immediately upstream and downstream of the impact point as they slid back and closed the gap between the edge of the plate-holes and the anchor bolts. The deflection-time history plots for the base plates are shown in Figure 26. The maximum dynamic deflection was 0.33 inches and 0.25 inches for rail splice and critical post CIP cases, respectively.

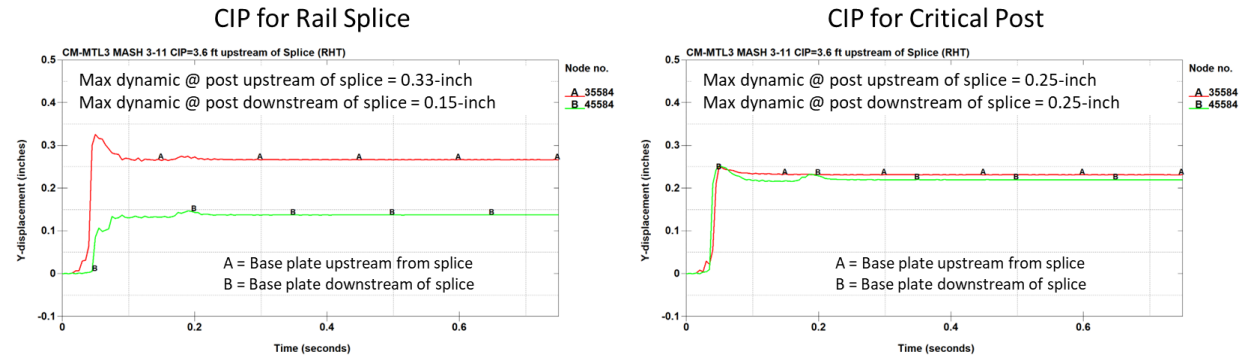

Figure 26. Deflection-time history of the base plates for Test 3-10.

Figure 27 shows a contour plot of effective plastic strain on the splice components, the maximum values were 0.004 and 0.008 for rail splice and critical post CIP cases, respectively. For the rail splice CIP case, the maximum plastic strain occurred at the lower edge of the flange on the splice bar on impact side. For the critical post CIP case, the maximum plastic strain occurred on the leading edge of downstream main rail on the traffic side. Figure 28 shows effective plastic strain contours for the weld regions at the top of the post. The maximum values were 0.01 for both cases. These values are considered minimal for the steel components of the barrier.

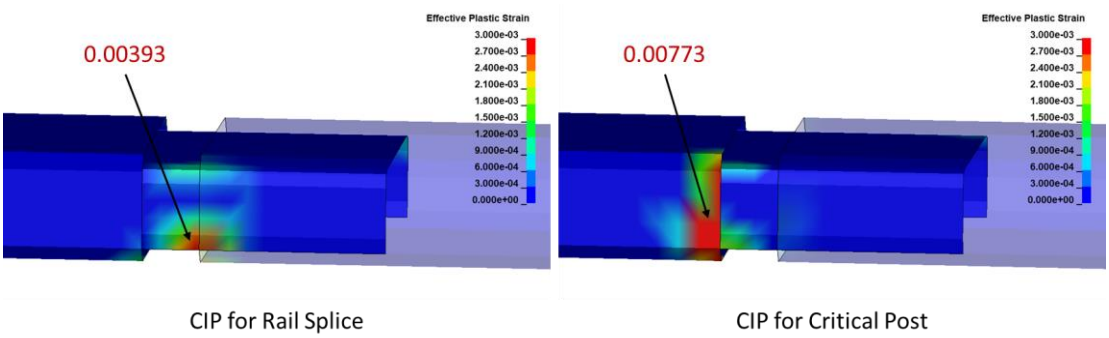

Figure 27. Effective plastic strain contours for the splice components for Test 3-10.

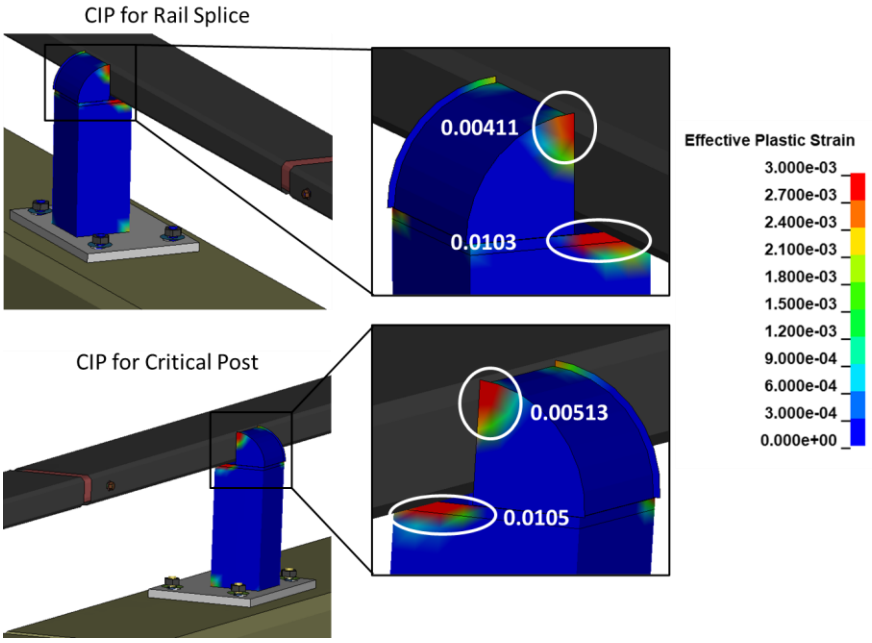

Figure 28. Effective plastic strain contours at critical welds for Test 3-10.

Figure 29 shows contour plots of the damage parameter computed in LS-DYNA for the concrete barrier. The results indicated a potential for concrete spalling on the front face of barrier but little to no potential for any major damage or cracks.

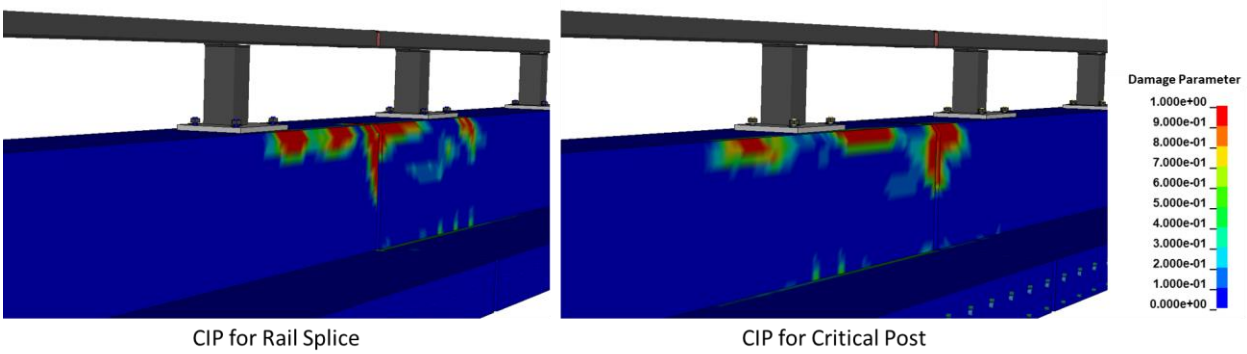

Figure 29. Contour plot of the damage variable for Test 3-10.

Damages to Vehicle

Figure 30 shows contour plots of effective plastic strain for the vehicle during Test 3-10 for CIP relative to the expansion splice and the critical post. The damages to the vehicle were limited to the impact side of the front cap, the front impact-side wheel assembly, leading edge of the front door, rear quarter panel, edge of windshield on impact side, and side windows. The damages to the side windows and windshield were not caused by direct contact with the barrier. The vehicle model, in these cases, did not include failure criteria for wheel joints or steering joints; however, with the extent of damage to the wheel assembly, it is likely that one or more of these joints are likely to fail.

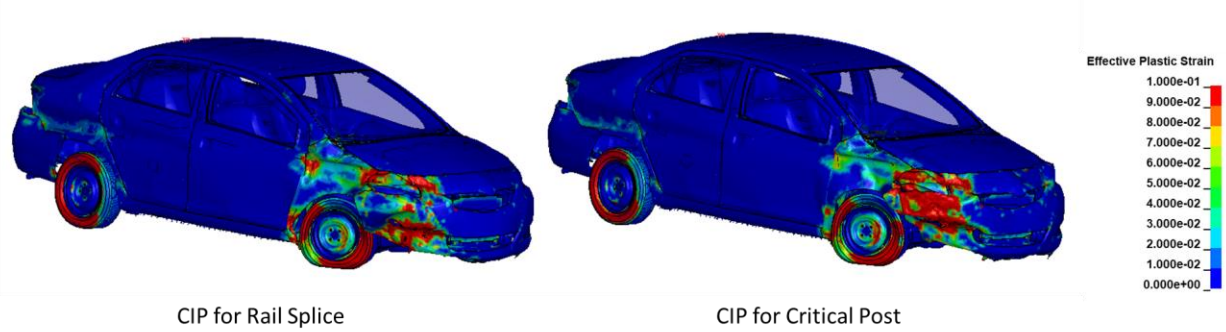

Figure 30. Damages to vehicle in Test 3-10.

Occupant Compartment Intrusion

CIP for Splice and Critical Post

The maximum deformation of the occupant compartment was 3.76 inches and 4.12 inches for Test 3-10 for rail splice and critical post CIP cases, respectively. The maximum deformation occurred at the right-front toe pan at the wheel well for both cases. Figure 31 shows a post-impact view of the vehicle floor pan with all other components removed to facilitate viewing. The maximum deformation was less than the critical limit of 9 inches specified in *MASH* for this area of the occupant compartment.

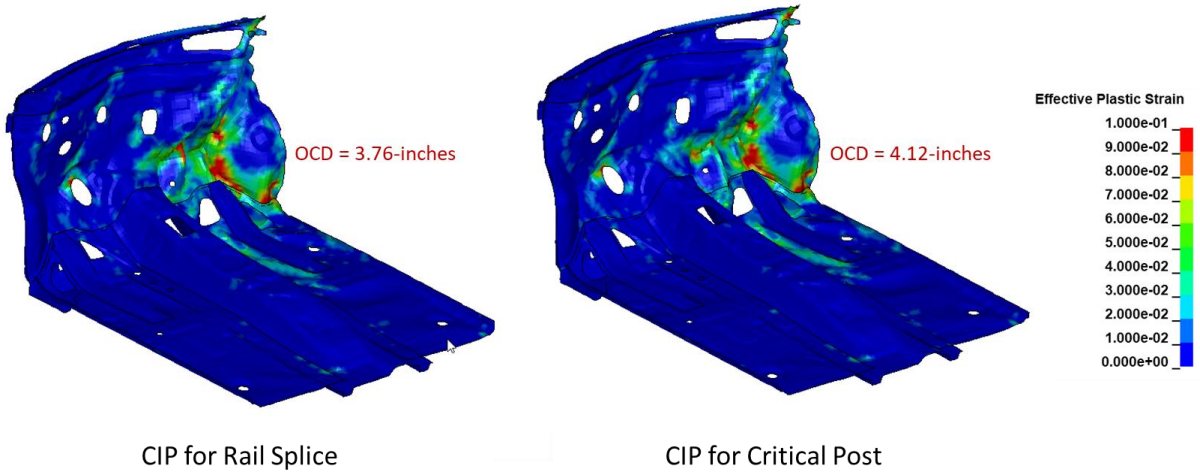

Figure 31. Occupant compartment deformation resulting from Test 3-10.

Exit Box

Figure 32 show the exit box for Test 3-10 for CIP relative to critical post and expansion splice, respectively. The post trajectory response was similar for both cases, and the vehicle was redirected with its path well within the exit box criteria of *MASH*.

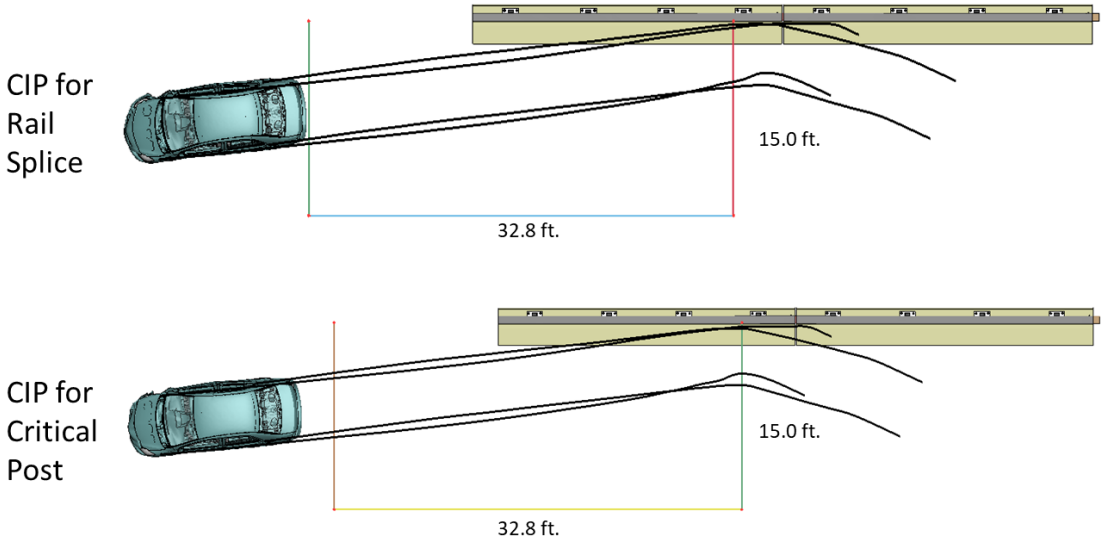

Figure 32. Exit box for Test 3-10.

Test 3-10 Results Summary

A summary of *MASH* Test 3-10 results for the CM-MTL3 with proposed design revisions is shown is shown in Table 6. The bridge rail successfully contained and redirected the small car with minimal damage to the concrete barrier and steel rail components. There were no detached elements from the barrier that showed potential for penetrating into the occupant compartment or presenting undue hazard to other traffic. The vehicle remained upright and did not experience excessive roll or pitch angle displacements. The OIV and maximum ORA values were within critical limits specified in *MASH*. Based on the results of this analysis, the barrier is expected to meet all structural and occupant risk criteria in *MASH* for Test 3-10 impact conditions.

Table 6. Summary of *MASH* Test 3-10 for the CM-MTL3 with proposed design revisions.

Evaluation Factors		Evaluation Criteria	Splice Reference	Post Reference
Structural Adequacy	A	Test article should contain and redirect the vehicle or bring the vehicle to a controlled stop; the vehicle should not penetrate, underride, or override the installation although controlled lateral deflection of the test article is acceptable.	Pass	Pass
Occupant Risk	D	Detached elements, fragments, or other debris from the test article should not penetrate or show potential for penetrating the occupant compartment, or present undue hazard to other traffic, pedestrians, or personnel in a work zone. Deformations of, or intrusions into, to occupant compartment should not exceed limits set forth in Section 5.2.2 and Appendix E.	Pass	Pass
	F	The vehicle should remain upright during and after collision. The maximum roll and pitch angles are not to exceed 75 degrees.	Pass	Pass
	H	The longitudinal and lateral occupant impact velocity (OIV) shall not exceed 40 ft/s (12.2 m/s), with a preferred limit of 30 ft/s (9.1 m/s)	Pass	Pass
	I	The longitudinal and lateral occupant ridedown acceleration (ORA) shall not exceed 20.49 G, with a preferred limit of 15.0 G	Pass	Pass

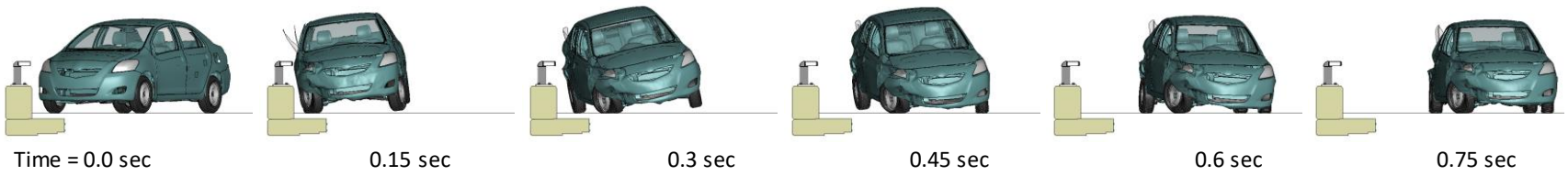

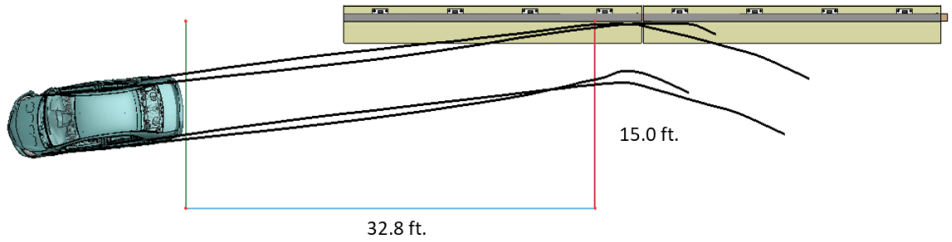

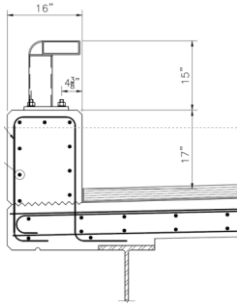

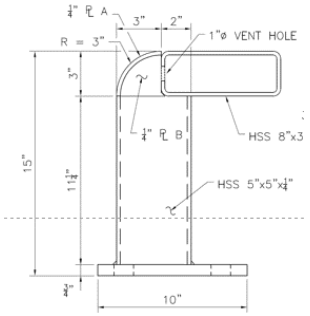

General Information

Analysis Agency	Roadsafe LLC
Test Standard Test No.	MASH Test 3-10
Analysis No.	CM-MTL3_IP01-Splice
Analysis Date	1/13/2023

Test Article

Type	Bridge Rail
Name	CM-MTL3
Installation Length	48.0 feet
Material or Key Elements	Continuous concrete with top mounted steel post-and-beam rail
Soil Type and Condition	NA

Analysis Vehicle

Type / Designation	1100C
FEA Model name	YarisC_V1l_R200522.k w/ RS tire
Mass	2,595 lb

Impact Conditions

Speed	62.2 mph
Angle	25 degrees
Location	3.6 ft upstream of splice
Impact Severity	59.8 kip-ft

Exit Conditions

Speed	44.2 mph
Angle	8.2 degrees
Time	0.27 seconds

Occupant Risk Values

Longitudinal OIV	22.3 ft/s
Lateral OIV	29.9 ft/s
Longitudinal ORA	5.6 g
Lateral ORA	13.9 g
THIV	36.7 ft/s
PHD	13.9 g
ASI	2.55

Max50-millisecond Avg. (G)

Longitudinal	13.2 g
Lateral	17.6 g
Vertical	2.9 g

Test Article Deflections (in)

Dynamic	0.92 inches
Permanent	0.36 inches
Working Width	16.0 inches
Max. OCD	3.76 inches

Vehicle Stability

Roll	9.9 degees
Pitch	6.4 degrees
Yaw	34.5 degrees

Figure 33. Summary results for MASH Test 3-10 on the CM-MTL3 for CIP relative to Rail Splice.

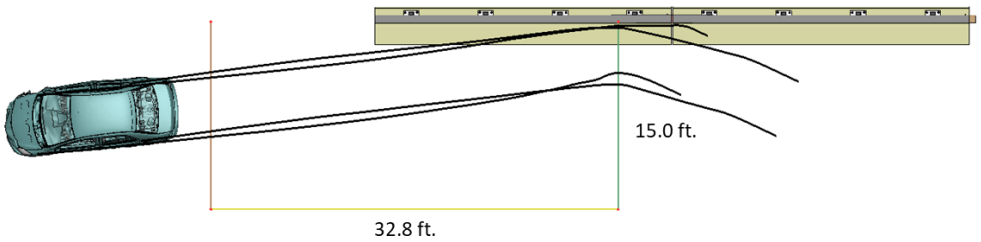

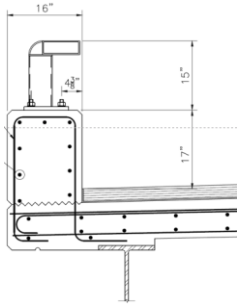

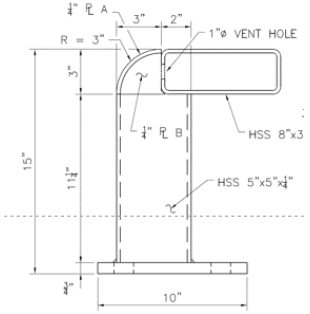

General Information

Analysis Agency	Roadsafe LLC
Test Standard Test No.	MASH Test 3-10
Analysis No.	CM-MTL3_IP02-Post
Analysis Date	1/13/2023

Test Article

Type	Bridge Rail
Name	CM-MTL3
Installation Length	48.0 feet
Material or Key Elements	Continuous concrete with top mounted steel post-and-beam rail
Soil Type and Condition	NA

Analysis Vehicle

Type / Designation	1100C
FEA Model name	YarisC_V1I_R200522.k w/ RS tire
Mass	2,595 lb

Impact Conditions

Speed	62.2 mph
Angle	25 degrees
Location	3.6 ft upstream of post
Impact Severity	59.8 kip-ft

Exit Conditions

Speed	44.0 mph
Angle	8.2 degrees
Time	0.28 seconds

Occupant Risk Values

Longitudinal OIV	22.6 ft/s
Lateral OIV	29.5 ft/s
Longitudinal ORA	4.0 g
Lateral ORA	13.9 g
THIV	37.1 ft/s
PHD	14.0 g
ASI	2.57

Max50-millisecond Avg. (G)

Longitudinal	13.6 g
Lateral	17.9 g
Vertical	3.2 g

Test Article Deflections (in)

Dynamic	0.98 inches
Permanent	0.36 inches
Working Width	16.0 inches
Max. OCD	4.12 inches

Vehicle Stability

Roll	9.2 degees
Pitch	6.5 degrees
Yaw	34.2 degrees

Figure 34. Summary results for MASH Test 3-10 on the CM-MTL3 for CIP relative to Critical Post.

Test 3-11 with CIP for Expansion Splice and Critical Post

Simulation of Test 3-11 included the 2270P Dodge Ram model ballasted to 5,182 lb (2,351 kg) impacting the railing at 62.2 mph and 25 degrees. Two critical impact cases were evaluated:

- Splice Reference Case - involved impact point at 4.3 ft upstream from the splice connection to maximize the potential for snagging at the splice and
- Post Reference Case - involved impact point at 4.3 ft upstream of the critical post (i.e., immediately downstream of expansion joint and rail splice) to maximize the potential for snagging on the post. Each of the impact points are illustrated in Figure 35.

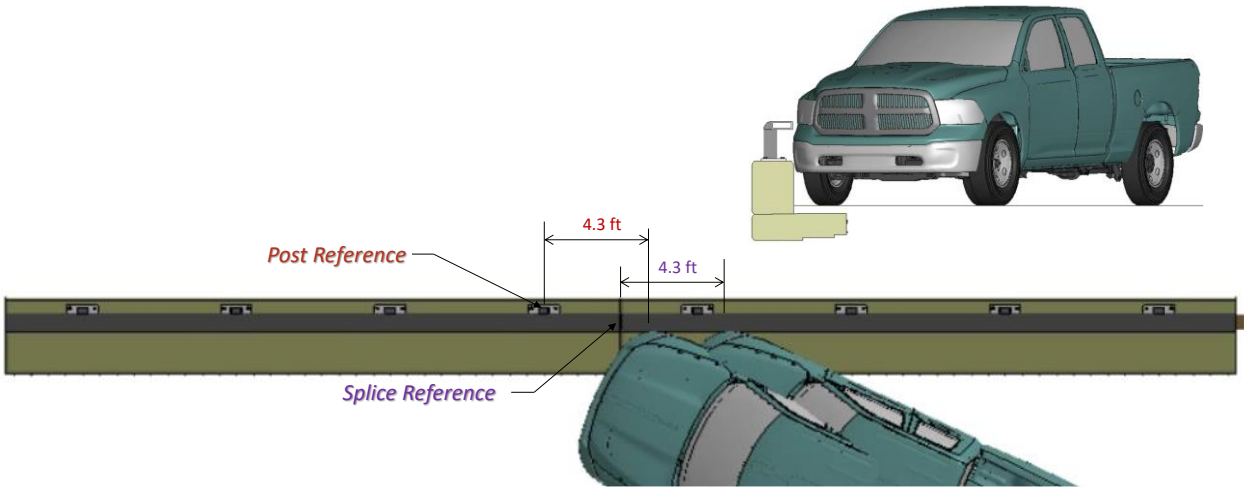

Figure 35. Critical impact points evaluated for Test 3-11.

Summary of Crash Event

CIP for Rail Splice and Critical Post

The 5,182-lb pickup model struck the face of the barrier at 4.3 feet upstream of the rail splice at a speed of 62.2 mph and at an angle of 25 degrees. The sequential views of the impact event with CIP relative to the splice are shown in Appendix D. The sequential views of the impact event with CIP relative to the critical posts are shown in Appendix E. Additional details regarding the sequence of key events for these two analysis cases are provided in Table 7. The following sections provide time-history data evaluation, occupant risk assessments, and damages sustained by the barrier and vehicle.

Table 7. Sequence of events for Test 3-11.

Event		Expansion Splice	Critical Post
1	Initial contact with barrier Right front fender and right front tire impacts vertical wall @ post 4	0.01 sec Impact speed = 62.2 mph Impact angle = 25 deg	0.01 sec Impact speed = 62.2 mph Impact angle = 25 deg
2	Right front wheel starts to climbs vertical face of barrier	0.030 sec	0.03 sec
3	Front right tire deflates	0.041 - 0.071 sec	0.038 - 0.071 sec
4	Peak 50-ms average x-acceleration	-10.3 G @ 0.0251 - 0.0751 sec	-10.5 G @ 0.0261 - 0.0761 sec
5	Peak 50-ms average y-acceleration	-12.5 G @ 0.0433 - 0.0933 sec	-13.0 G @ 0.0392 - 0.0892 sec
6	Vehicle contacts critical splice - no snag	0.05 sec	0.025 sec(*)
7	Vehicle begins to yaw counterclockwise	≈ 0.06 sec	≈ 0.06 sec
8	Maximum dynamic barrier deflection occurs at splice	0.09 sec 1.41 in	0.08 sec 1.13 in
9	Wheel rim crossed expansion joint gap	≈ 0.09 sec (gouge w/spalling)	≈ 0.05 sec (no snag)(*)
10	Max positive pitch (front pitched upward)	≈ 5.5 deg @ 0.0780 sec (*)	≈ 5.3 deg @ 0.0803 sec
11	Occupant impact with vehicle interior	0.0996 sec OIV-x = 23.0 ft/s OIV-y = 26.6 ft/s	0.0987 sec OIV-x = 23.0 ft/s OIV-y = 27.2 ft/s
12	Maximum occupant compartment intrusion. Maximum OCI Location Maximum OCI Magnitude	0.105 sec Right front toe pan 7.34 in (pernament)	0.100 sec Right front toe pan 7.77 in (permanent)
13	Left front wheel leaves the ground	0.11 sec	0.11 sec
14	Left rear wheel leaves the ground	0.13 sec	0.13 sec
15	Front tire at critical post - no contact with post	0.13 sec	0.095 sec(*)
16	Tail slap with barrier Right rear fender and right rear tire impacts vertical wall	0.22 sec (*) Speed = 44.0 mph	0.22 sec Speed = 44.3 mph
17	Vehicle parallel with barrier	0.225 sec	0.22 sec
18	Maximum ORA-y	12.1 G @ 0.2355 - 0.2455 sec	11.8 G @ 0.2298 - 0.2398 sec
19	Maximum ORA-x	6.5 G @ 0.4010 - 0.4110 sec(*)	4.4 G @ 0.2206 - 0.2306 sec
20	Rear right tire deflates	0.243 - 0.352 sec sec	0.235 - 0.320 sec
21	Max negative pitch (front pitched downward)	≈ -2.3 deg @ 0.40 sec (*)	≈ -1.5 deg @ 0.42 sec
22	Max positive roll (top of vehicle toward barrier)	≈ 7.2 deg @ 0.40 sec	≈ 8.3 deg @ 0.45 sec
23	Left front wheel returns to ground	0.41 sec	0.44 sec(*)
24	Vehicle body exits barrier	0.42 sec Exit speed = 40.6 mph Exit angle = -9.7 deg	0.42 sec(*) Exit speed = 41.6 mph Exit angle = -9.6 deg
25	Right front wheel returns to ground	0.425 sec	0.35 sec (*)
26	Right rear wheel leaves the ground	NA	0.55 sec
27	Right rear wheel returns to ground	NA	0.60 sec
28	Left rear wheel returns to ground	0.635 sec	0.65 sec
29	Analysis Terminated	0.75 sec Speed = 38.8 mph Yaw angle = -39.9 deg (total angle) Roll angle = -3.0 deg (away from barrier) Pitch angle = 1.8 deg (rear pitched down)	0.75 sec Speed = 39.5 mph Yaw angle = -40.8 deg (total angle) Roll angle = -0.7 deg (away from barrier) Pitch angle = 1.6 deg (rear pitched down)

(*) *Out of sequence*

Time History Plots and Occupant Risk Measures

Figure 36 through Figure 38 show the longitudinal, transverse, and vertical acceleration-time histories, respectively, computed from the center of gravity of the vehicle; Figure 39 through Figure 41 show the comparison of the angular rates and angular displacements (i.e., yaw, roll, and pitch) at the center of gravity of the vehicle. Table 8 shows the results for the occupant risk calculations for the two cases.

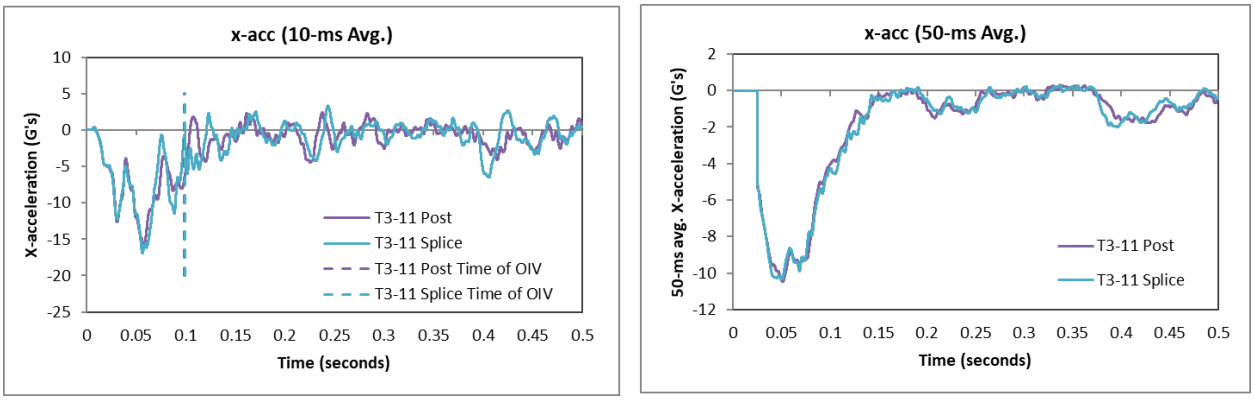

Figure 36. 10- and 50-millisecond average X-acceleration from FEA of Test 3-11.

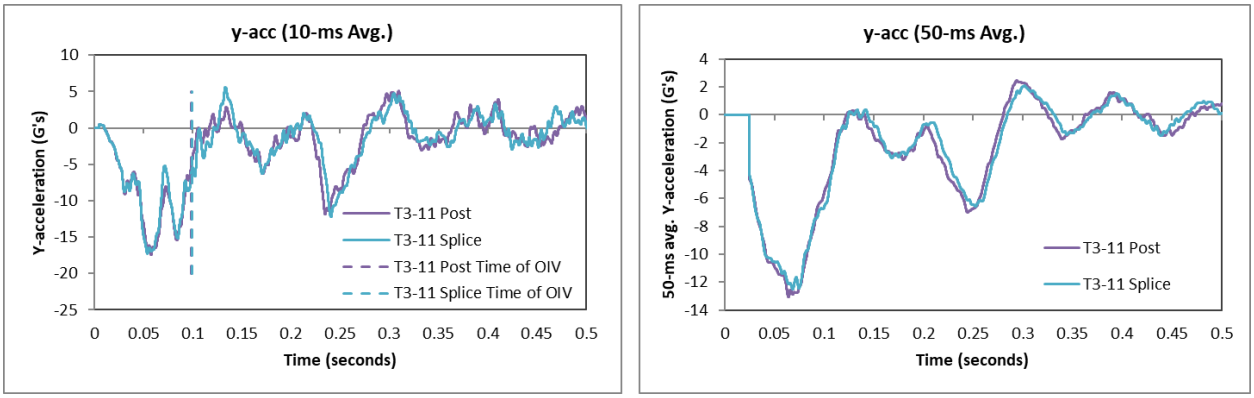

Figure 37. 10- and 50-millisecond average Y-acceleration from FEA of Test 3-11.

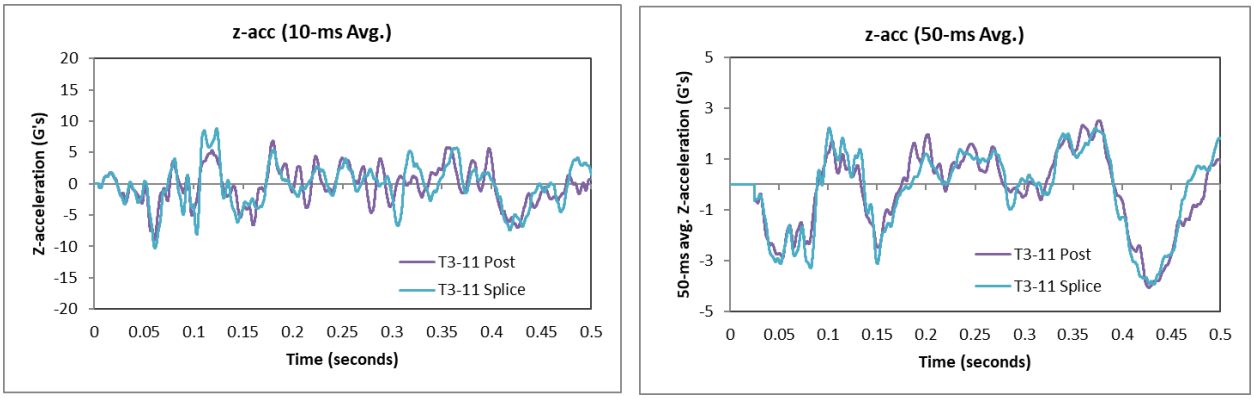

Figure 38. 10- and 50-millisecond average Z-acceleration from FEA of Test 3-11.

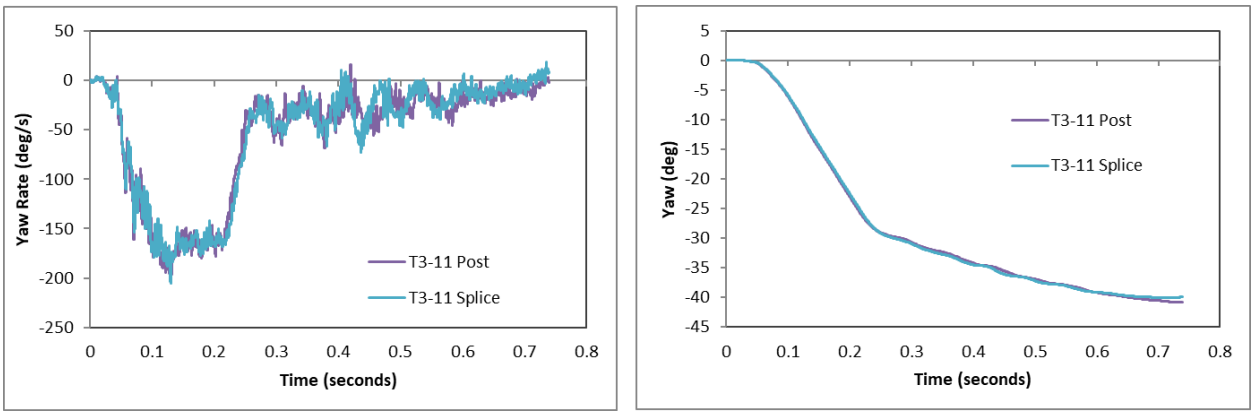

Figure 39. Yaw rate and yaw angle time-history from FEA of Test 3-11.

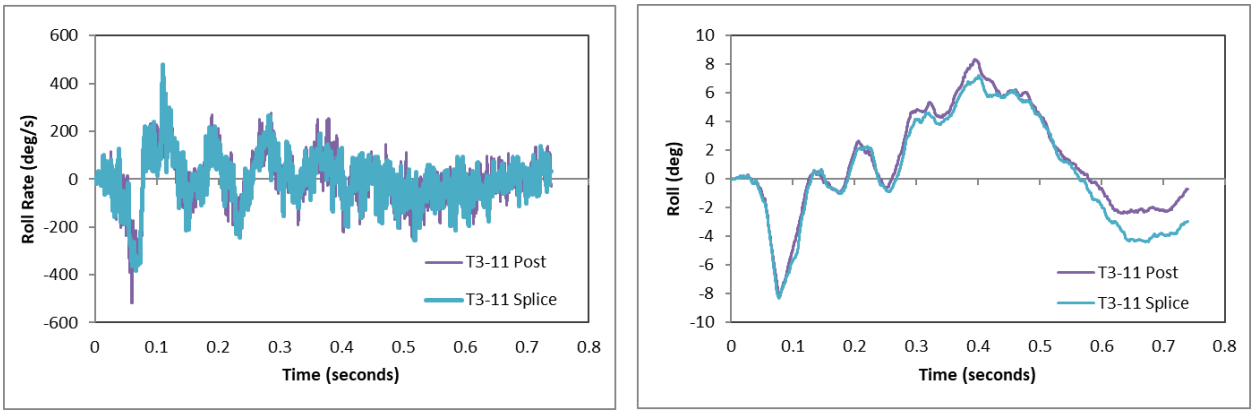

Figure 40. Roll rate and roll angle time-history from FEA of Test 3-11.

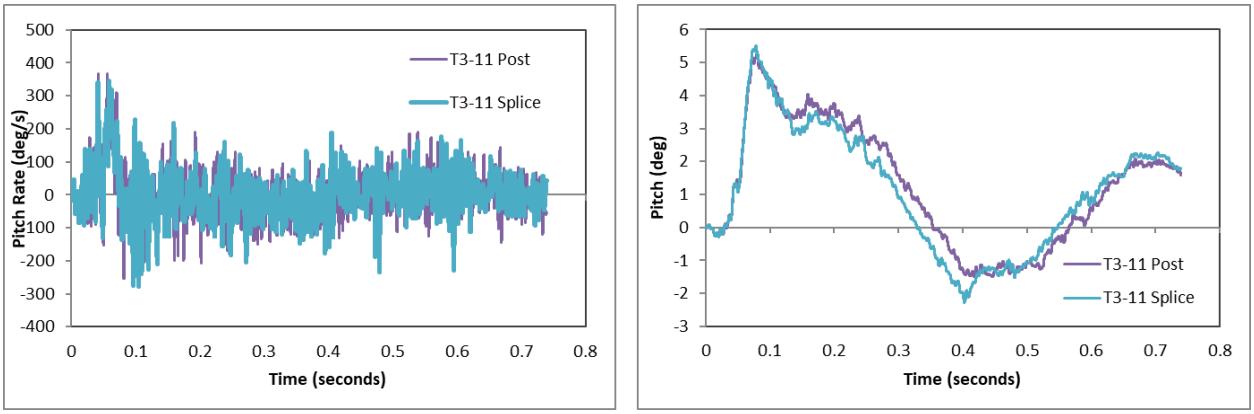

Figure 41. Pitch rate and pitch angle time-history from FEA of Test 3-11.

CIP for Rail Splice and Critical Post

The peak 10-ms running average acceleration was 16.1 G and 16.0 G in the longitudinal direction for CIP relative to rail splice and critical post, respectively, and was 16.7 G and 16.5 G, respectively, in the lateral direction, as shown in Figure 36, Figure 37, and Table 8. The OIV values in the longitudinal direction were 23.0 ft/s for both cases; the occupant impact velocity in the lateral direction was 26.6 ft/s and 27.2 ft/s for CIP relative to splice and critical post, respectively. The maximum ORA in the longitudinal direction was -6.5 g and -4.4 g for CIP

relative to splice and critical post, respectively; the maximum ORA in the lateral direction was -12.2 g and -11.8 g for CIP relative to splice and critical post, respectively. The first peak roll angle occurred at approximately 0.078 seconds with magnitude 8.3 degrees and 8.0 degrees away from barrier for CIP relative to splice and critical post, respectively. This event marked the maximum roll angle for the rail splice CIP case; however, in both cases the floor of the truck deformed slightly at the accelerometer mounting causing the accelerometer to tilt. The sequential views shown in Appendix D and E indicate that the roll angle during this time-period was minimal. A second peak roll angle occurred during post trajectory at approximately 0.4 seconds with magnitude 7.2 degrees and 8.3 toward the barrier for the two cases, respectively. This event marked the maximum roll angle for the critical post CIP case. The maximum pitch angle of the vehicle occurred at approximately 0.08 seconds during impact with the barrier with magnitude 5.5 degrees and 5.3 degrees (rear pitching up) for CIP relative to splice and critical post, respectively. All occupant risk metrics were within the preferred limits of *MASH*.

Table 8. Summary of MASH occupant risk metrics for Test 3-11.

Occupant Risk Factors		MASH Test 3-11	
		T3-11 Post	T3-11 Splice
Occupant Impact Velocity (ft/s)	x-direction	23.0	23.0
	y-direction	27.2	26.6
	at time	at 0.0987 seconds on right side of interior	at 0.0996 seconds on right side of interior
THIV (ft/s)		35.1 at 0.0962 seconds on right side of interior	33.8 at 0.0968 seconds on right side of interior
Ridedown Acceleration (g's)	x-direction	-4.4 (0.2206 - 0.2306 seconds)	-6.5 (0.4010 - 0.4110 seconds)
	y-direction	-11.8 (0.2298 - 0.2398 seconds)	-12.2 (0.2355 - 0.2455 seconds)
PHD (g's)		11.8 (0.2298 - 0.2398 seconds)	12.3 (0.2356 - 0.2456 seconds)
ASI		1.76 (0.0605 - 0.1105 seconds)	1.72 (0.0592 - 0.1092 seconds)
Max 50-ms moving avg. acc. (g's)	x-direction	-10.5 (0.0261 - 0.0761 seconds)	-10.3 (0.0251 - 0.0751 seconds)
	y-direction	-13 (0.0392 - 0.0892 seconds)	-12.5 (0.0433 - 0.0933 seconds)
	z-direction	-4.1 (0.4023 - 0.4523 seconds)	-3.9 (0.4071 - 0.4571 seconds)
Maximum Angular Disp. (deg)	Roll	8.3 (0.3952 seconds)	-8.3 (0.0775 seconds)
	Pitch	5.3 (0.0803 seconds)	5.5 (0.0780 seconds)
	Yaw	-40.8 (0.7325 seconds)	-40.1 (0.7064 seconds)

MASH Criteria

< 30 ft/s (preferred) ✓
< 40 ft/s (limit)

< 15 G (preferred) ✓
< 20.49 G (limit)

< 75 deg ✓

Damages to the Barrier System

CIP for Rail Splice and Critical Post

Figure 42 shows images of maximum deflection of the barrier with a contour plot for lateral displacement on the steel railing components. The maximum dynamic deflection was

1.41 inches and 1.13 inches for CIP relative to splice and critical post, respectively, and occurred at the splice for both cases. The maximum deflection occurred at 0.09 seconds CIP relative to splice, and at 0.08 seconds for CIP relative to critical post during impact with the front corner of the vehicle. The maximum permanent dynamic deflection was 0.50 inches and 0.41 inches for CIP relative to splice and critical post, respectively.

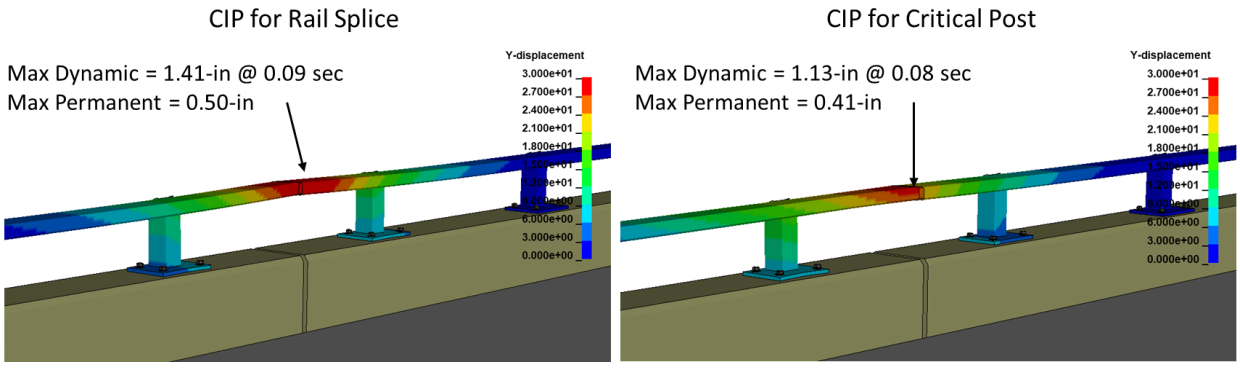

Figure 42. Contour plot of lateral displacement for Test 3-11.

The baseplates immediately upstream and downstream of the impact point slid back during impact due to the over-sized anchor-bolt holes. The deflection-time history plots are shown in Figure 43. The maximum dynamic deflection was 0.31 inches and 0.30 inches for CIP relative to splice and critical post, respectively, and occurred at the upstream base plate for CIP relative to splice and the downstream base plate for CIP relative to post.

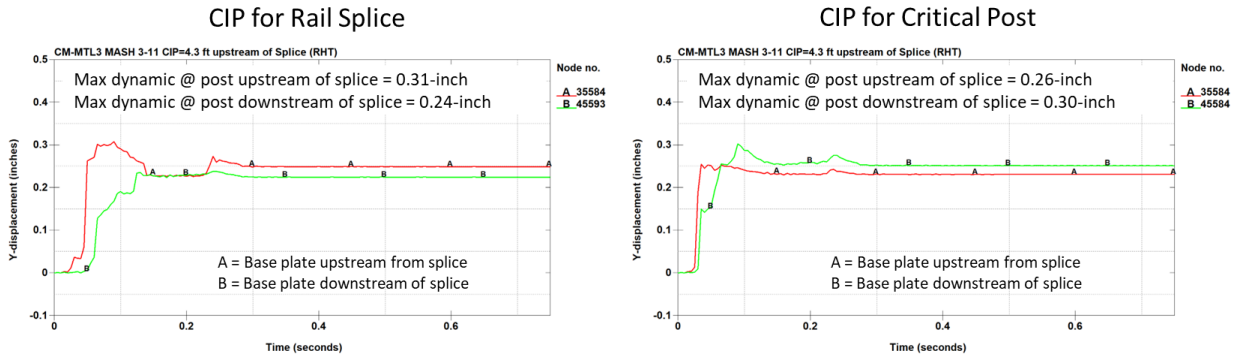

Figure 43. Deflection-time history of the base plates for Test 3-11.

Figure 44 shows a contour plot of effective plastic strain on the splice components. The maximum plastic strain values were 0.03 for CIP relative to splice, and 0.01 for CIP relative to critical post and occurred at the lower edge of the flange of the splice bar and at the leading edge of downstream main rail. Figure 45 shows effective plastic strain contours at the top of the post, where the highest strains occurred at the weld regions. These values were 0.057 and 0.038 for CIP relative to splice and critical post, respectively, which are negligible for the welds.

Figure 46 shows contour plots of the damage parameter computed in LS-DYNA for the concrete barrier. The results indicate potential spalling on the front face of barrier but low potential for any major damage or cracks.

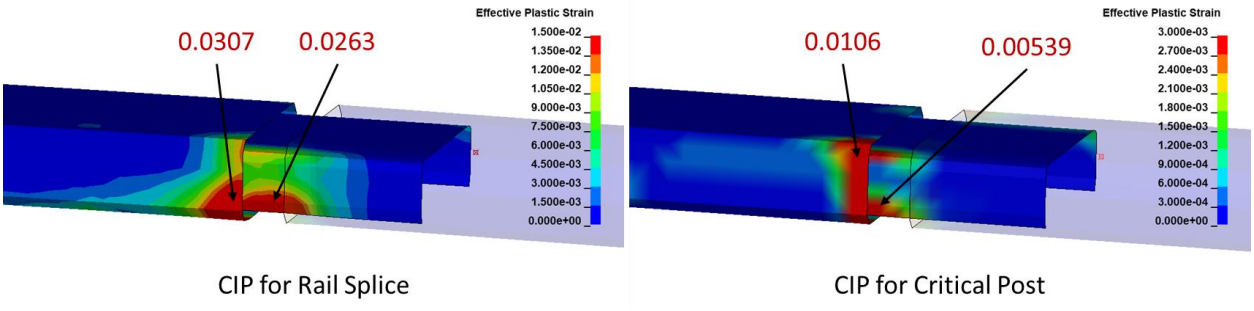

Figure 44. Effective plastic strain contours for the splice components for Test 3-11.

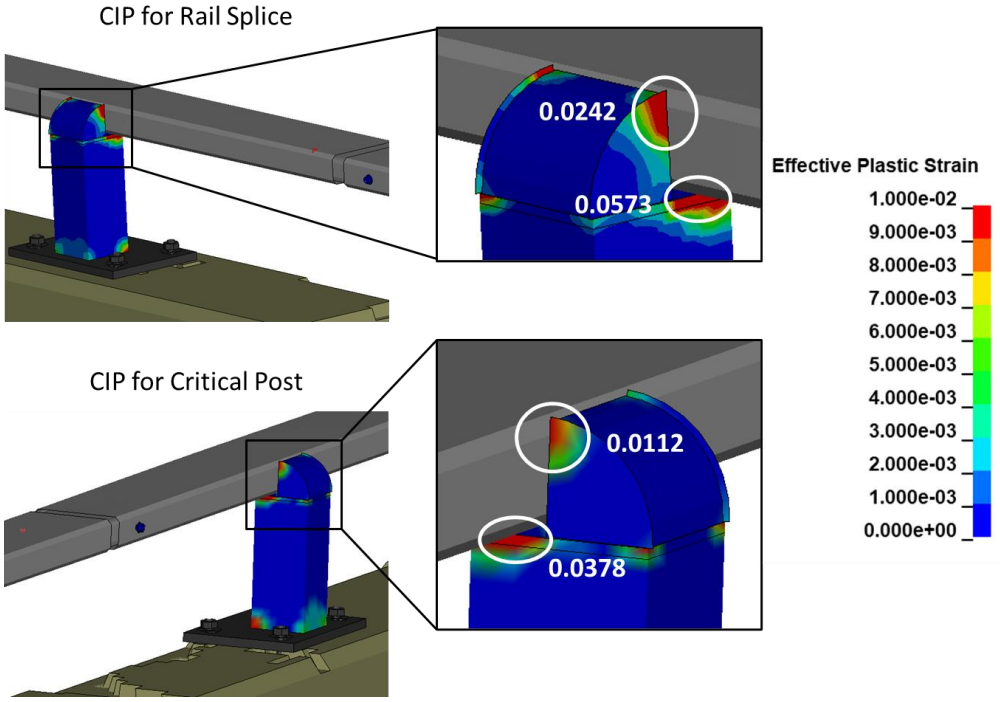

Figure 45. Effective plastic strain contours at critical welds for CIP at splice.

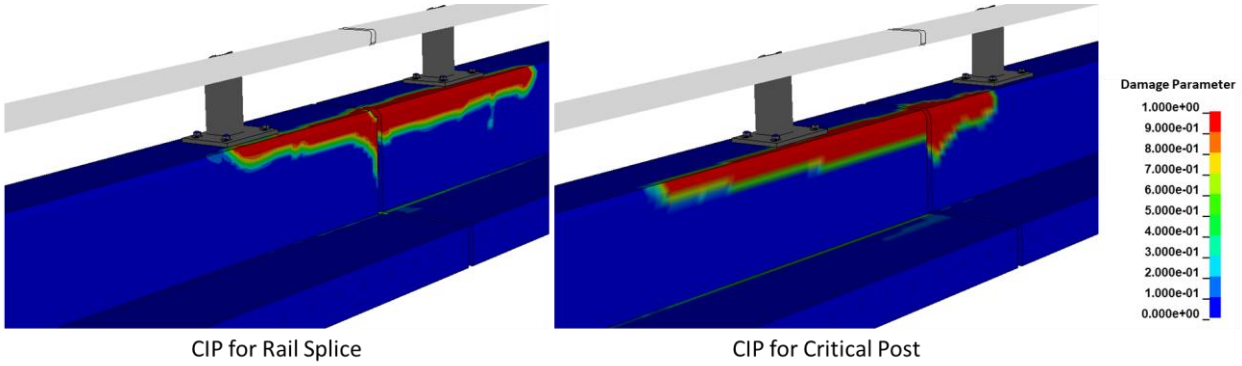

Figure 46. Contour plot of the damage variable for Test 3-11.

Damages to Vehicle

Figure 47 shows contour plots of effective plastic strain for the vehicle during Test 3-11 with CIP relative to the splice and relative to the critical post. The damages to the vehicle were similar for both analysis cases and were limited to the impact side of the vehicle. The damages extended from the front-right corner to the rear bumper. The most significant damages were caused by impact with the concrete barrier and included the front bumper, fender, and the wheel assembly on the impact side. There was also a "crease" that formed along the length of the vehicle which was caused by contact with the steel railing.

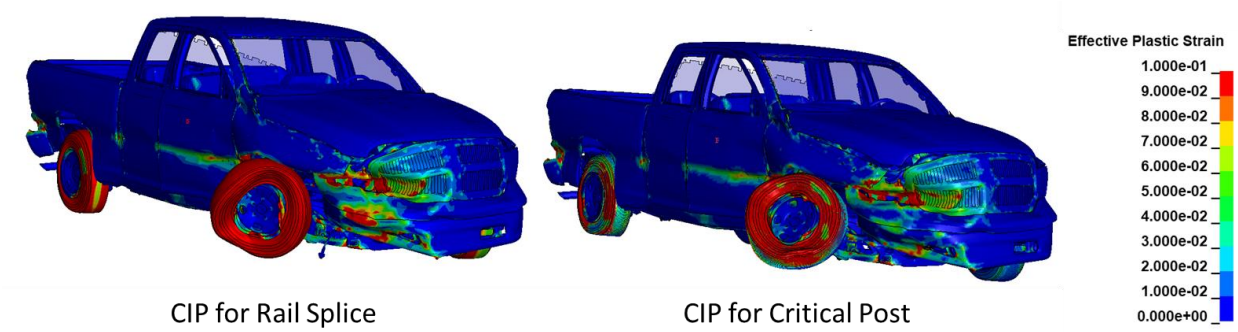

Figure 47. Damages to vehicle in Test 3-11.

Occupant Compartment Intrusion

CIP for Splice and Critical Post

The maximum deformation of the occupant compartment for Test 3-11 was 7.34 inches, for CIP at the splice and 7.77 inches for CIP at critical post. The maximum deformation occurred at the right-front toe pan at the wheel well for both cases. Figure 48 shows a view of the vehicle floor pan after the impact with all other components removed to facilitate viewing. The maximum deformation was less than the critical limit of 9 inches specified in *MASH* for this area of the occupant compartment. However, the magnitude is considered relatively high and, although the model has been shown to be relatively accurate for deformations up to approximately 5.5 inches, the model has not been validated for higher levels of deformation.

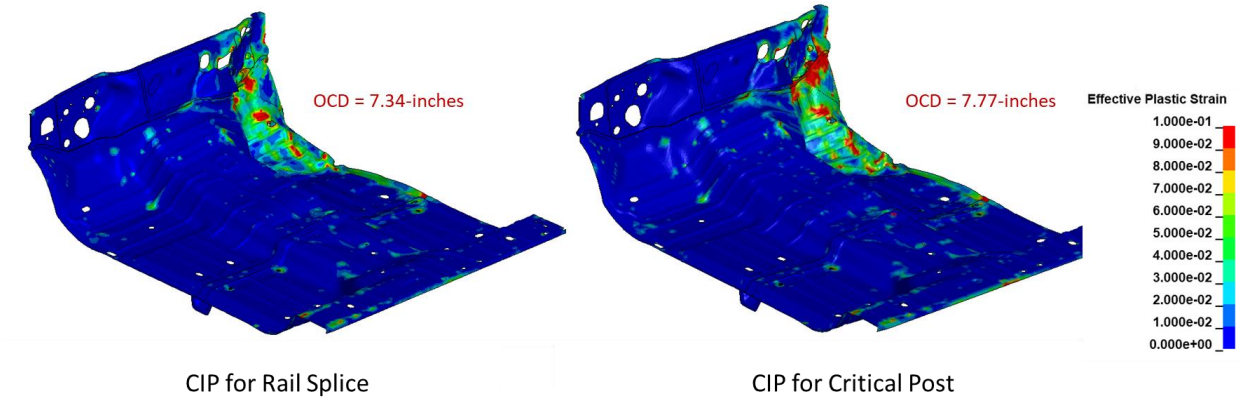

Figure 48. Occupant compartment deformation resulting from Test 3-11.

Exit Box

Figure 49 shows the exit box for Test 3-11 for CIP relative to rail splice and the critical post, respectively. Although the exit box analysis is not required in *MASH*, it was included here for completeness. The post trajectory response was similar for all cases, and the vehicle was redirected with its path well within the exit box criteria of *MASH*.

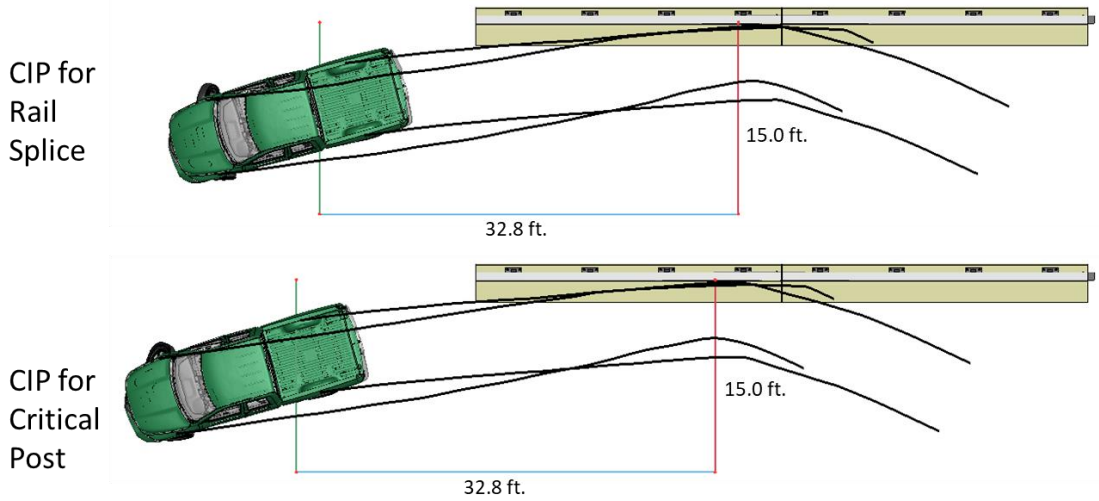

Figure 49. Exit box for Test 3-11.

Test 3-11 Results Summary

A summary of the *MASH* Test 3-11 results for the CM-MTL3 with proposed design revisions is shown in Table 9 and in Figures **Error! Reference source not found.** through **Error! Reference source not found.**. The bridge rail successfully contained and redirected the p ickup with minimal damage to the concrete barrier and moderate damage to the steel rail components. There were no detached elements from the barrier that showed potential for penetrating into the occupant compartment or presenting undue hazard to other traffic. The vehicle remained upright and did not experience excessive roll or pitch angle displacements. The OIV and maximum ORA values were within preferred limits specified in *MASH*. Based on the results of this analysis, the barrier is expected to meet all structural and occupant risk criteria in *MASH* for Test 3-11 impact conditions.

Table 9. Summary of *MASH* Test 3-11 for the CM-MTL3 with proposed design revisions.

Evaluation Factors		Evaluation Criteria	Splice Reference (Contact 1 & 2)	Post Reference (Contact 1)
Structural Adequacy	A	Test article should contain and redirect the vehicle or bring the vehicle to a controlled stop; the vehicle should not penetrate, underride, or override the installation although controlled lateral deflection of the test article is acceptable.	Pass	Pass
Occupant Risk	D	Detached elements, fragments, or other debris from the test article should not penetrate or show potential for penetrating the occupant compartment, or present undue hazard to other traffic, pedestrians, or personnel in a work zone. Deformations of, or intrusions into, to occupant compartment should not exceed limits set forth in Section 5.2.2 and Appendix E.	Pass	Pass
	F	The vehicle should remain upright during and after collision. The maximum roll and pitch angles are not to exceed 75 degrees.	Pass	Pass
	H	The longitudinal and lateral occupant impact velocity (OIV) shall not exceed 40 ft/s (12.2 m/s), with a preferred limit of 30 ft/s (9.1 m/s)	Pass	Pass
	I	The longitudinal and lateral occupant ridedown acceleration (ORA) shall not exceed 20.49 G, with a preferred limit of 15.0 G	Pass	Pass

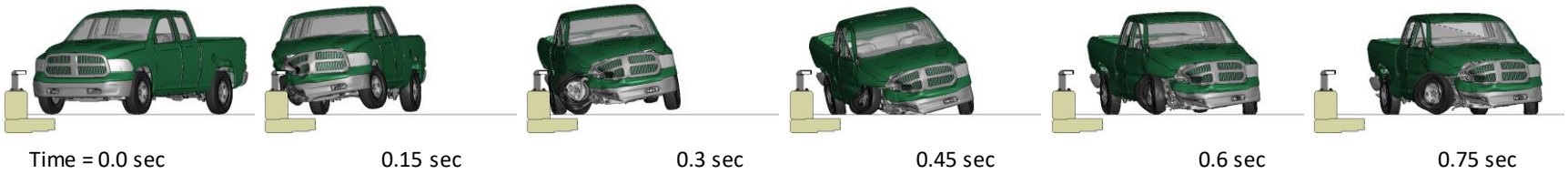

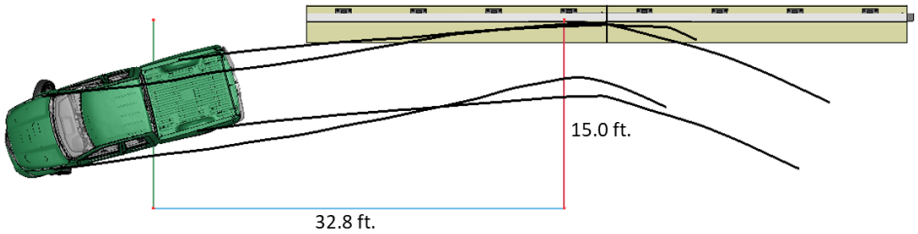

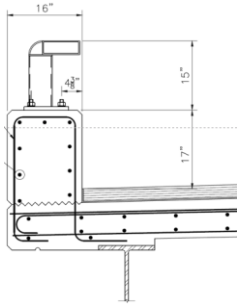

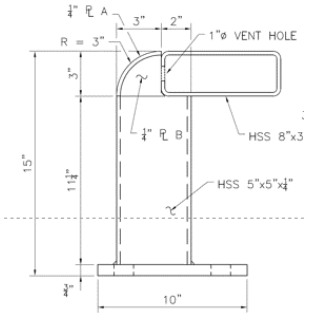

General Information

Analysis Agency	Roadsafe LLC
Test Standard Test No.	MASH Test 3-11
Analysis No.	CM-MTL3_IP01-Splice
Analysis Date	1/13/2023

Test Article

Type	Bridge Rail
Name	CM-MTL3
Installation Length	48.0 feet
Material or Key Elements	Continuous concrete with top mounted steel post-and-beam rail
Soil Type and Condition	NA

Analysis Vehicle

Type / Designation	2270P
FEA Model name	Ram2018C_V2u.k w/RS tire
Mass	5,001 lb

Impact Conditions

Speed	62.2 mph
Angle	25 degrees
Location	4.3 ft upstream of splice
Impact Severity	115.4 kip-ft

Exit Conditions

Speed	40.6 mph
Angle	9.7 degrees
Time	0.42 seconds

Occupant Risk Values

Longitudinal OIV	23.0 ft/s
Lateral OIV	26.6 ft/s
Longitudinal ORA	6.5 g
Lateral ORA	12.2 g
THIV	33.8 ft/s
PHD	12.3 g
ASI	1.72

Max50-millisecond Avg. (G)

Longitudinal	10.3 g
Lateral	12.5 g
Vertical	3.9 g

Test Article Deflections (in)

Dynamic	1.41 inches
Permanent	0.50 inches
Working Width	16.0 inches
Max. OCD	7.34 inches

Vehicle Stability

Roll	8.3 degees
Pitch	5.5 degrees
Yaw	40.1 degrees

Figure 50. Summary results for MASH Test 3-11 on the CM-MTL3 for CIP relative to Rail Splice.

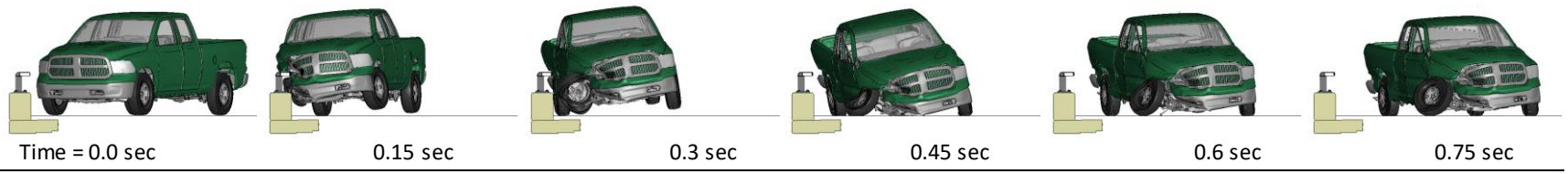

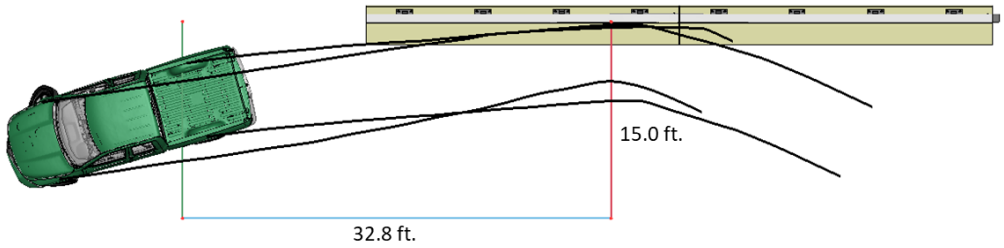

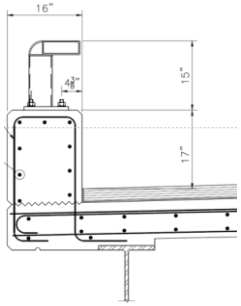

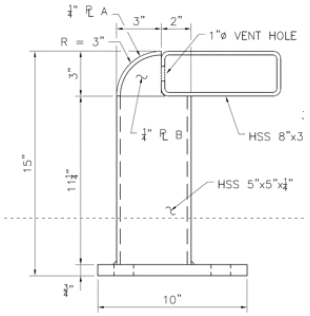

General Information

Analysis Agency	Roadsafe LLC
Test Standard Test No.	MASH Test 3-11
Analysis No.	CM-MTL3_IP02-Post
Analysis Date	1/13/2023

Test Article

Type	Bridge Rail
Name	CM-MTL3
Installation Length	48.0 feet
Material or Key Elements	Continuous concrete with top mounted steel post-and-beam rail
Soil Type and Condition	NA

Analysis Vehicle

Type / Designation	2270P
FEA Model name	Ram2018C_V2u.k w/RS tire
Mass	5,001 lb

Impact Conditions

Speed	62.2 mph
Angle	25 degrees
Location	4.3 ft upstream of post
Impact Severity	115.4 kip-ft

Exit Conditions

Speed	41.6 mph
Angle	9.6 degrees
Time	0.42 seconds

Occupant Risk Values

Longitudinal OIV	23.0 ft/s
Lateral OIV	27.2 ft/s
Longitudinal ORA	4.4 g
Lateral ORA	11.8 g
THIV	35.1 ft/s
PHD	11.8 g
ASI	2.57

Max50-millisecond Avg. (G)

Longitudinal	10.5 g
Lateral	13.0 g
Vertical	4.1 g

Test Article Deflections (in)

Dynamic	1.13 inches
Permanent	0.41 inches
Working Width	16.0 inches
Max. OCD	7.77 inches

Vehicle Stability

Roll	8.3 degees
Pitch	5.3 degrees
Yaw	40.8 degrees

Figure 51. Summary results for MASH Test 3-11 on the CM-MTL3 for CIP relative to Critical Post.

CHAPTER 7 – CONCLUSIONS

The objective of this project was to use finite element analysis (FEA) to evaluate the crash performance of the MassDOT CM-MTL3 bridge rail with the proposed design revisions. The impact conditions and assessment procedures for the evaluations conformed to the specifications in *MASH* for test level 3. Two critical impact cases were evaluated for Test 3-10 and Test 3-11:

- Splice Reference Case – critical impact point for maximizing potential for snag on the rail expansion splice, and
- Post Reference Case – critical impact point for maximizing loading and potential snag on the critical bridge rail post located immediately downstream of the rail splice and expansion joint.

In total, four analysis cases were evaluated, including two cases for Test 3-10 and two cases for Test 3-11. A summary of the analysis results regarding eight key metrics is shown in Table 10. Based on the results of all analysis cases, the CM-MTL3 with the proposed design revisions is expected to meet all performance criteria specified in *MASH* for test level 3. However, as stated previously, the magnitude of occupant compartment deformation on the floor pan area is considered relatively high and poses some concern, since the model has not been validated for this level of deformation inside the occupant compartment. Recently, MwRSF tested a similar barrier design for Minnesota DOT in which the OCD for Test 3-11 was 5.8 inches.[*Hinojosa21*] Based on comparison to those results, it is expected that the values from the FEA model are likely over-predicted.

Table 10. Summary of FEA results for CM-MTL3 with proposed design revisions.

MASH Test	Ref. Point	OIVx (ft/s)	OIVy (ft/s)	ORAx (G)	ORAy (G)	Deflection (in)		Roll	Pitch	OCD (in)
						Dynamic	Permanent	(deg)	(deg)	
Test 3-10	Splice	22.3	29.9	5.6	13.9	0.92	0.36	9.9	6.4	3.76
	Post	22.6	29.5	4.0	13.9	0.98	0.36	9.2	6.5	4.12
Test 3-11	Splice	23.0	26.6	6.5	12.2	1.41	0.5	8.3	5.5	7.34
	Post	23.0	27.2	4.4	11.8	1.13	0.41	8.3	5.3	7.78

REFERENCES

AASHTO16 Technical Committee for Roadside Safety, "Manual for Assessing Safety Hardware," American Association of State Highway and Transportation Officials, Washington, D.C. (2016).

Carrigan22 Carrigan, C.E. and Chuck A. Plaxico, "Guide for Bridge Curb/Rail and Approach Treatment for Extremely Low Volume Road," 2022 Expected.

CCSA16 George Mason University Center for Collision Safety and Analysis, "2010 Toyota Yaris Finite Element Model Validation Detailed Mesh." https://doi.org/10.13021/G8CC7G. Accessed 7/30/2021.

CCSA18 George Mason University Center for Collision Safety and Analysis, "2018 Dodge Ram Model Development." https://www.ccsa.gmu.edu/models/ Accessed 7/30/2021.

Bligh19 Bligh, R.P, W.L. Menges, B.L. Griffith, G.E. Schroeder, and D.L. Kuhn, "*MASH* Evaluation of TXDOT Roadside Safety Features – Phase II," Report No. FHWA-TX-18/0-6946-R2, Texas Transportation Institute, College Station, TX, (2019).

Hinojosa21 Hinojosa, M.A., R.K. Faller, S. Rosenbaugh, C.S. Stolle, R.W. Bielenberg, J.D. Rasmussen, J.S. Steelman, and J.C. Holloway, "MASH 2016 Test Level 4 Evaluation of MNDOT Concrete Parapet with Brush Curb and Upper Beam and Post Rail with New Tapered End Section," MwRSF Research Report No. TRP-03-403-21, Midwest Roadside Safety Facility, University of Nebraska-Lincoln, (2021).

LSDYNA20 "LSDYNA User's Manual" Volumes I, II and III, Livermore Software Technology Corporation (LSTC), Livermore, CA (2020).

Marzougui12 Marzougui, D., R.R. Samaha, C. Cui, and C.D. Kan, "Extended Validation of the Finite Element Model for the 2010 Toyota Yaris Passenger Sedan." https://media.ccsa.gmu.edu/cache/NCAC-2012-W-005.pdf. Accessed 7/30/2021.

Plaxico19 Plaxico, C.A., "*MASH* TL4 Evaluation of MassDOT's Curb-Mounted and Sidewalk-Mounted S3-TL4 Steel Bridge Railing Using Finite Element Analysis," Technical Report No. TR 19-0429-GEA, Performed for Gill Engineering Associates, Performed by Roadsafe LLC, Canton, ME (April 2019).

Plaxico20 Plaxico, C.A. and E.M. Ray, "Development of *MASH* Computer Simulated Steel Bridge Rail and Transition Details," Technical Report No. TR-200323-NETC115, Performed for New England Transportation Consortium, Performed by Roadsafe LLC, Canton, ME (April 2020).

Plaxico21a Plaxico, C.A., "*MASH* TL2 Evaluation of MassDOT's Curb-Mounted and Sidewalk-Mounted CT-TL2 Bridge Rail Using Finite Element Analysis," Technical Report No. TR 21-0121-GEA, Performed for Gill Engineering Associates, Performed by Roadsafe LLC, Canton, ME (April 2021).

Plaxico21b Plaxico, C.A., "*MASH* TL3 Evaluation of MassDOT's CM-MTL3 Bridge Rail Using Finite Element Analysis," Technical Report No. TR 21-0730-GEA, Performed for Gill Engineering Associates, Performed by Roadsafe LLC, Canton, ME (July 2021).

Plaxico22 Plaxico, C.A., "Modifications to the Steer Mechanism for the 1100C Vehicle Model," Unpublished work, Roadsafe, LLC, Canton, Maine, 2022.

Ray07 Ray, M.H. and M. Mongiardini, "A LS-DYNA Crash Simulation of the Annisquam River Bridge for Report 350 Test Level Three Conditions," Final Report, Worcester Polytechnic Institute, Worcester, MA (2007).

Ray10 Ray, M.H., C.A. Plaxico and M. Anghileri, "Procedures for Verification and Validation of Computer Simulations Used for Roadside Safety Applications," NCHRP Web-Only Document 179, National Academy of Sciences, Washington, D.C. (2010).

TFHRC15 "Stress vs strain for ASTM A615 Grade 69 steel", Provided by Z.B. Haber, Bridge engineer for Professional Service Industries and consultant for Turner-Fairbanks Highway Research Center, McLean, VA, (2015).

TTI22 TTI, "Test Risk Assessment Program (TRAP) Version 1.01: User's Manual," Texas Transportation Institute, College Station, TX (2022).

Appendix A

Drawings for the MassDOT CM-MTL3 Bridge Rail

with Proposed Revisions

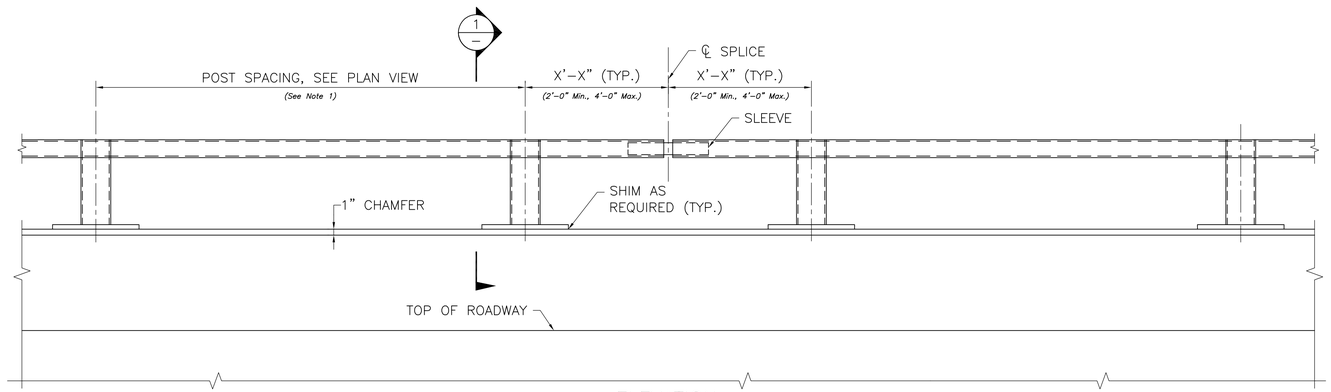

ELEVATION

SCALE: 1" = 1'–0"

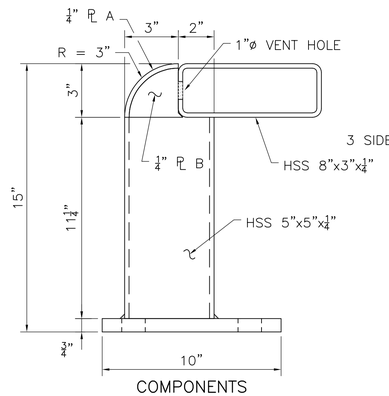

COMPONENTS

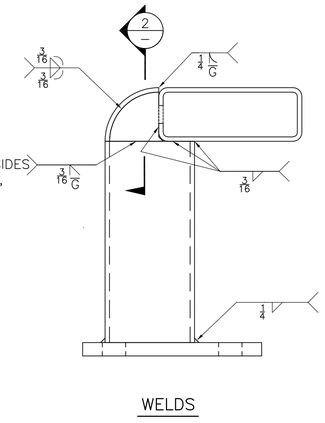

WELDS

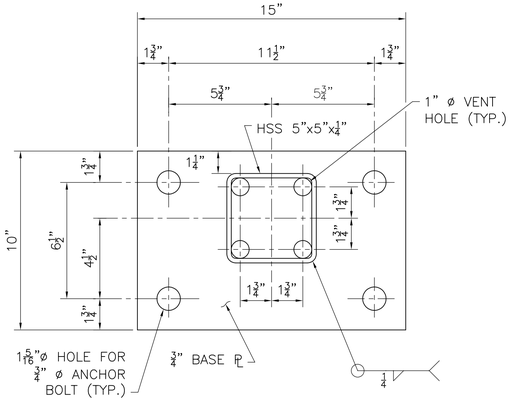

BASE PLATE

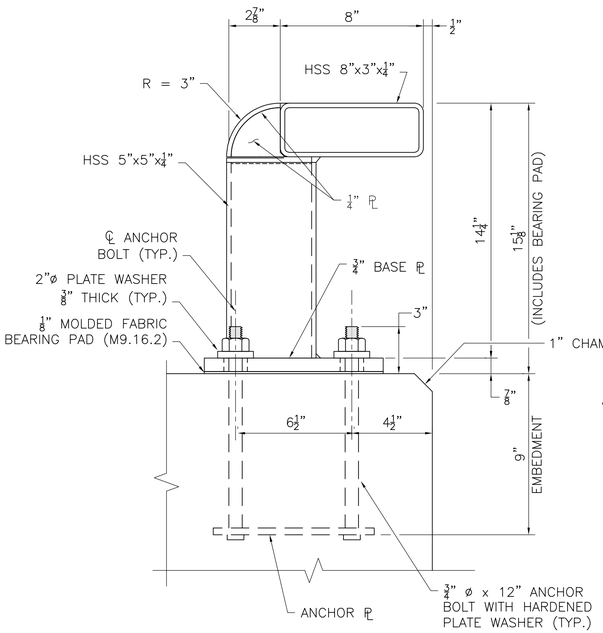

SECTION 1

SCALE: 3" = 1'–0"

MUNICIPALITY
STREET NAME/ROUTE #

STATE	FED. AID PROJ. NO.	SHEET NO.	TOTAL SHEETS
MA	######	####	X
	PROJECT FILE NO.	######	

CM-MTL3 BRIDGE RAILING

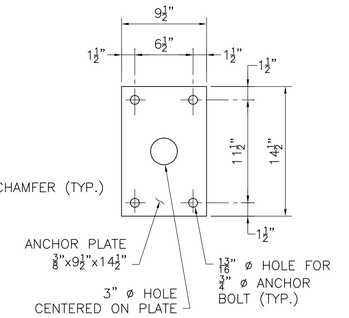

ANCHOR PLATE

SCALE: 1½" = 1'–0"

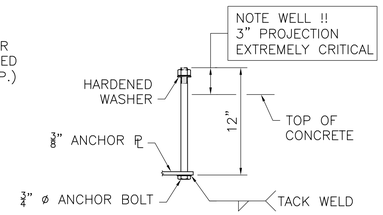

ANCHOR BOLT

SCALE: 1½" = 1'–0"

GENERAL NOTES:

1. MAXIMUM RAIL LENGTH IS 24'–0". MAXIMUM POST SPACING IS 6'–0". RAILS SHALL BE CONTINUOUS OVER A MINIMUM OF TWO (2) AND A MAXIMUM OF FOUR (4) POSTS.
2. RAILS SHALL HAVE A TUBE SPLICE BETWEEN CONTINUOUS LENGTHS OF RAIL AND IN THE PANEL OVER A BRIDGE EXPANSION JOINT.
3. ALL STEEL SHALL BE GALVANIZED. ALL PIPE SLEEVE SPLICES SHALL BE GALVANIZED SEPARATELY AND NOT WHILE BOLTED TO THE RAIL.
4. ALL GALVANIZED STEEL (EXCEPT THE ANCHOR PLATE AND FASTENERS) SHALL BE PAINTED DARK BRONZE (AMS STANDARD 595A COLOR NUMBER 10045 OF THE FEDERAL STANDARD 595B).
5. ANCHOR BOLTS SHALL BE SET WITH TEMPLATES. THE NUT SECURING THE POST BASE PLATE TO THE CONCRETE SHALL BE TIGHTENED TO A SNUG FIT AND GIVEN A ADDITIONAL ⅛ TURN AFTER STEEL IS IN PLACE.
6. ALL POSTS SHALL BE SET PERPENDICULAR TO GRADE.
7. END TUBE SECTIONS SHALL BE SAWED. GRIND SMOOTH EXPOSED EDGES. ALL CUT ENDS SHALL BE TRUE AND SMOOTH.
8. WELDING SHALL CONFORM TO THE REQUIREMENTS OF ANSI/AASHTO/AWS D.1.5, EXCEPT THAT WELDING OF THE TUBE–WELDED SPLICE SHALL CONFORM TO THE REQUIREMENTS OF ANSI/AWS D.1.1

SECTION

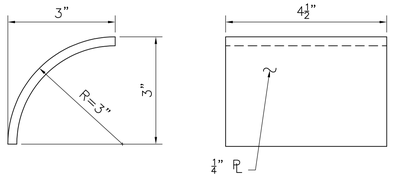

PLATE A

SCALE: 6" = 1'–0"

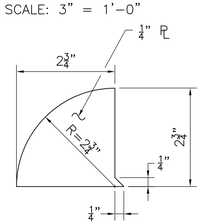

PLATE B

SCALE: 6" = 1'–0"

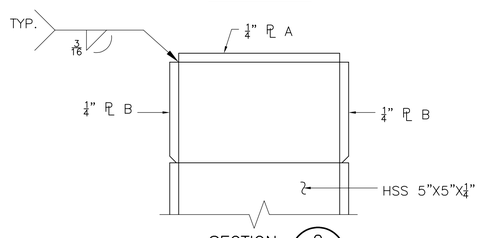

SECTION 2

POST CAP ASSEMBLY

SCALE: 6" = 1'–0"

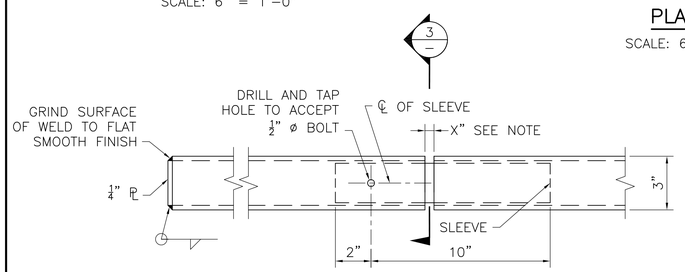

NOTE: AT RAIL SPLICES X = ½" AT BRIDGE EXPANSION JOINTS X = THERMAL EXPANSION + ½"

END RAIL CAP

RAIL ELEVATION

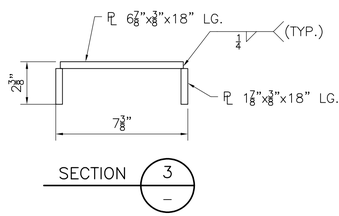

SECTION 3

TYPICAL SPLICE DETAILS

SCALE: 3" = 1'–0"

MATERIALS:

STRUCTURAL STEEL TUBING_____	ASTM A 500 GRADE B (GALVANIZED)
POST AND BASE PLATE _____	AASHTO M 270 GRADE 36 OR GRADE 50 (GALVANIZED)
ANCHOR BOLT PLATE WASHERS _	AASHTO M 270 GRADE 36 OR GRADE 50 (GALVANIZED)
ANCHOR BOLTS _____	ASTM F1554 GRADE 105 TYPE 2A (GALVANIZED)

MMMM DD, YYYY	ISSUED FOR CONSTRUCTION
DATE	DESCRIPTION

THIS SHEET IS APPROVED FOR CONSTRUCTION BY MASSDOT
AUTHORIZED SIGNATORY: _____ STATE BRIDGE ENGINEER

USE ONLY PRINTS OF LATEST DATE

SHEET X OF X SHEETS BRIDGE NO. X–XX–XXX (BIN1)

Date: MONTH 20XX

CM-MTL3.DWG Plotted on 28-Oct-2022 9:47 AM

DD-Month-YYYY

Xxxxxx Structural Submittal (S#)

MUNICIPALITY
STREET NAME/ROUTE #

STATE	FED. AID PROJ. NO.	SHEET NO.	TOTAL SHEETS
MA	######	####	X
	PROJECT FILE NO.	######	

TERMINUS FOR CM-MTL3 BRIDGE RAILING

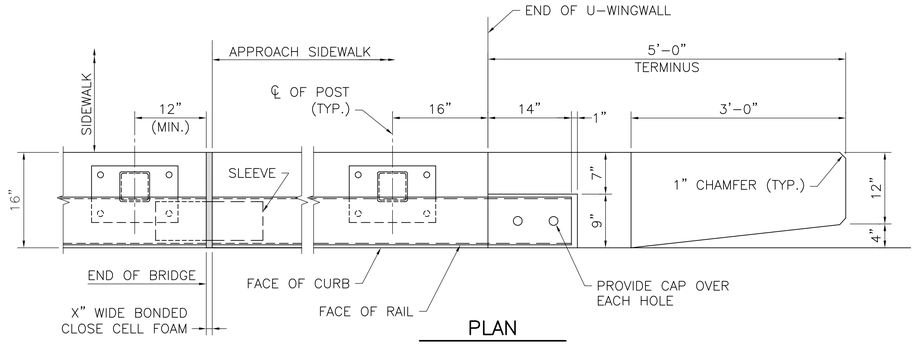

PLAN
SCALE: 1" = 1'-0"

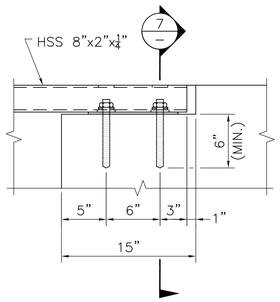

RAIL ATTACHMENT
SCALE: 1½" = 1'-0"

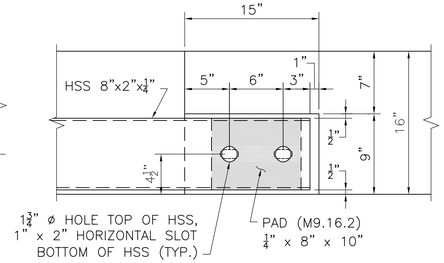

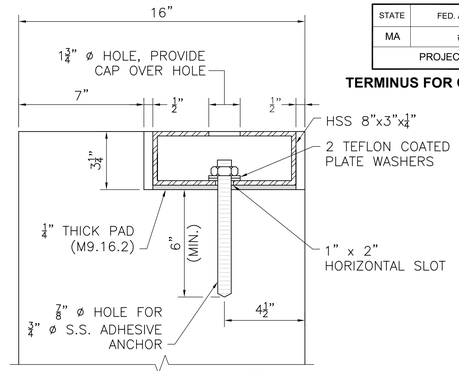

SECTION 7
SCALE: 3" = 1'-0"

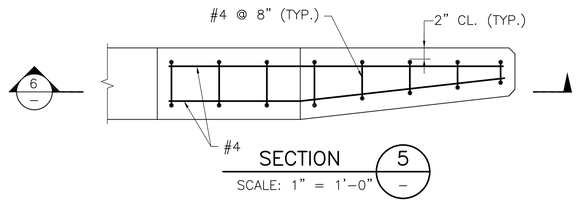

SECTION 5
SCALE: 1" = 1'-0"

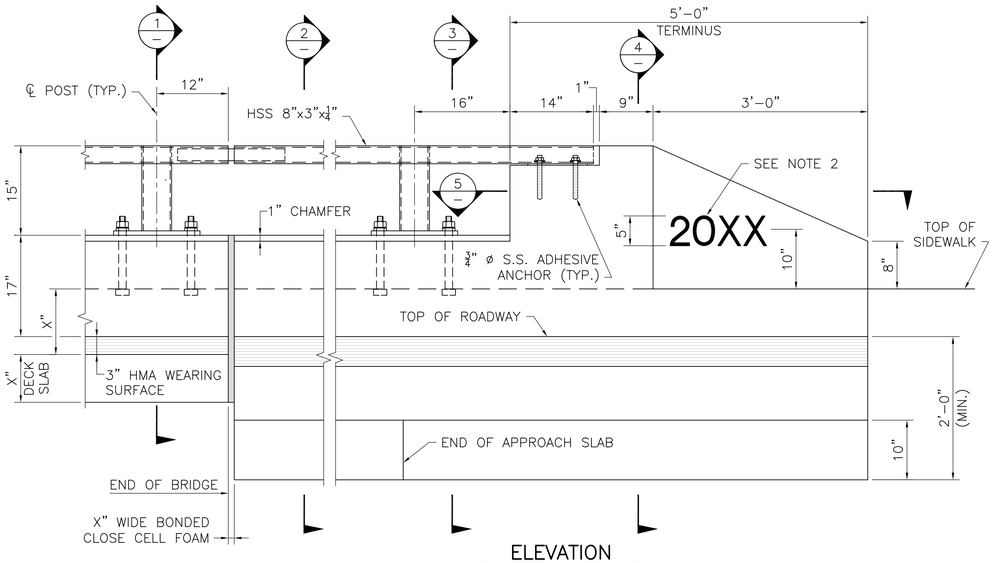

ELEVATION
SCALE: 1" = 1'-0"

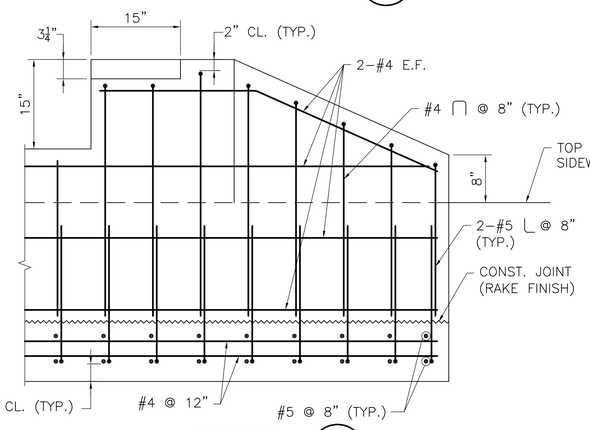

SECTION 6
SCALE: 1" = 1'-0"

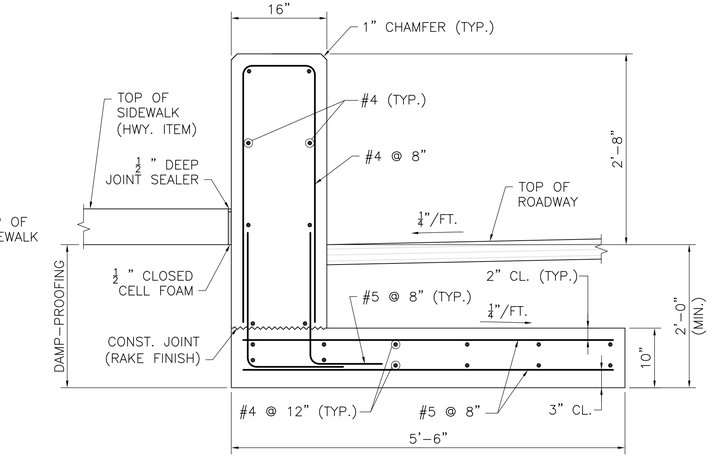

SECTION 4
SCALE: 1" = 1'-0"

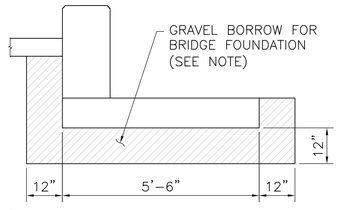

NOTE:
GRAVEL BORROW SHALL BE PLACED AND THOROUGHLY COMPACTED TO THE GRADE OF THE BOTTOM OF THE SLAB.

CM-MTL3 MOMENT SLAB BACKFILL
SCALE: ½" = 1'-0"

NOTE: USE LATEST CONTRACT COMPLETION YEAR IN EFFECT WHEN THE FIRST TERMINUS IS CAST.

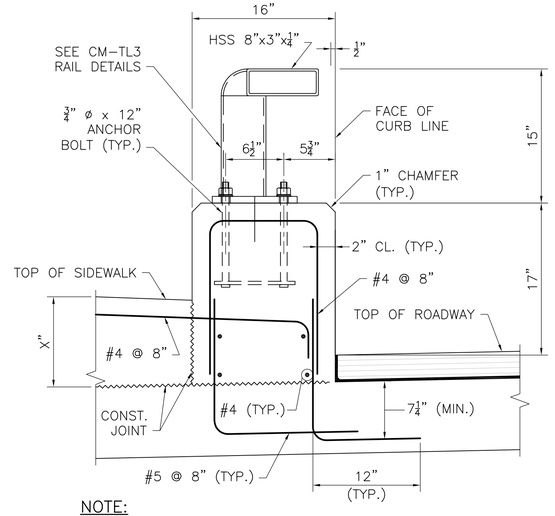

NOTE:
SIDEWALK AND DECK SLAB REINFORCEMENT NOT SHOWN FOR CLARITY.

SECTION 1
SCALE: 1" = 1'-0"

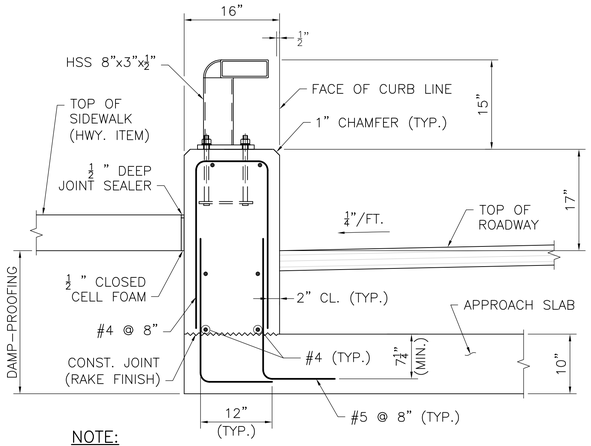

NOTE:
APPROACH SLAB REINFORCEMENT NOT SHOWN FOR CLARITY.

SECTION 2
SCALE: 1" = 1'-0"

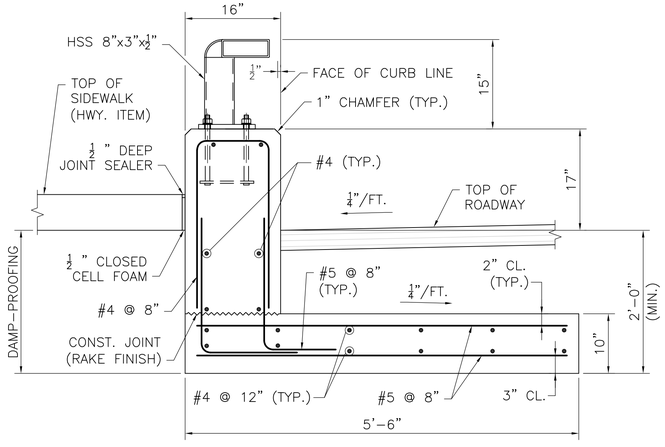

SECTION 3
SCALE: 1" = 1'-0"

MMMM DD, YYYY	ISSUED FOR CONSTRUCTION
DATE	DESCRIPTION

THIS SHEET IS APPROVED FOR CONSTRUCTION BY MASSDOT
AUTHORIZED SIGNATORY: STATE BRIDGE ENGINEER
USE ONLY PRINTS OF LATEST DATE

SHEET X OF X SHEETS BRIDGE NO. X-XX-XXX (BIN1)

Date: MONTH 20XX

Appendix B

Sequential Views for Test 3-10 for the

CM-MTL3 Bridge Rail Design with Proposed Revisions

for CIP Relative to Splice

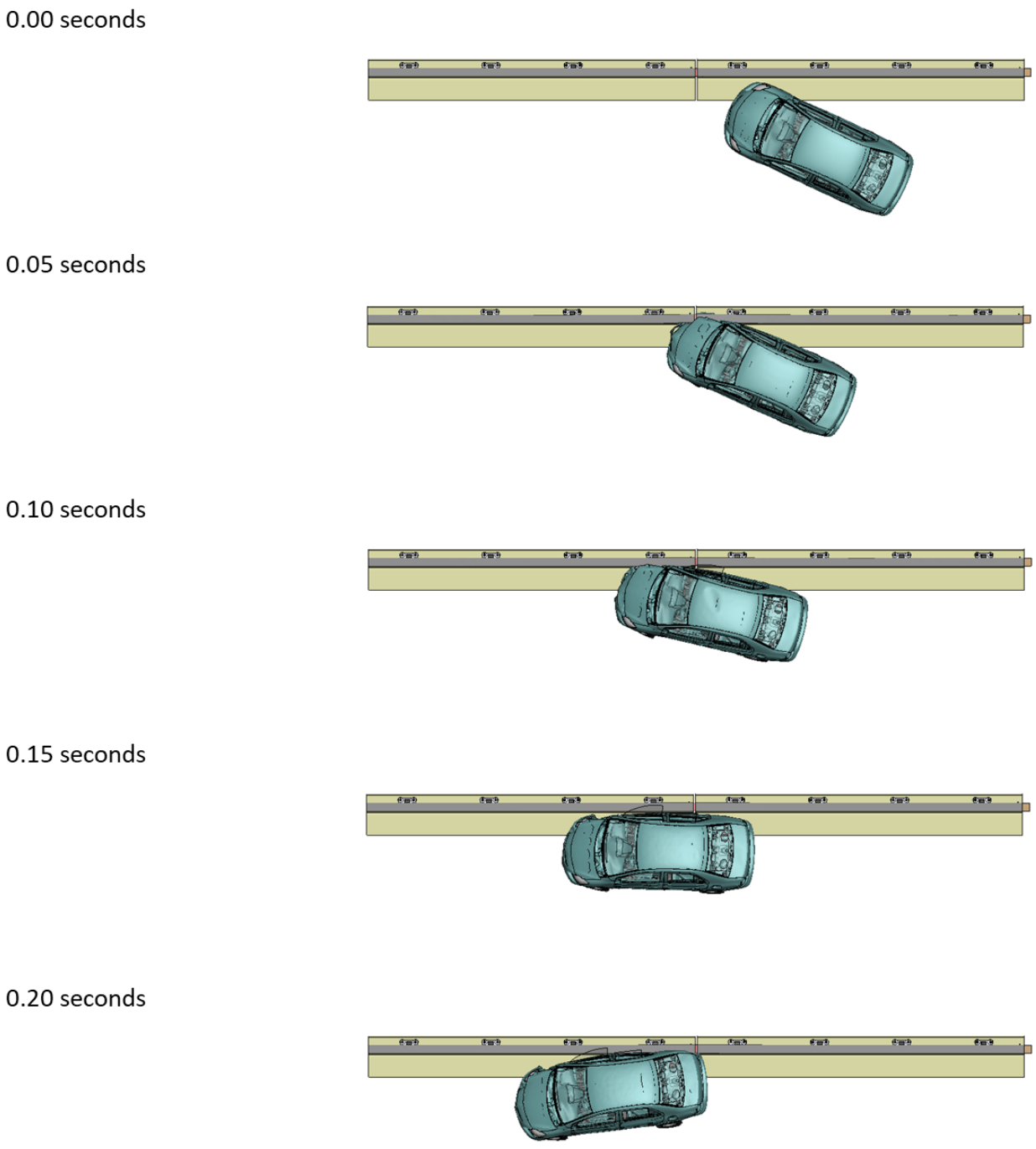

Figure 1. Sequential views from analysis of MASH Test 3-10 for CIP relative to Splice from an overhead viewpoint.

0.25 seconds

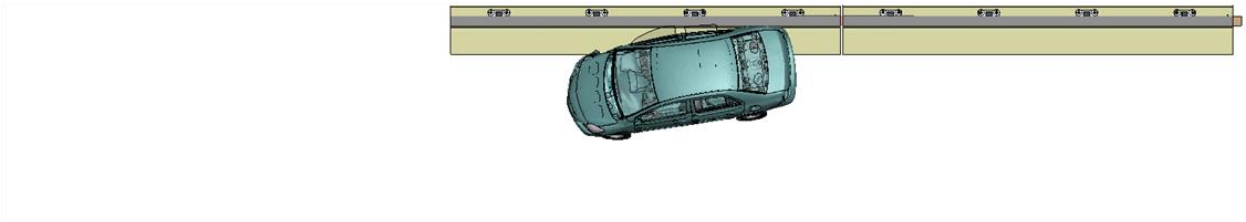

0.30 seconds

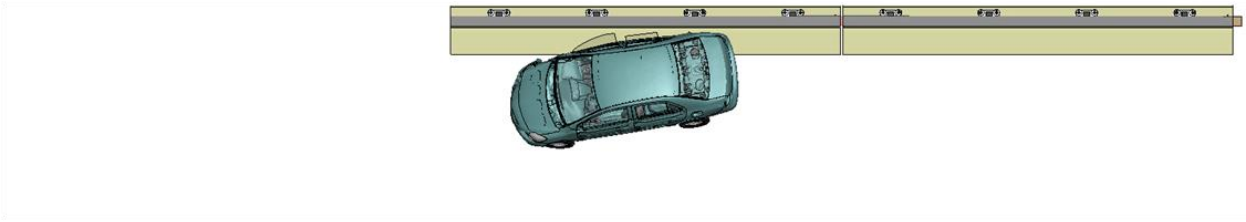

0.35 seconds

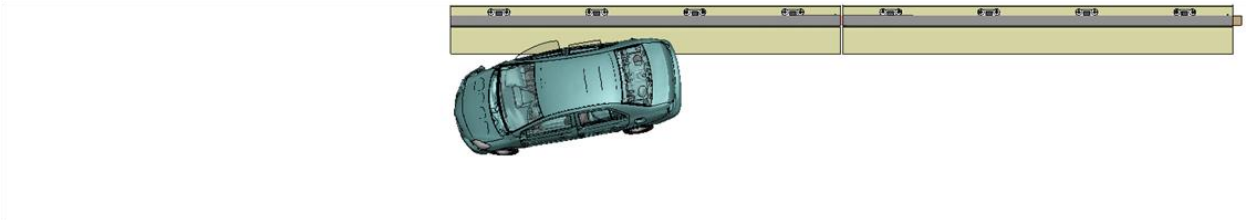

0.40 seconds

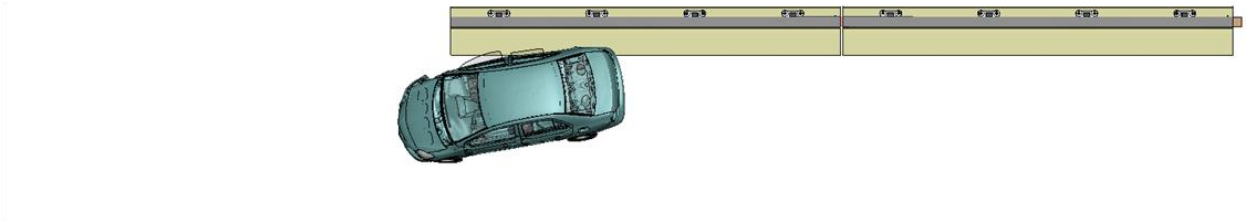

0.45 seconds

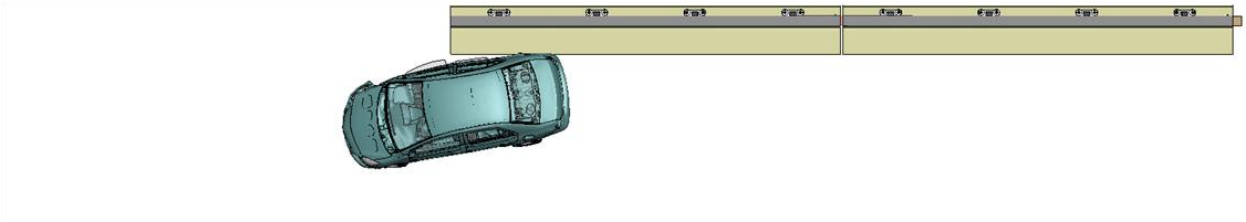

Figure 1 [CONTINUED] Sequential views from analysis of MASH Test 3-10 for CIP relative to Splice from an overhead viewpoint.

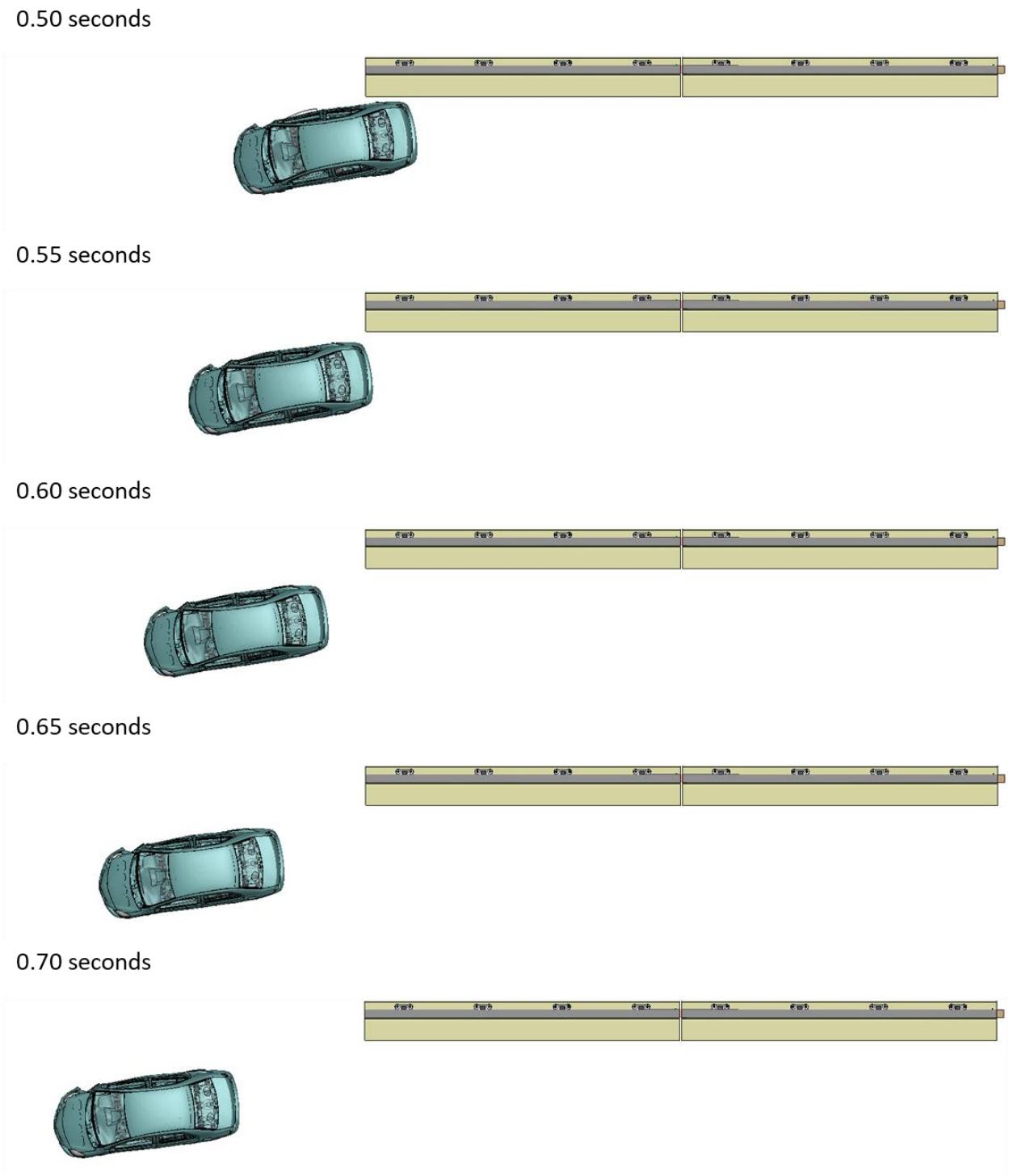

Figure 1 [CONTINUED] Sequential views from analysis of MASH Test 3-10 for CIP relative to Splice from an overhead viewpoint.

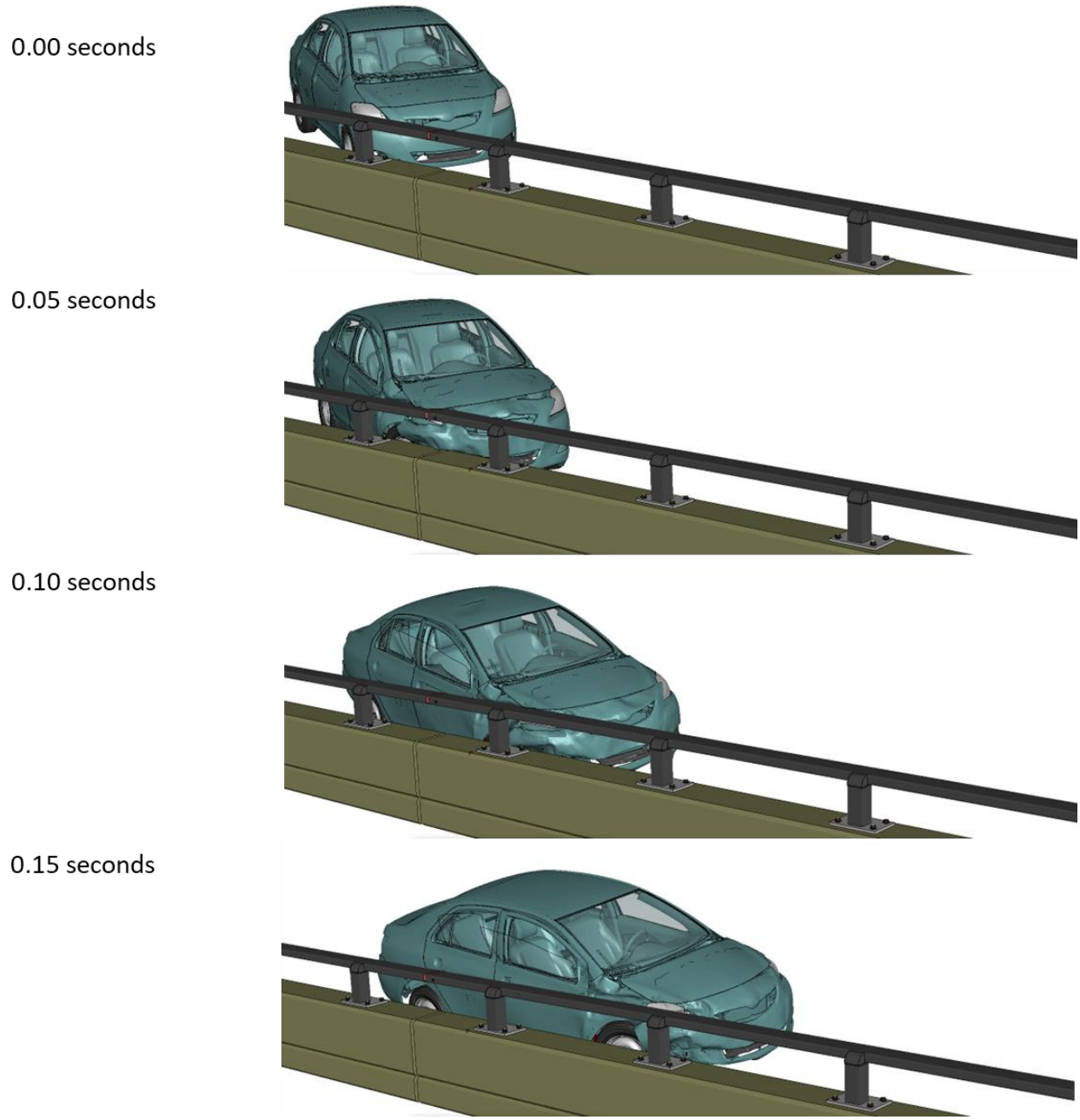

Figure 2. Sequential views from analysis of MASH Test 3-10 for CIP relative to Splice from an oblique viewpoint.

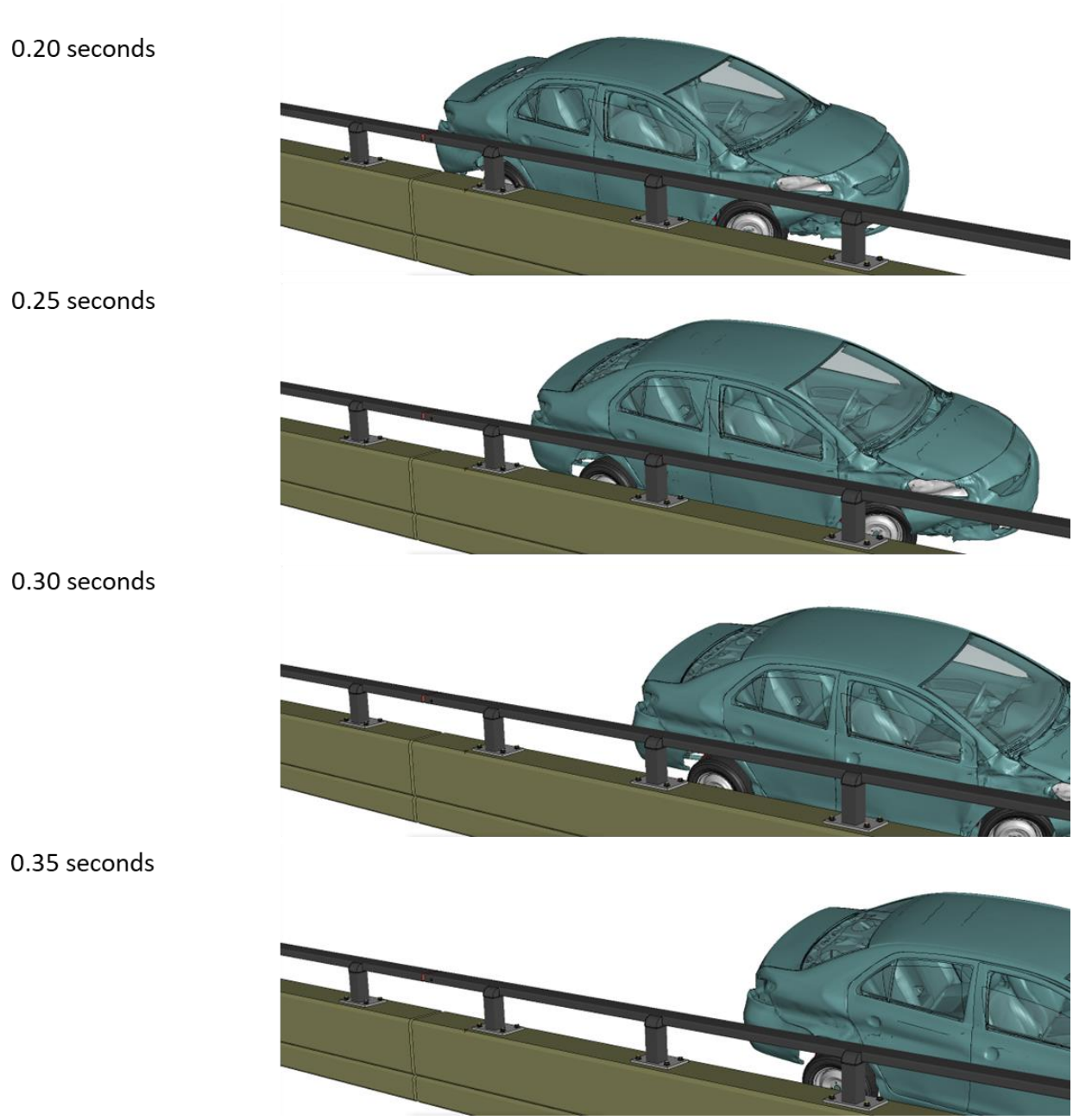

Figure 2 [CONTINUED] Sequential views from analysis of MASH Test 3-10 for CIP relative to Splice from an oblique viewpoint.

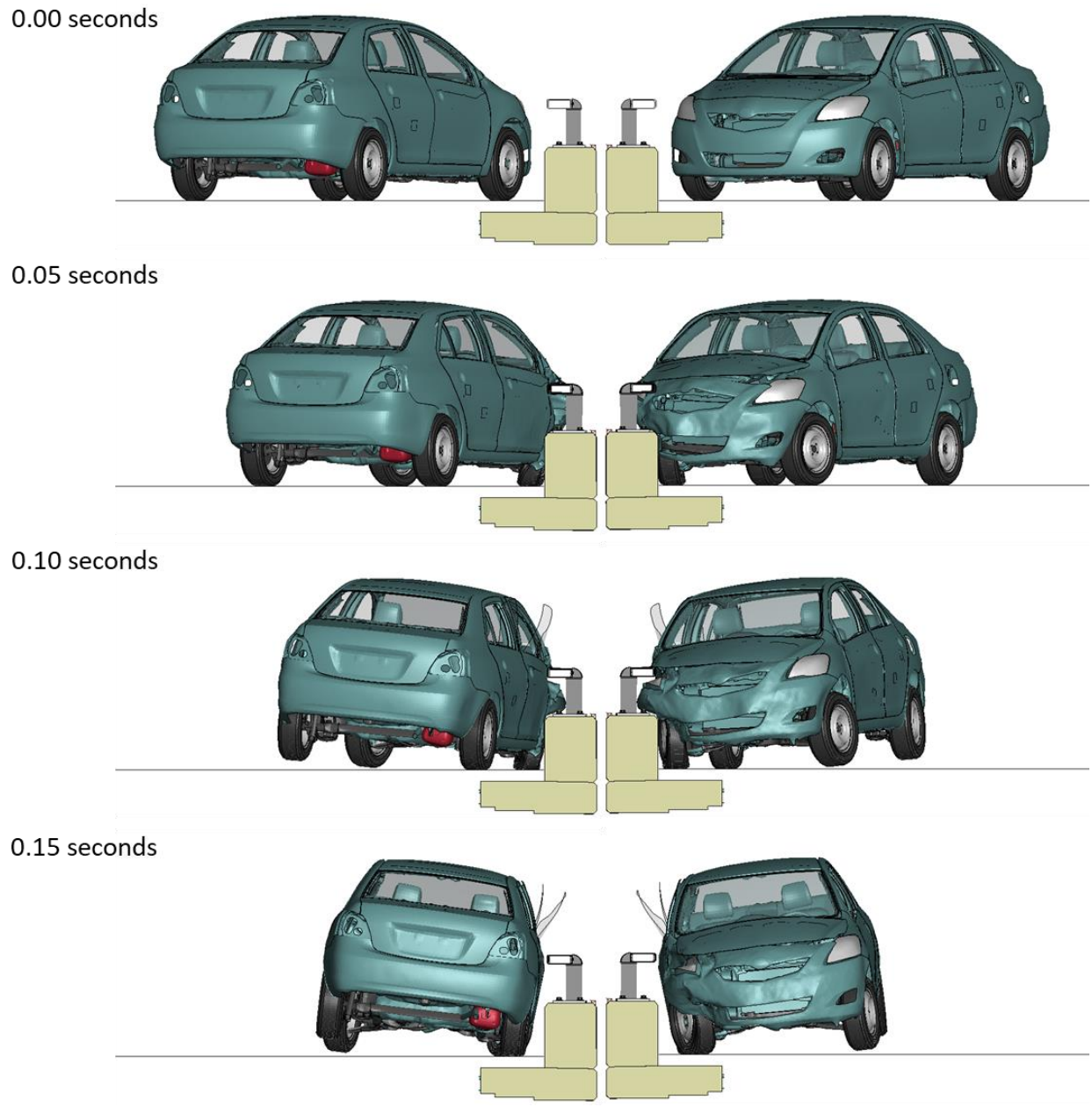

Figure 3. Sequential views from analysis of MASH Test 3-10 for CIP relative to Splice from a front and rear viewpoint.

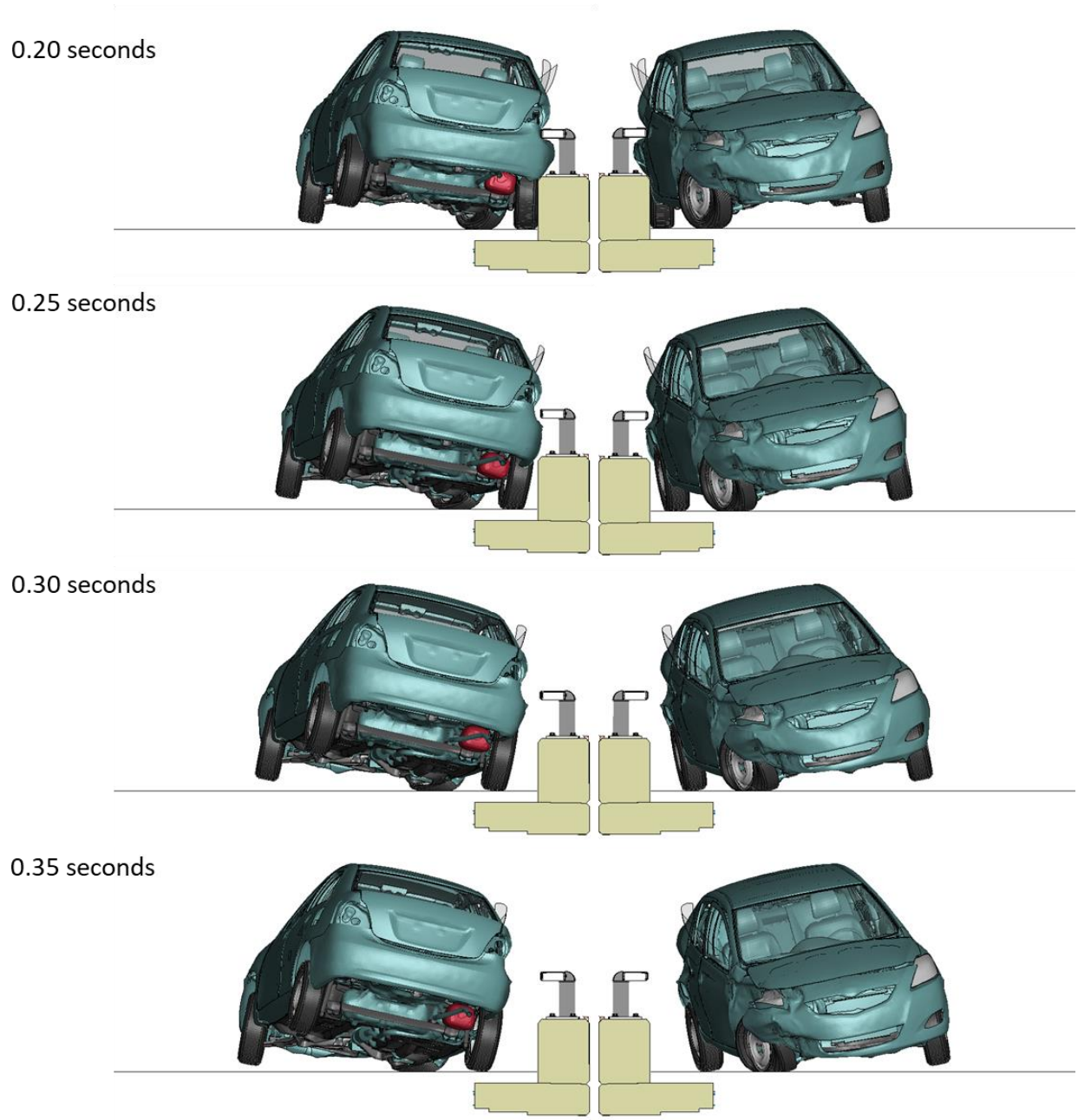

Figure 3 [CONTINUED] Sequential views from analysis of MASH Test 3-10 for CIP relative to Splice from a front and rear viewpoint.

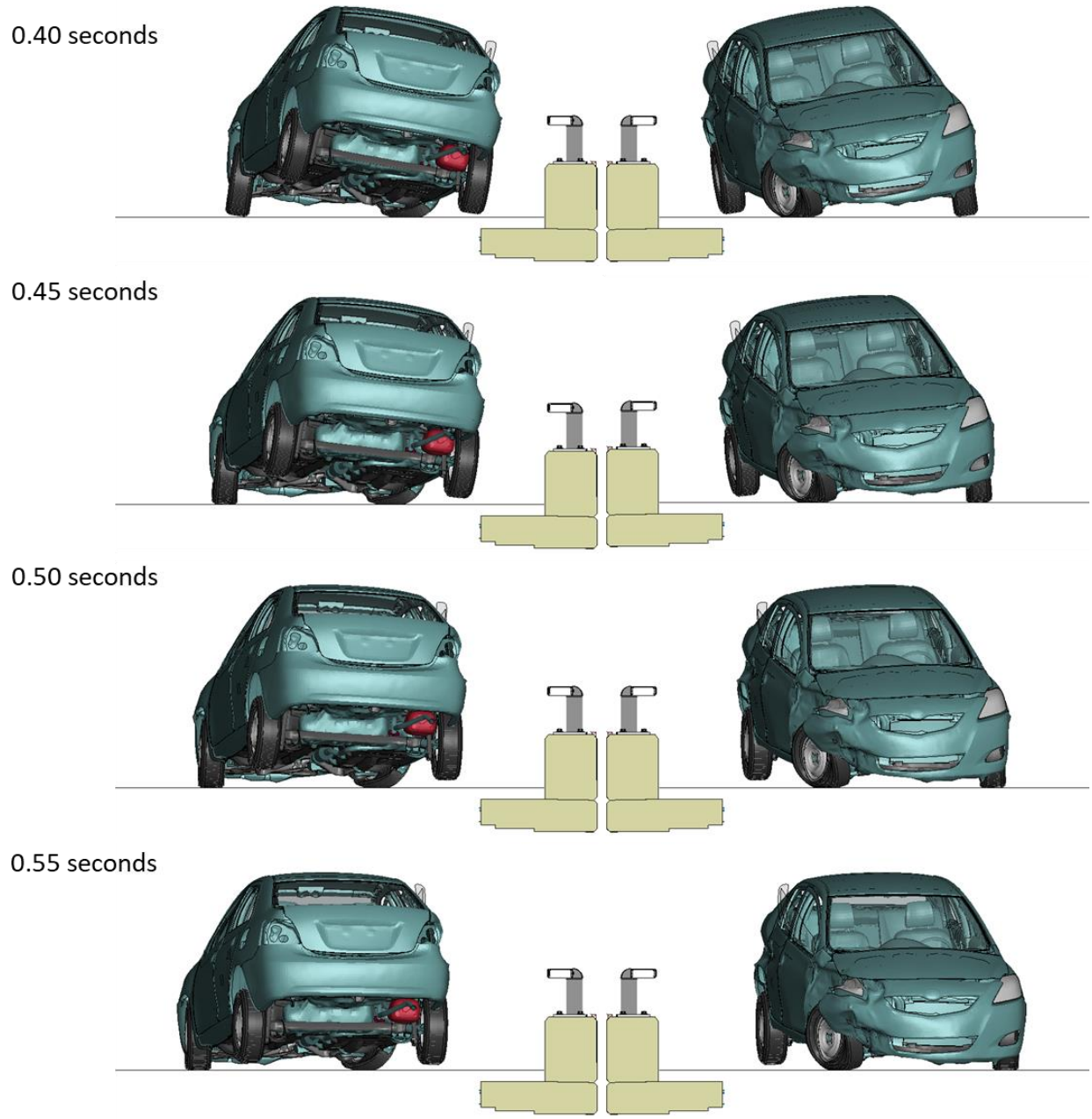

Figure 3 [CONTINUED] Sequential views from analysis of MASH Test 3-10 for CIP relative to Splice from a front and rear viewpoint.

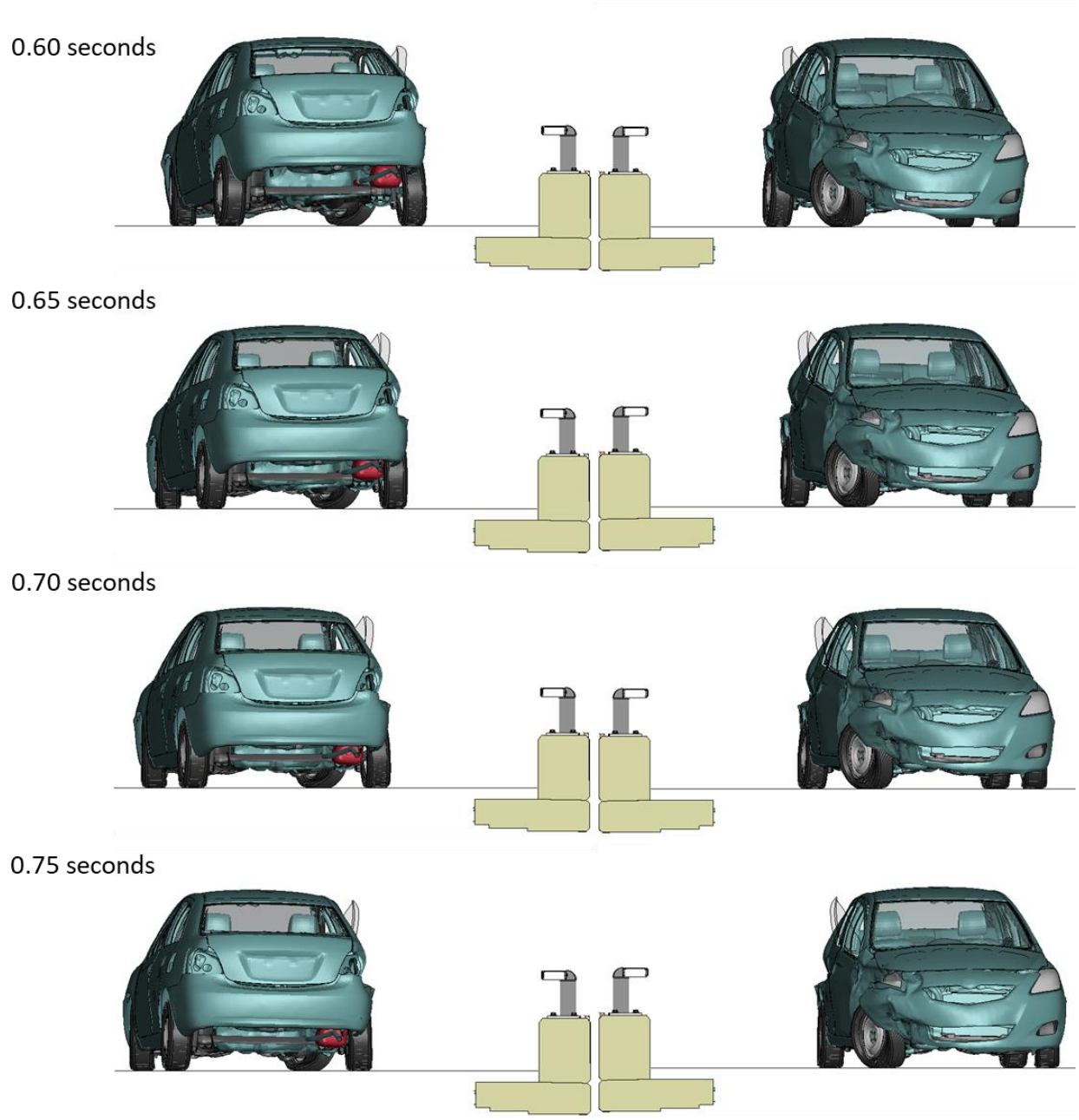

Figure 3 [CONTINUED] Sequential views from analysis of MASH Test 3-10 for CIP relative to Splice from a front and rear viewpoint.

Appendix C

Sequential Views for Test 3-10 for the

CM-MTL3 Bridge Rail Design with Proposed Revisions

for CIP Relative to Post

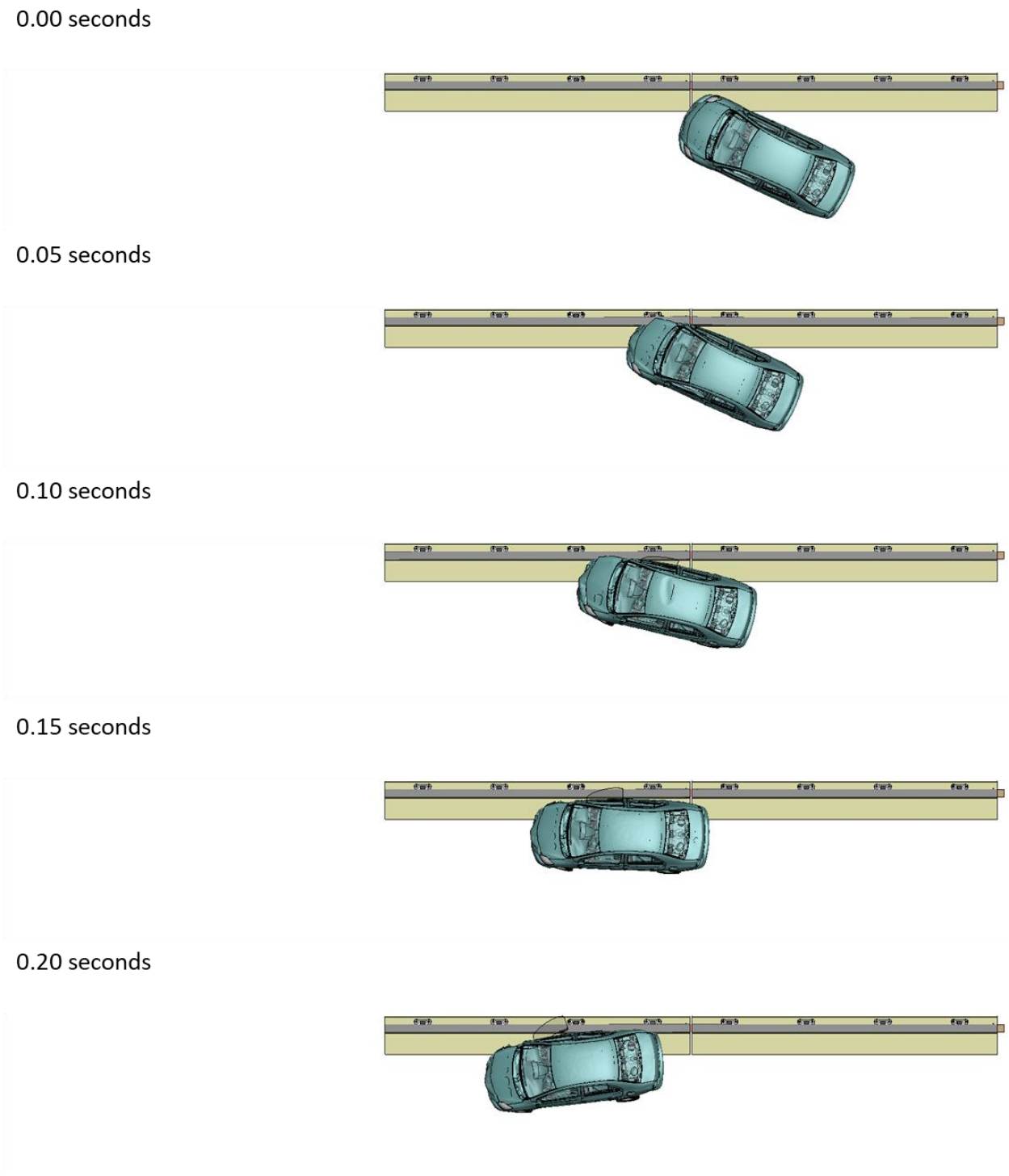

Figure 1. Sequential views from analysis of MASH Test 3-10 for CIP relative to Post from an overhead viewpoint.

0.25 seconds

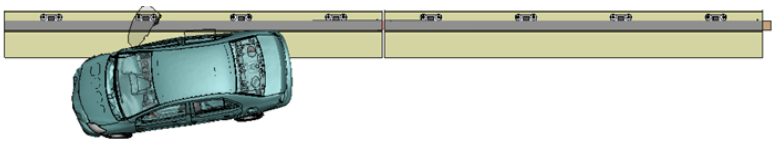

0.30 seconds

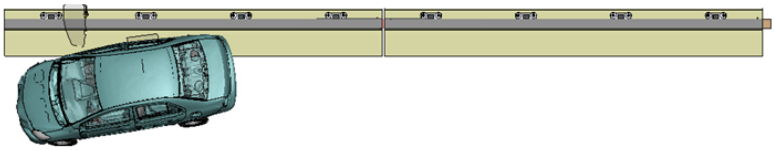

0.35 seconds

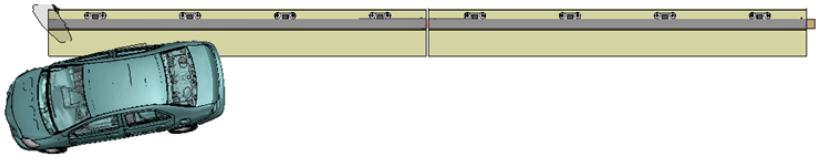

0.40 seconds

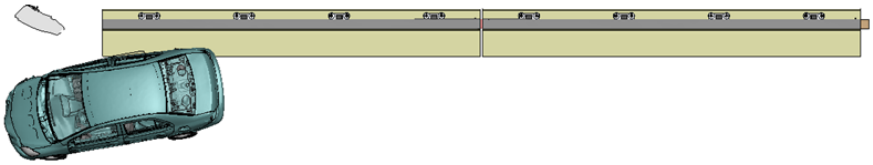

0.45 seconds

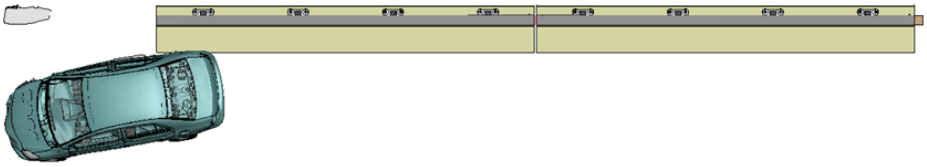

Figure 1 [CONTINUED] Sequential views from analysis of MASH Test 3-10 for CIP relative to Post from an overhead viewpoint.

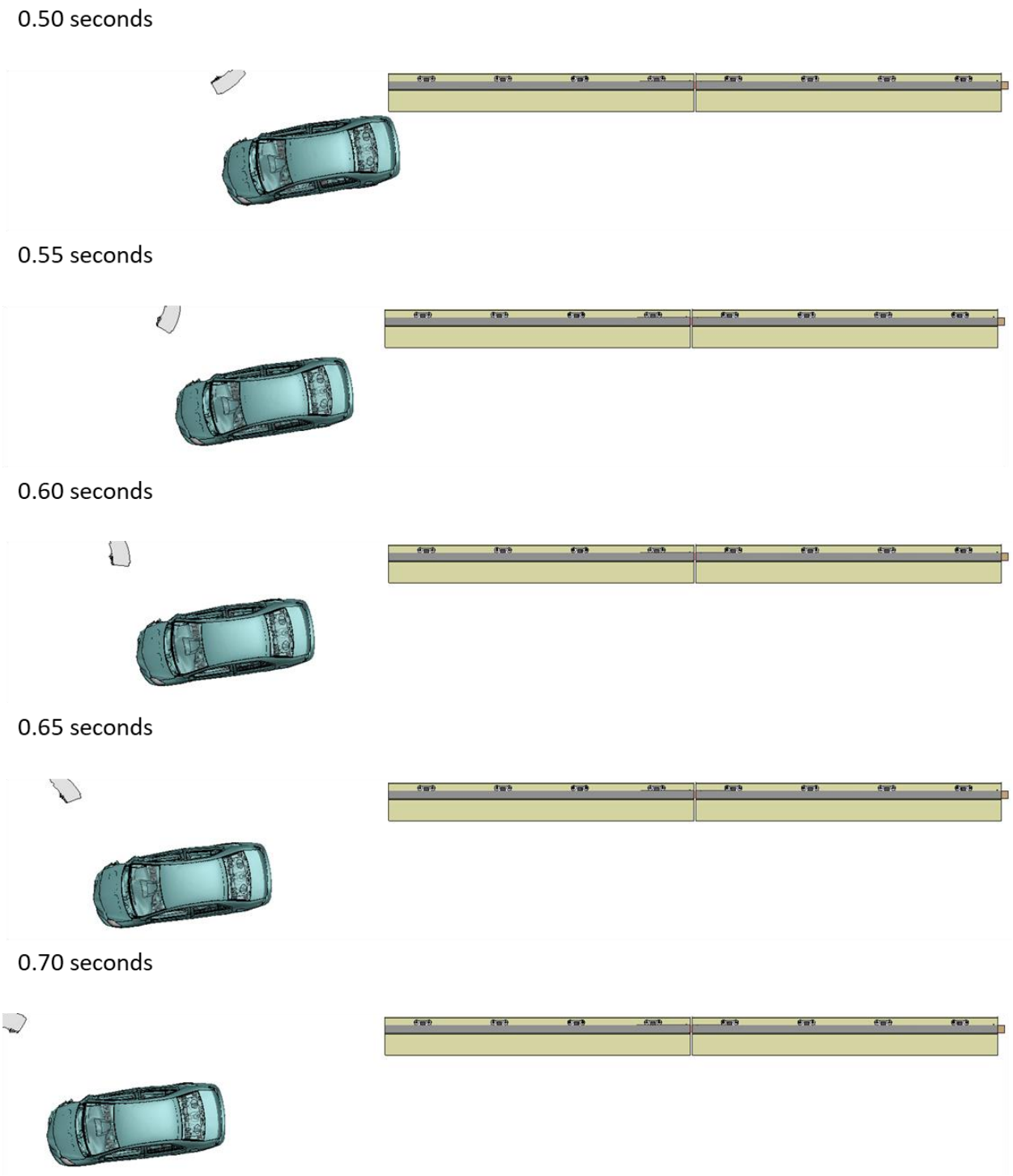

Figure 1 [CONTINUED] Sequential views from analysis of MASH Test 3-10 for CIP relative to Post from an overhead viewpoint.

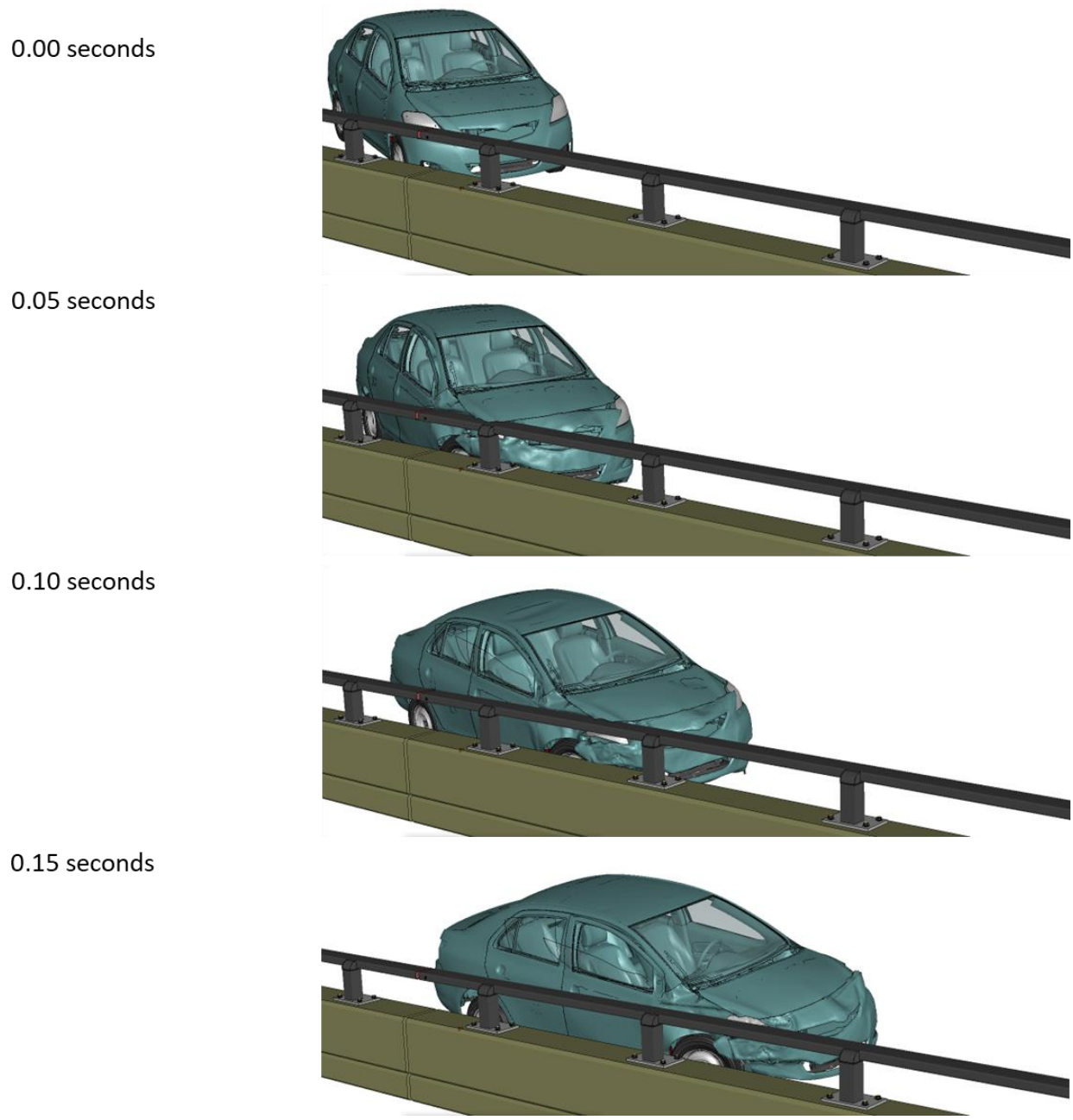

Figure 2. Sequential views from analysis of MASH Test 3-10 for CIP relative to Post from an oblique viewpoint.

0.20 seconds

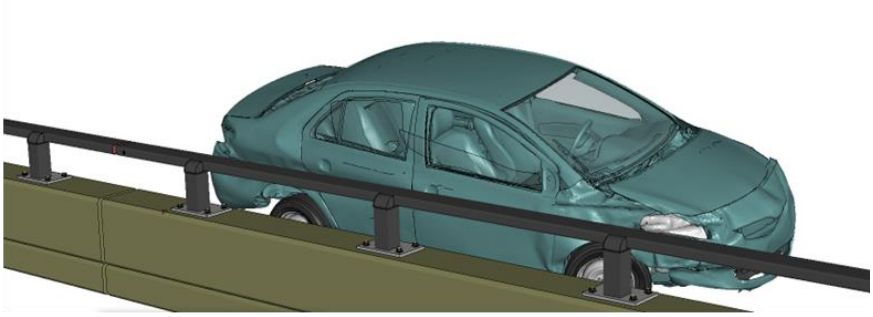

0.25 seconds

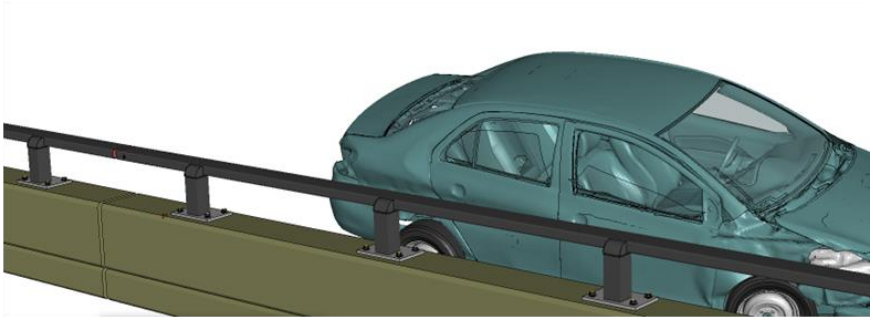

0.30 seconds

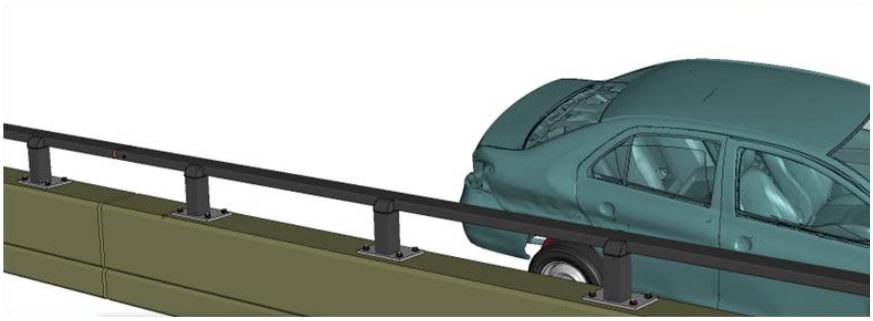

0.35 seconds

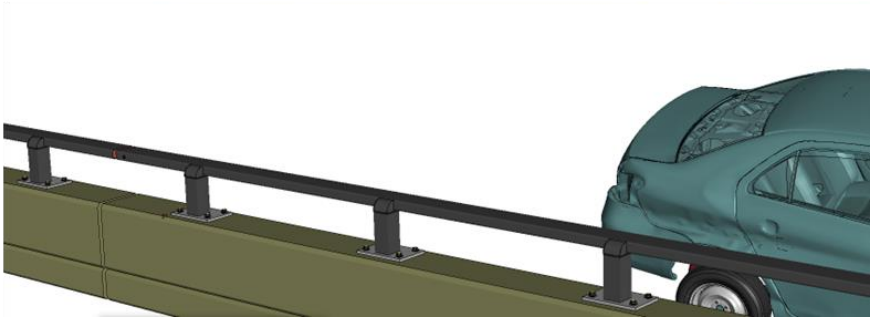

Figure 2 [CONTINUED] Sequential views from analysis of MASH Test 3-10 for CIP relative to Post from an oblique viewpoint.

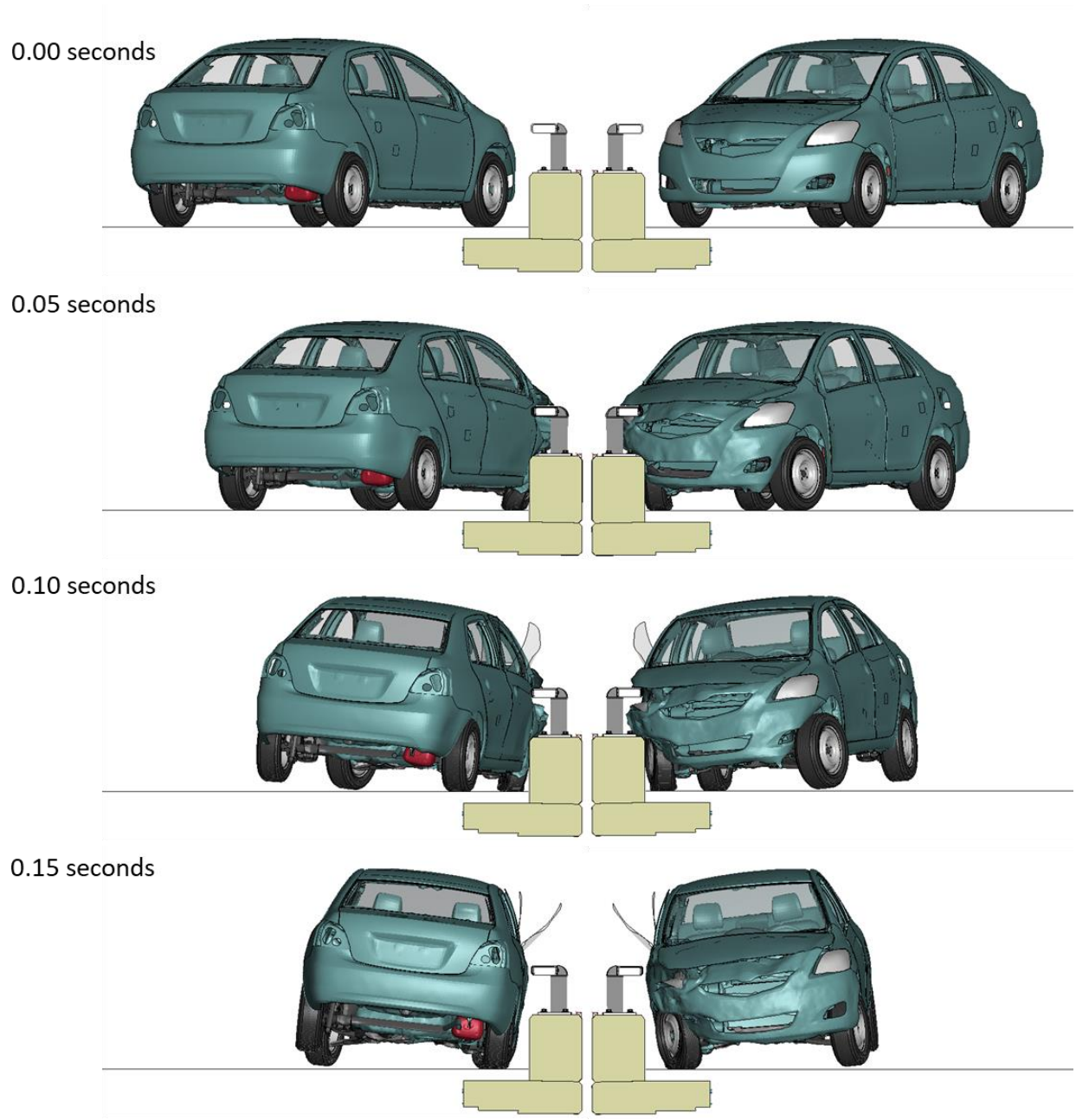

Figure 3. Sequential views from analysis of MASH Test 3-10 for CIP relative to Post from a front and rear viewpoint.

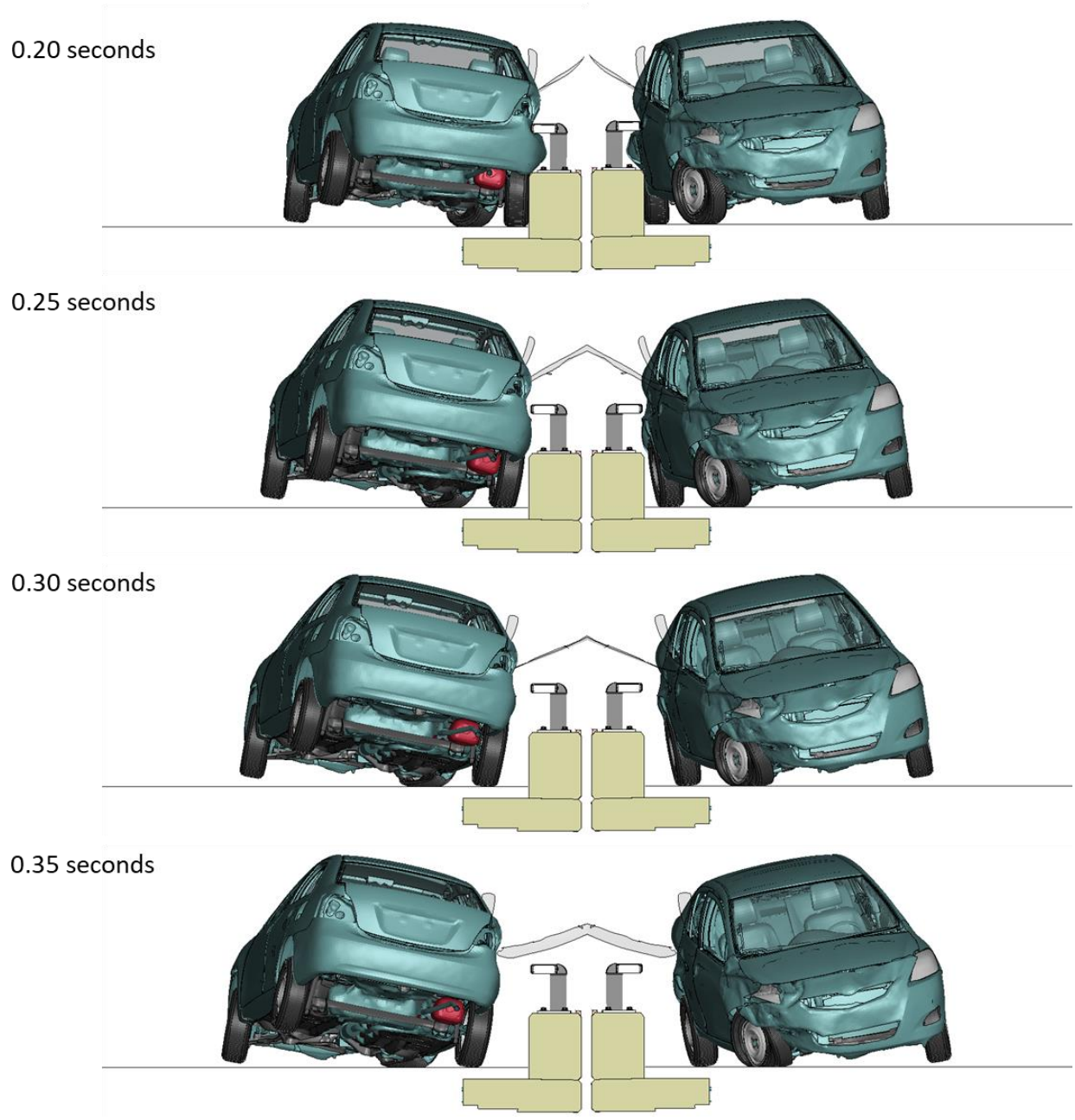

Figure 3 [CONTINUED] Sequential views from analysis of MASH Test 3-10 for CIP relative to Post from a front and rear viewpoint.

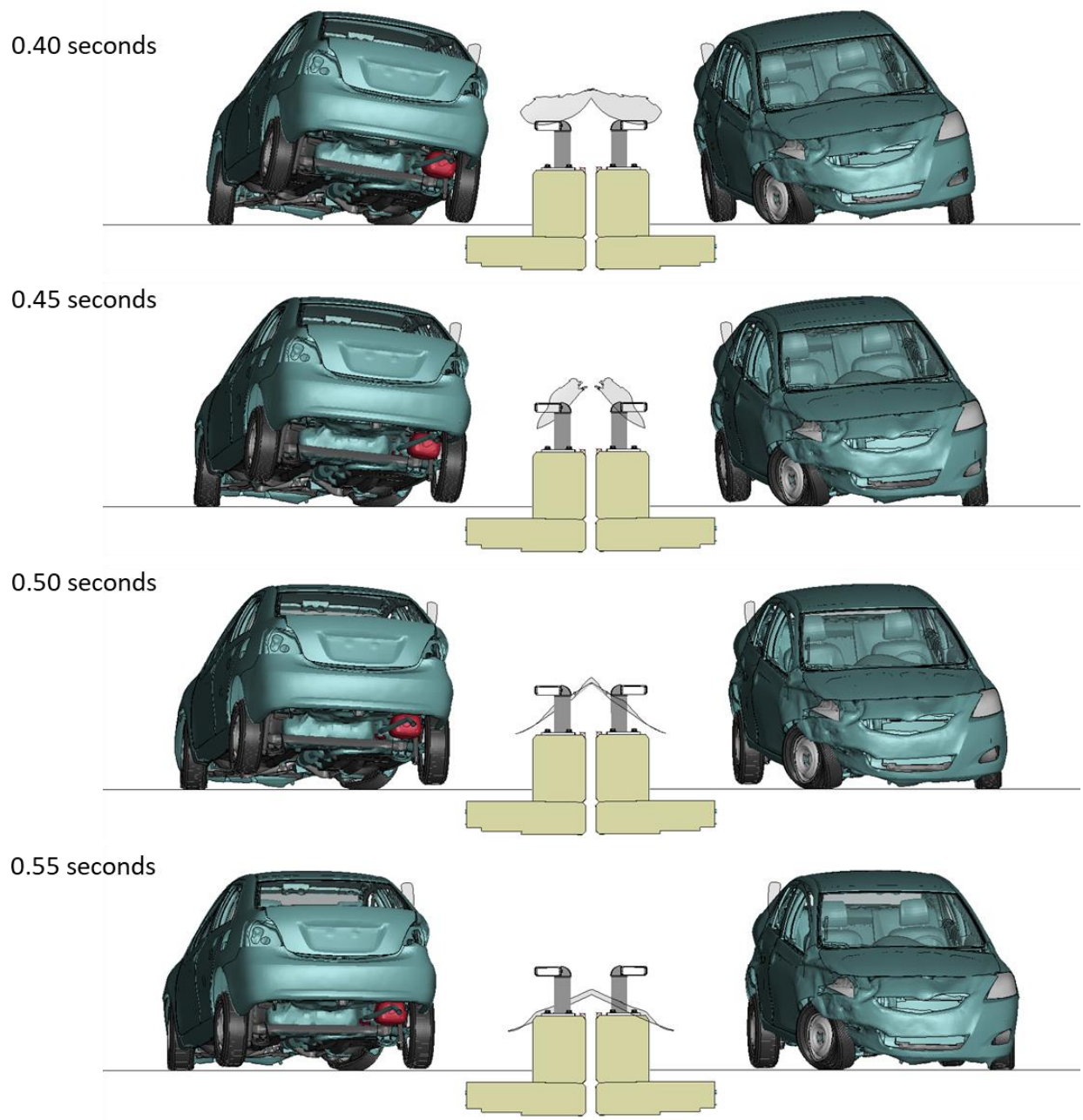

Figure 3 [CONTINUED] Sequential views from analysis of MASH Test 3-10 for CIP relative to Post from a front and rear viewpoint.

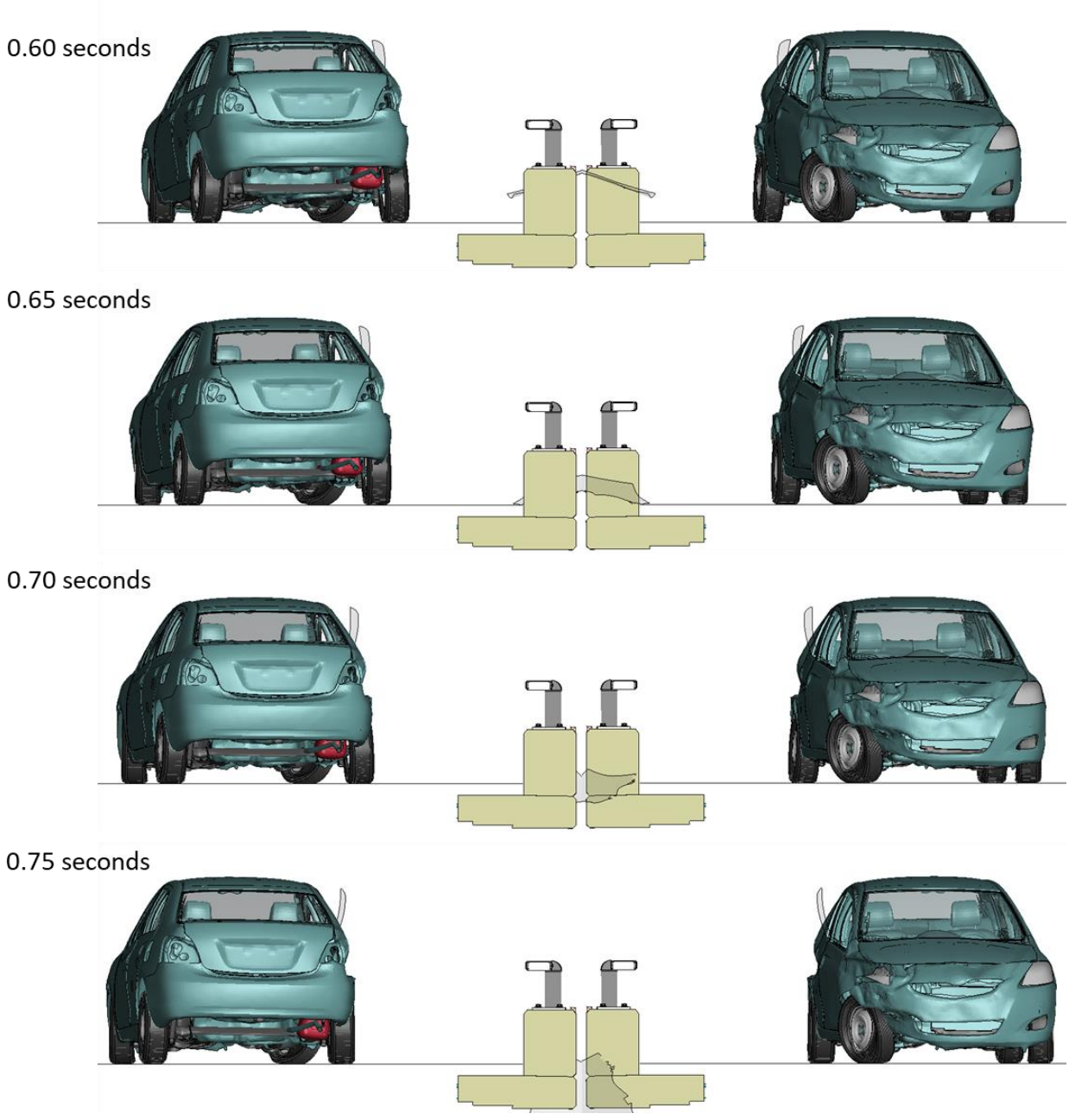

Figure 3 [CONTINUED] Sequential views from analysis of MASH Test 3-10 for CIP relative to Post from a front and rear viewpoint.

Appendix D

Sequential Views for Test 3-11 for the

CM-MTL3 Bridge Rail Design with Proposed Revisions

for CIP Relative to Splice

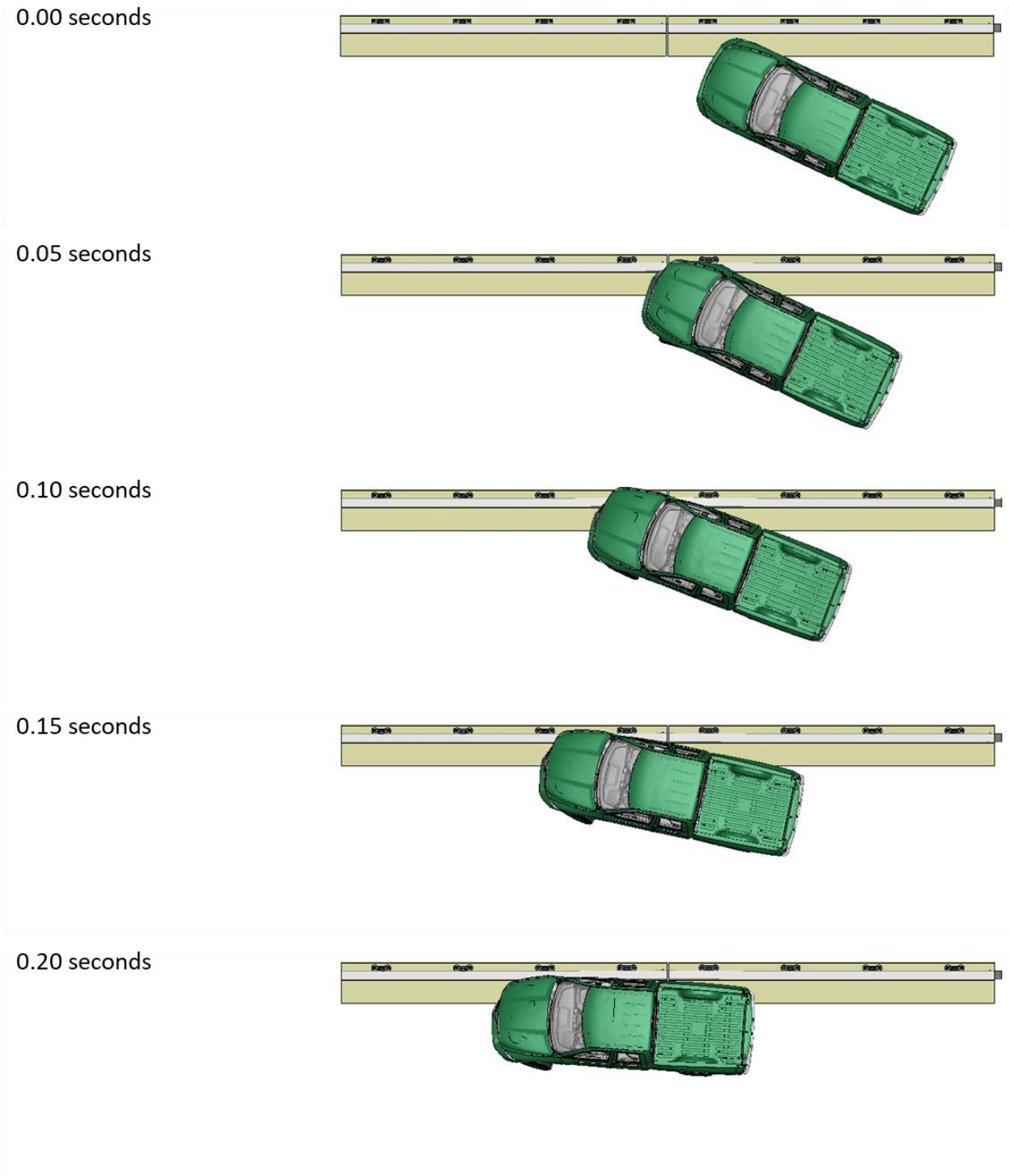

Figure 1. Sequential views from analysis of MASH Test 3-11 for CIP relative to splice from an overhead viewpoint.

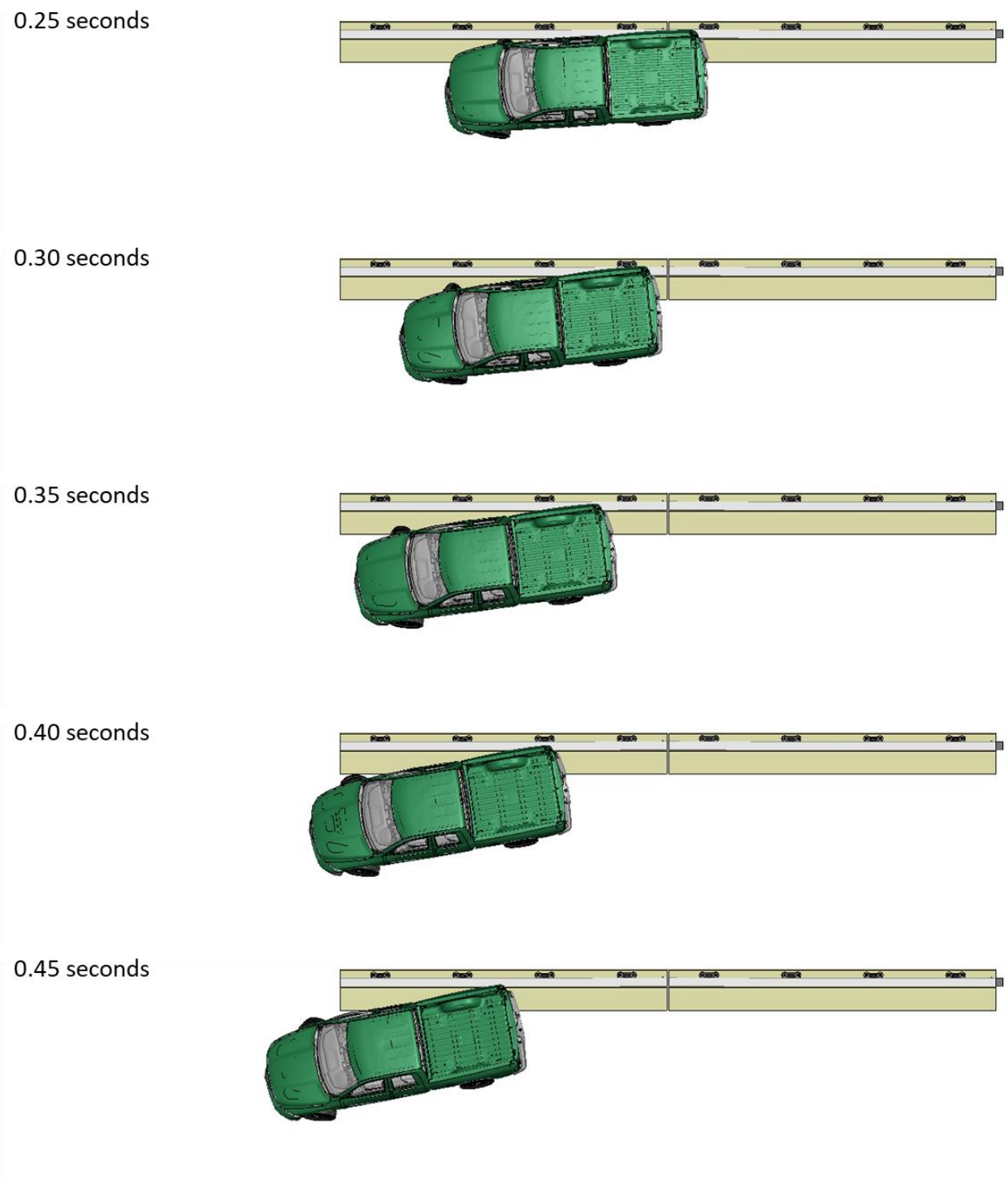

Figure 1 [CONTINUED] Sequential views from analysis of MASH Test 3-11 for CIP relative to splice from an overhead viewpoint.

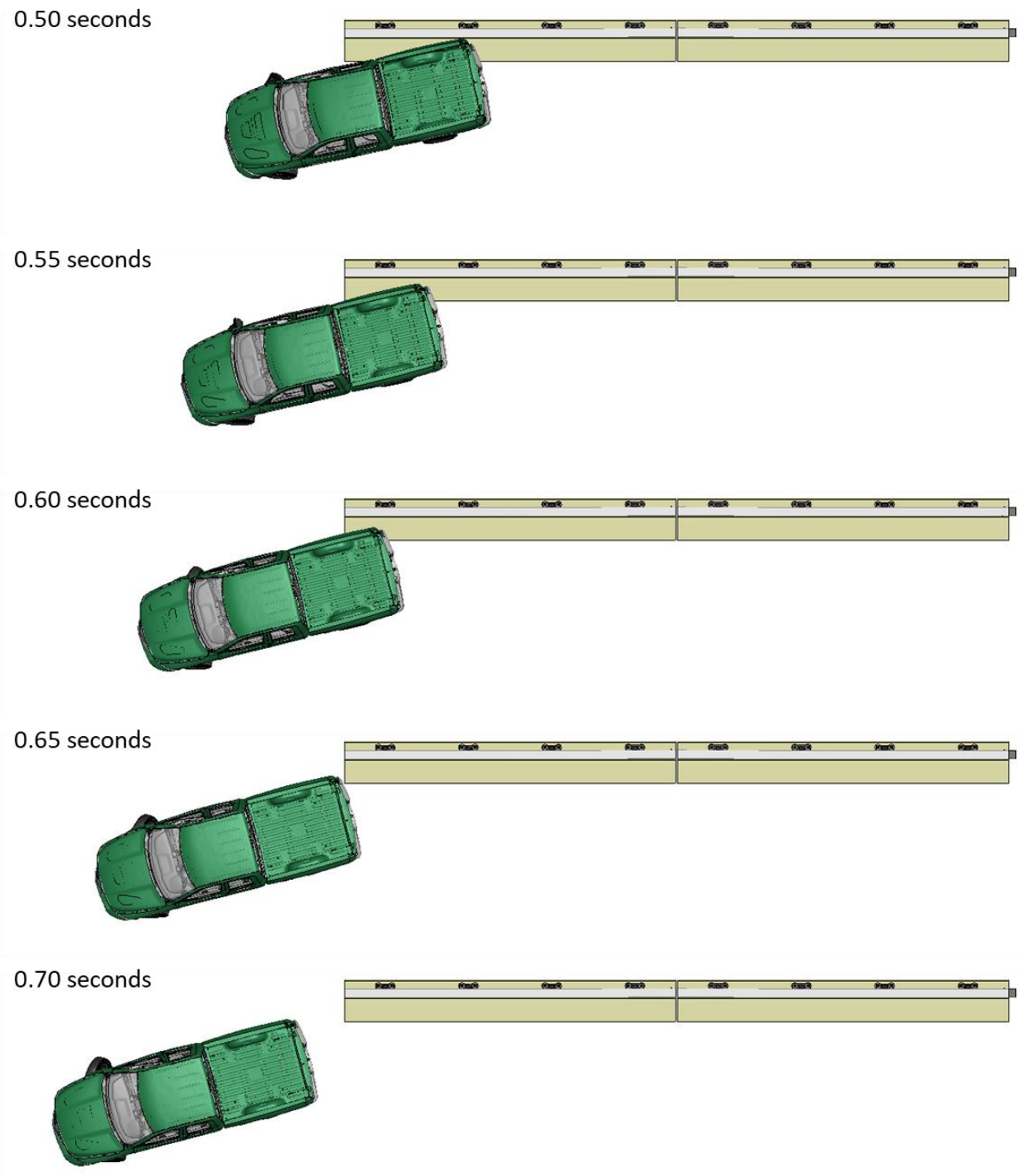

Figure 1 [CONTINUED] Sequential views from analysis of MASH Test 3-11 for CIP relative to splice from an overhead viewpoint.

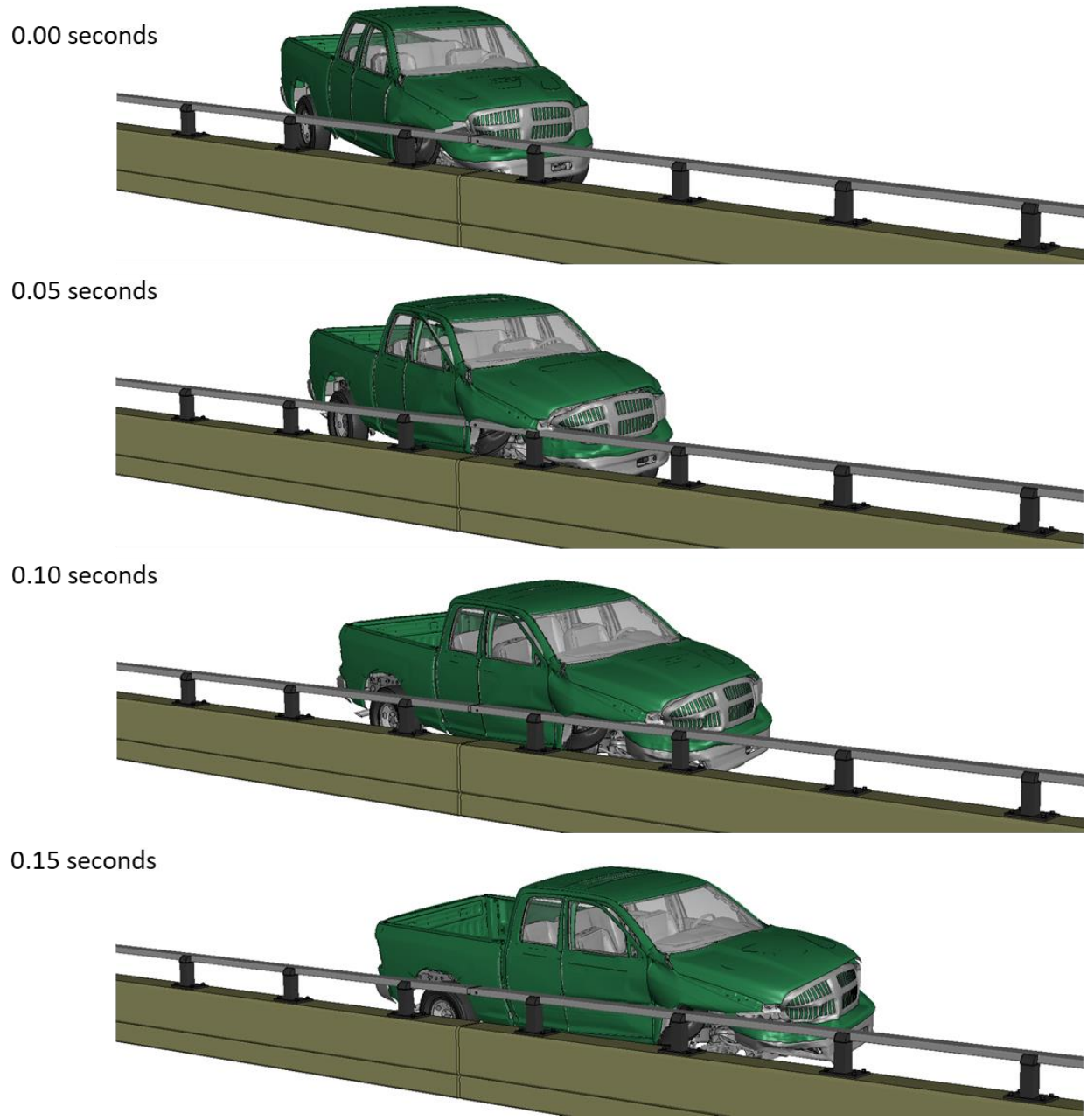

Figure 2. Sequential views from analysis of MASH Test 3-11 for CIP relative to splice from an oblique viewpoint.

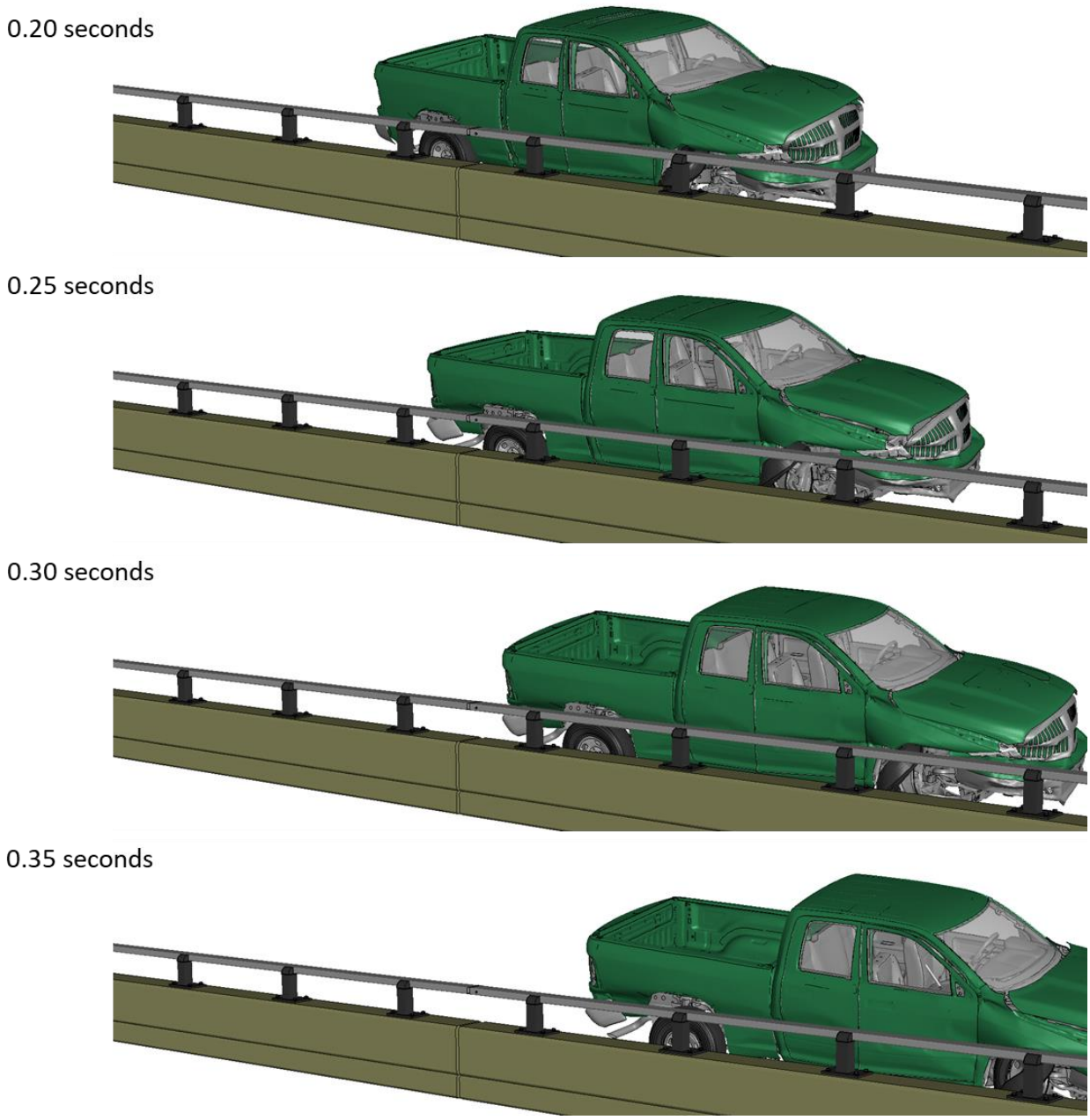

Figure 2 [CONTINUED] Sequential views from analysis of MASH Test 3-11 for CIP relative to splice from an oblique viewpoint.

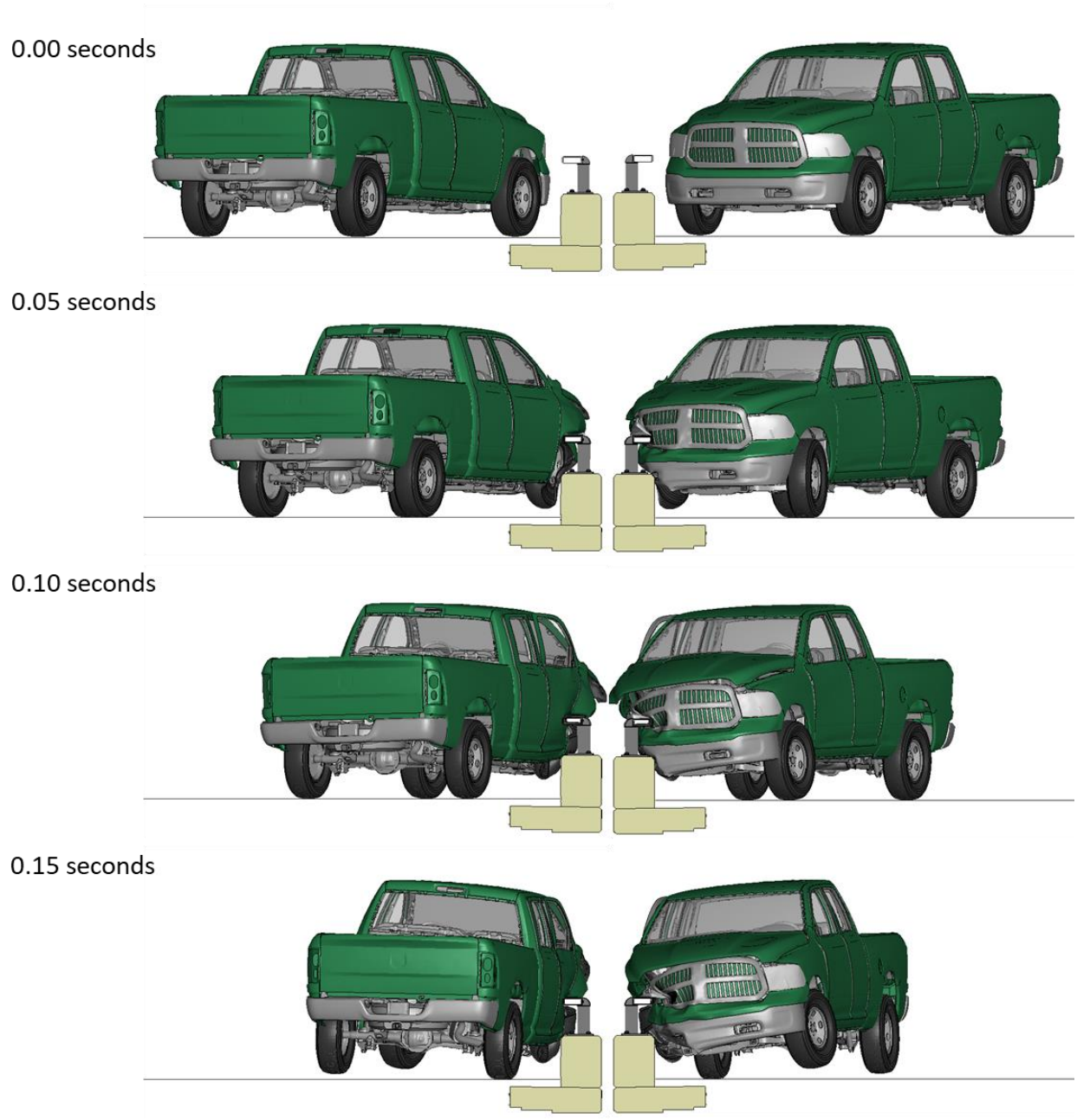

Figure 3. Sequential views from analysis of MASH Test 3-11 for CIP relative to splice from a front and rear viewpoint.

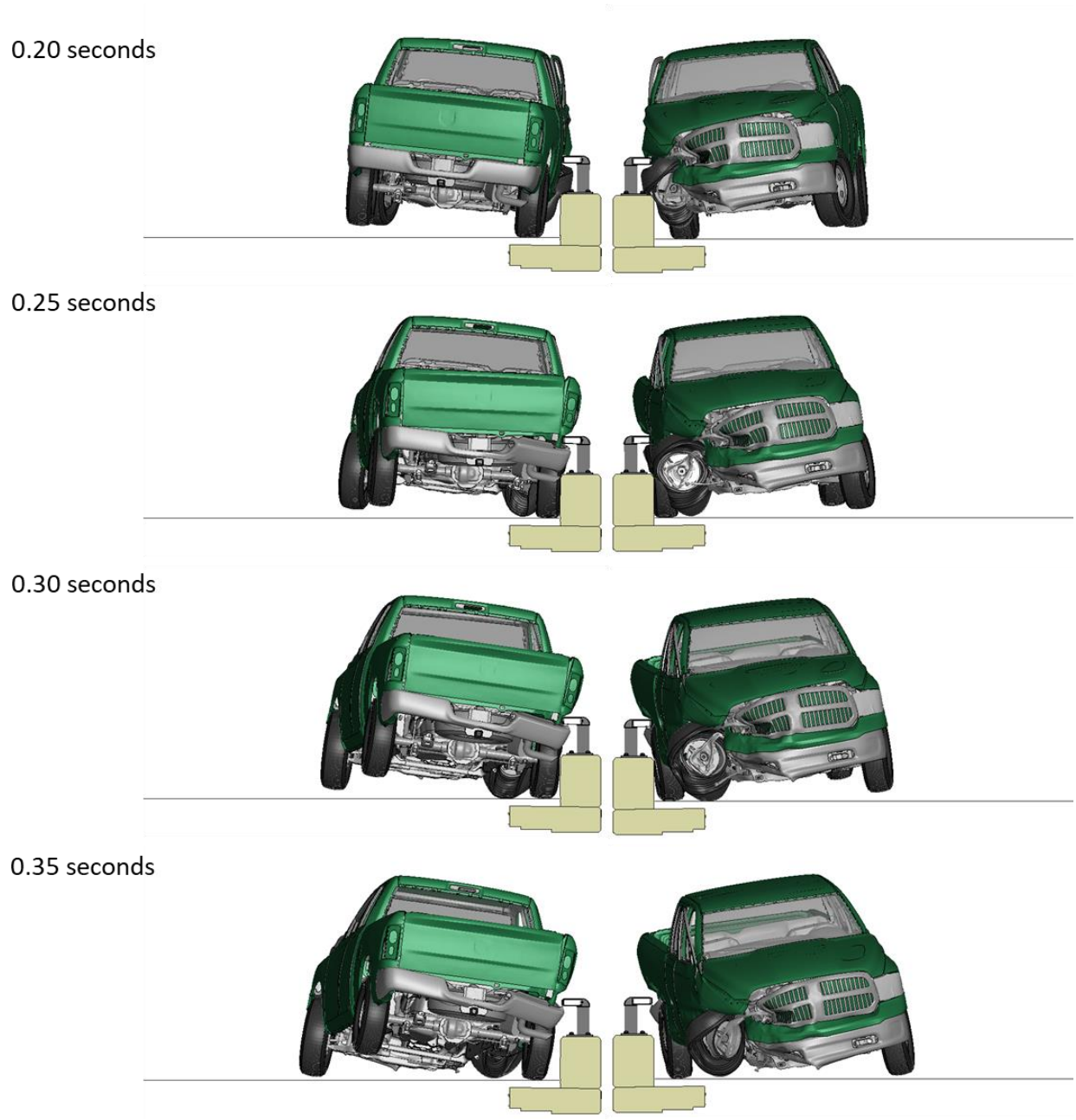

Figure 3 [CONTINUED] Sequential views from analysis of MASH Test 3-11 for CIP relative to splice from a front and rear viewpoint.

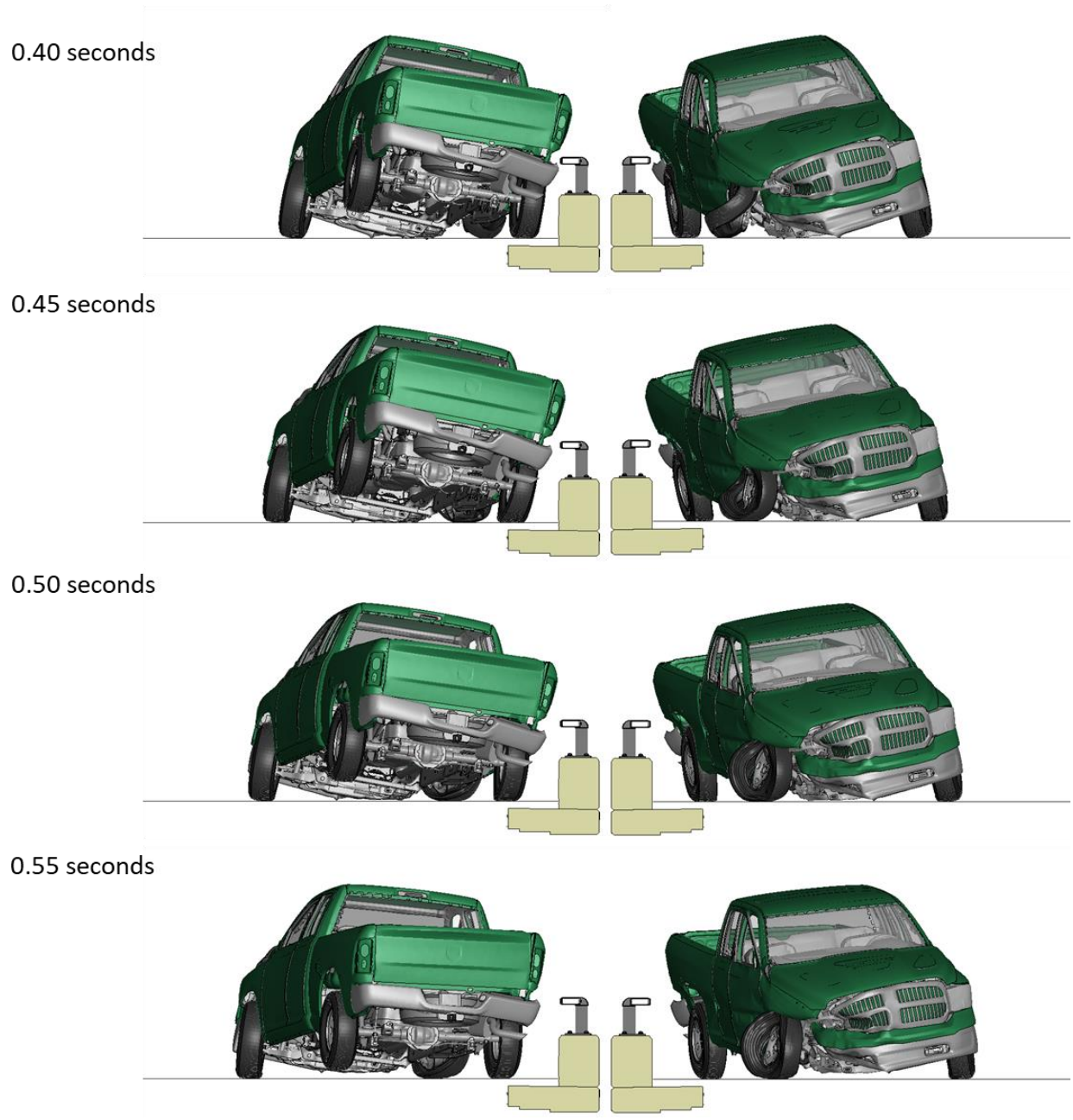

Figure 3 [CONTINUED] Sequential views from analysis of MASH Test 3-11 for CIP relative to splice from a front and rear viewpoint.

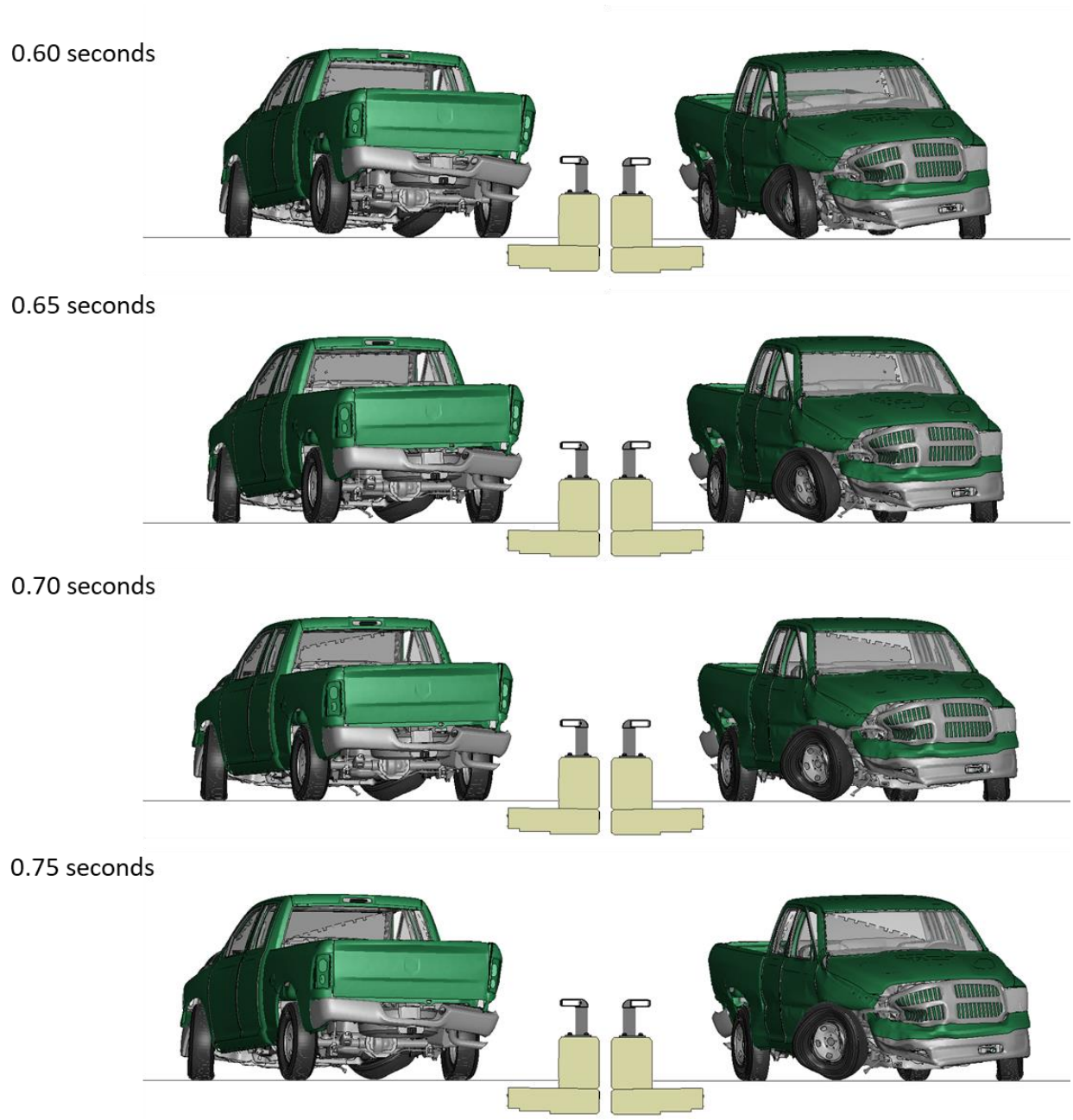

Figure 3 [CONTINUED] Sequential views from analysis of MASH Test 3-11 for CIP relative to splice from a front and rear viewpoint.

Appendix E

Sequential Views for Test 3-11 for the

CM-MTL3 Bridge Rail Design with Proposed Revisions

for CIP Relative to Post

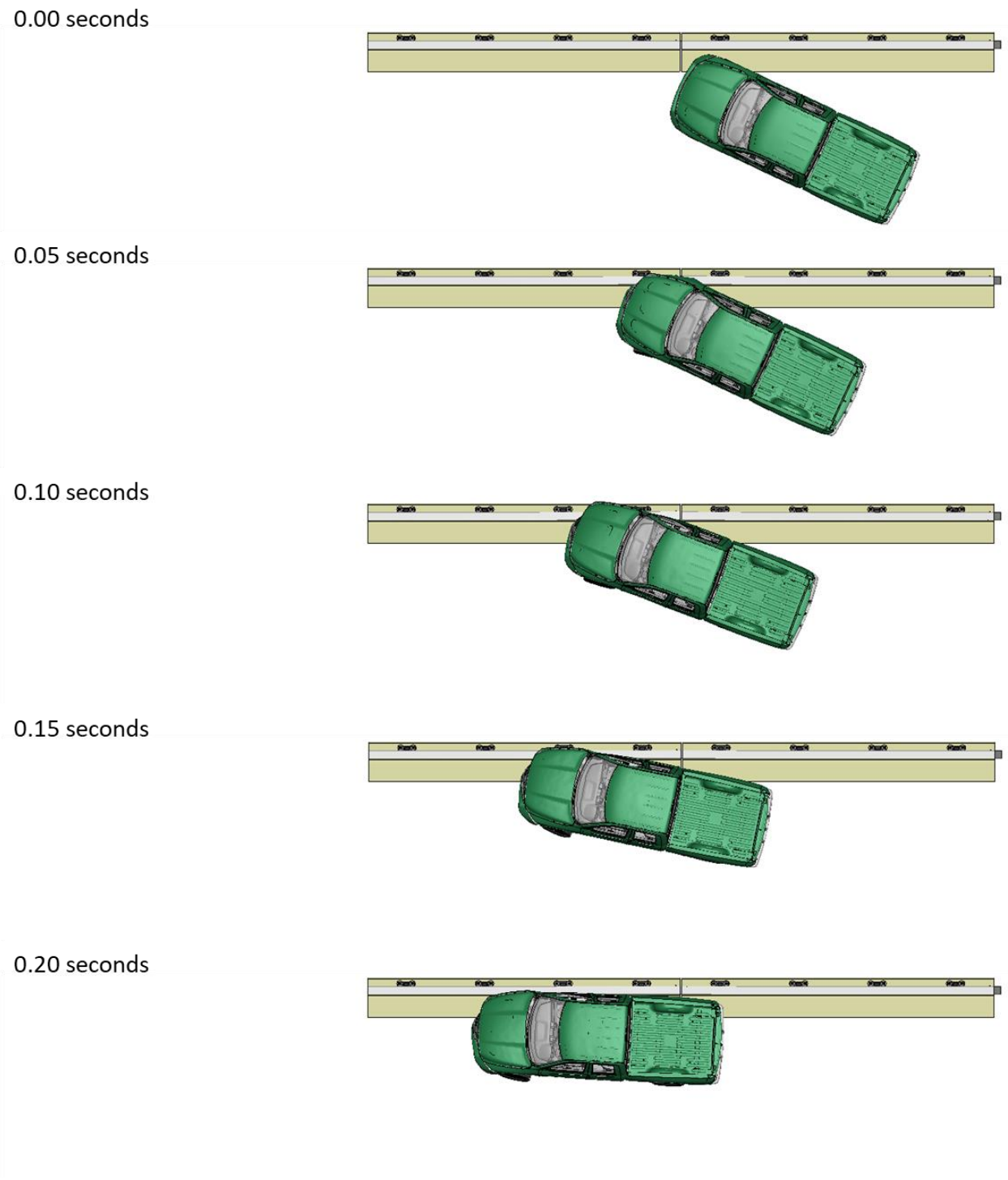

Figure 1. Sequential views from analysis of MASH Test 3-11 for CIP relative to Post from an overhead viewpoint.

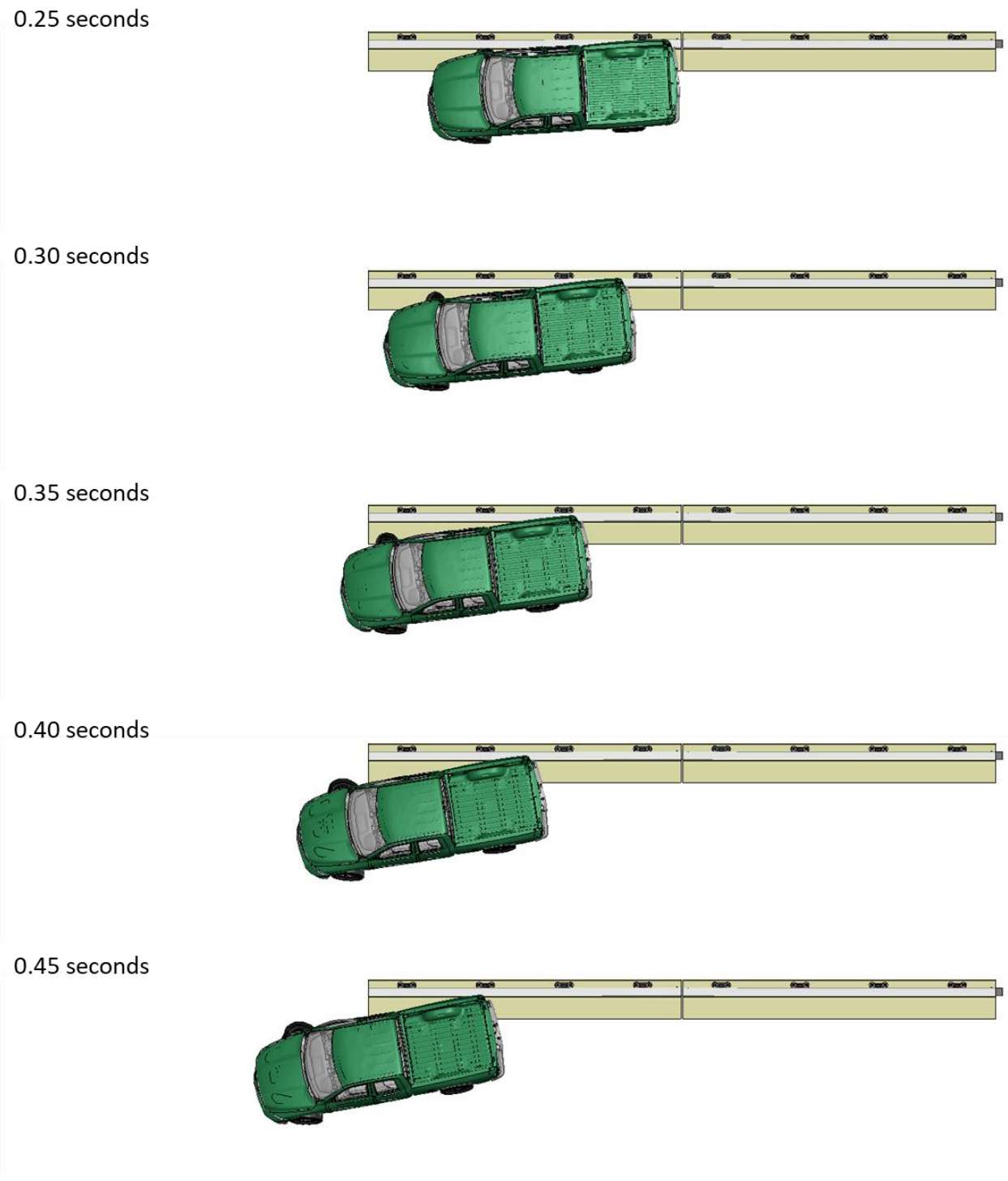

Figure 1 [CONTINUED] Sequential views from analysis of MASH Test 3-11 for CIP relative to Post from an overhead viewpoint.

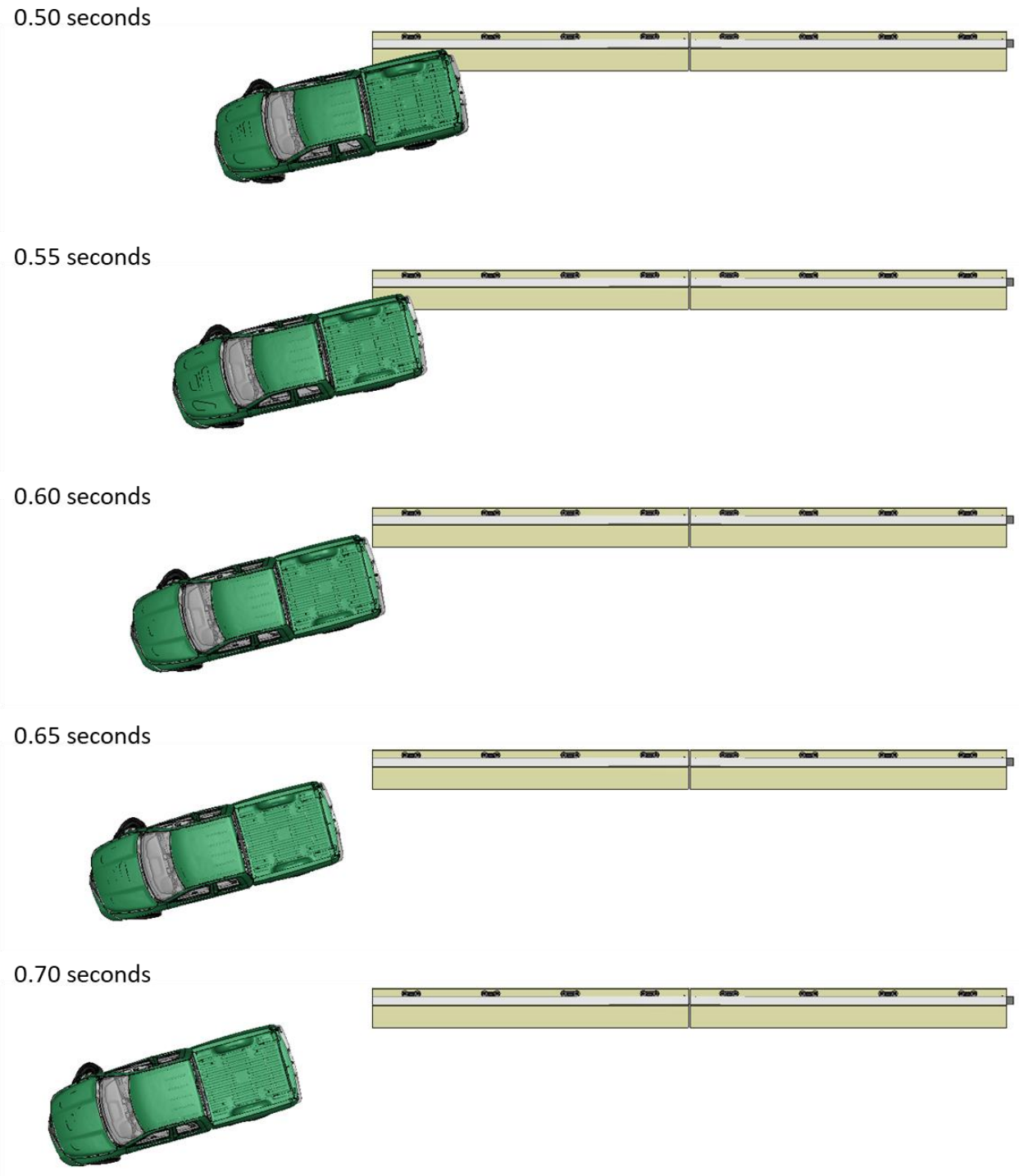

Figure 1 [CONTINUED] Sequential views from analysis of MASH Test 3-11 for CIP relative to Post from an overhead viewpoint.

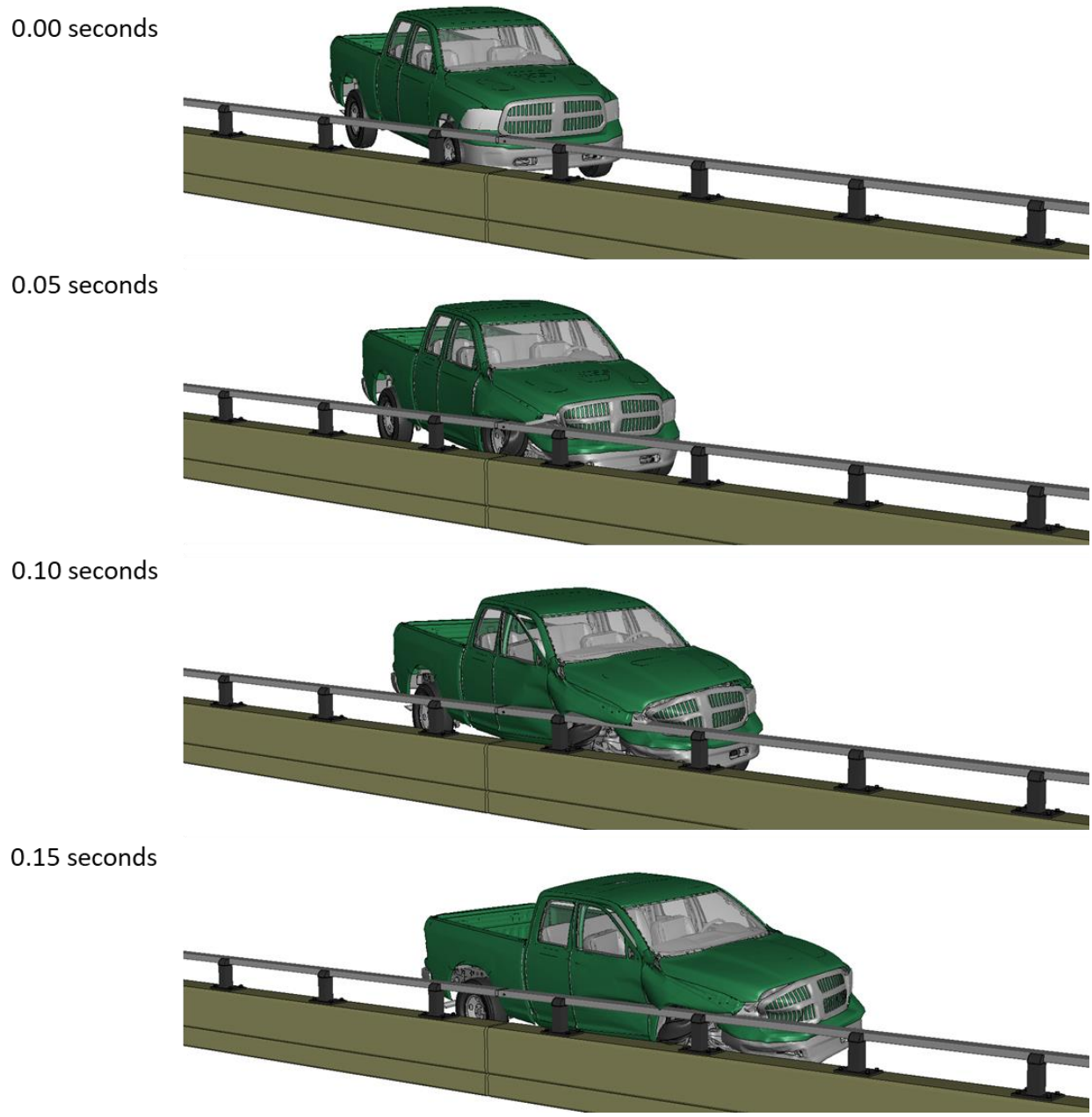

Figure 2. Sequential views from analysis of MASH Test 3-11 for CIP relative to Post from an oblique viewpoint.

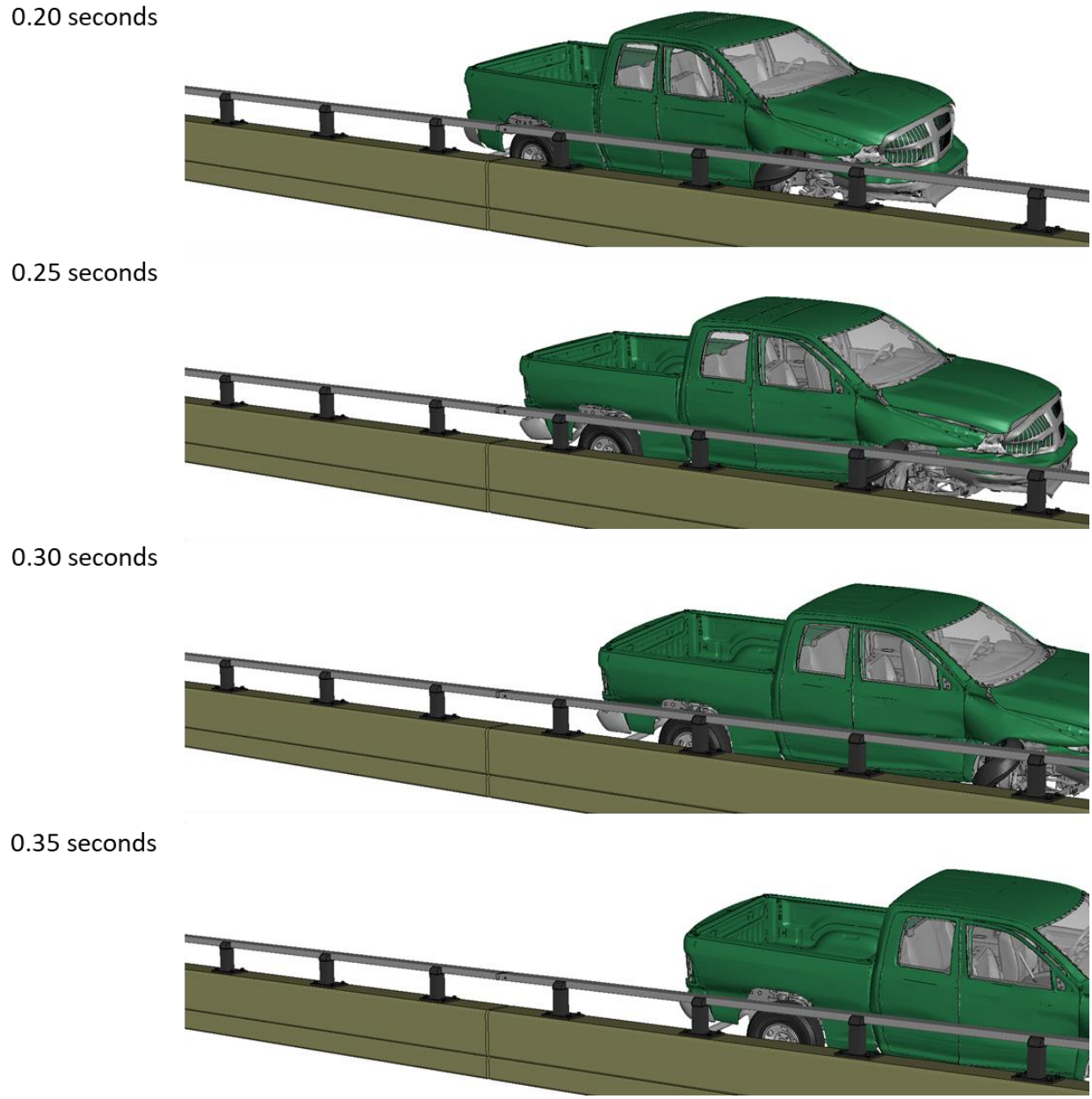

Figure 2 [CONTINUED] Sequential views from analysis of MASH Test 3-11 for CIP relative to Post from an oblique viewpoint.

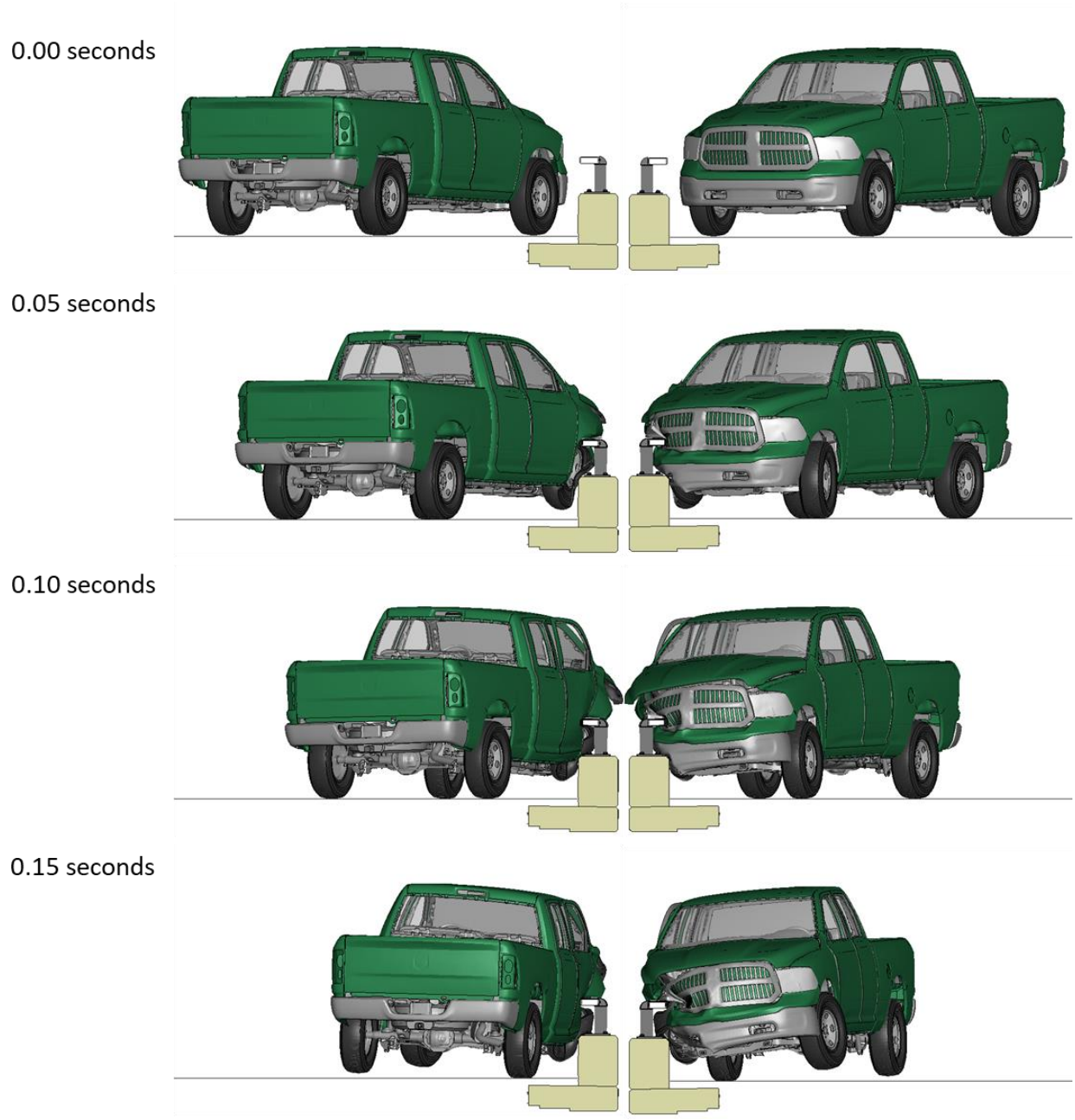

Figure 3. Sequential views from analysis of MASH Test 3-11 for CIP relative to Post from a front and rear viewpoint.

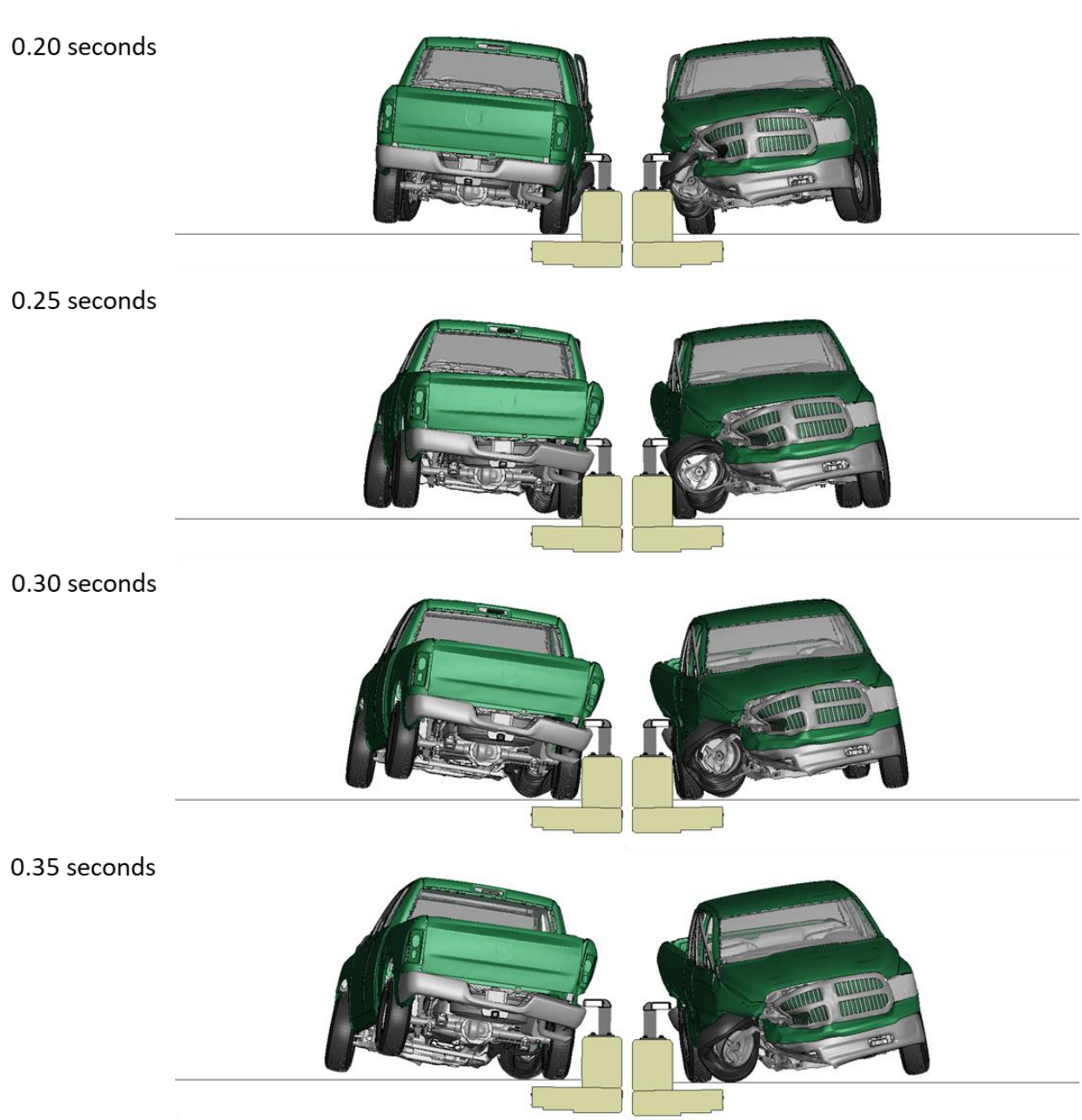

Figure 3 [CONTINUED] Sequential views from analysis of MASH Test 3-11 for CIP relative to Post from a front and rear viewpoint.

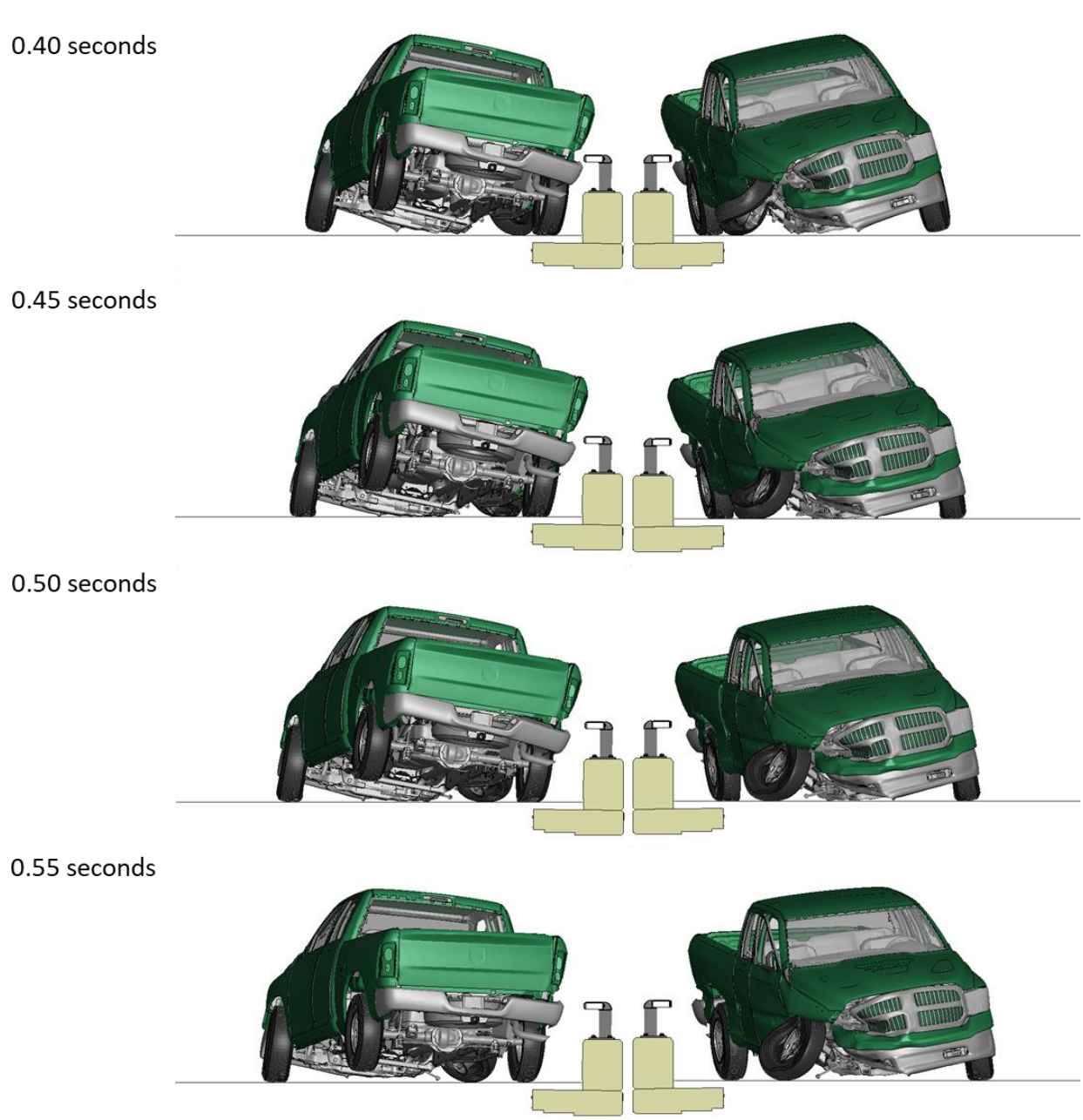

Figure 3 [CONTINUED] Sequential views from analysis of MASH Test 3-11 for CIP relative to Post from a front and rear viewpoint.

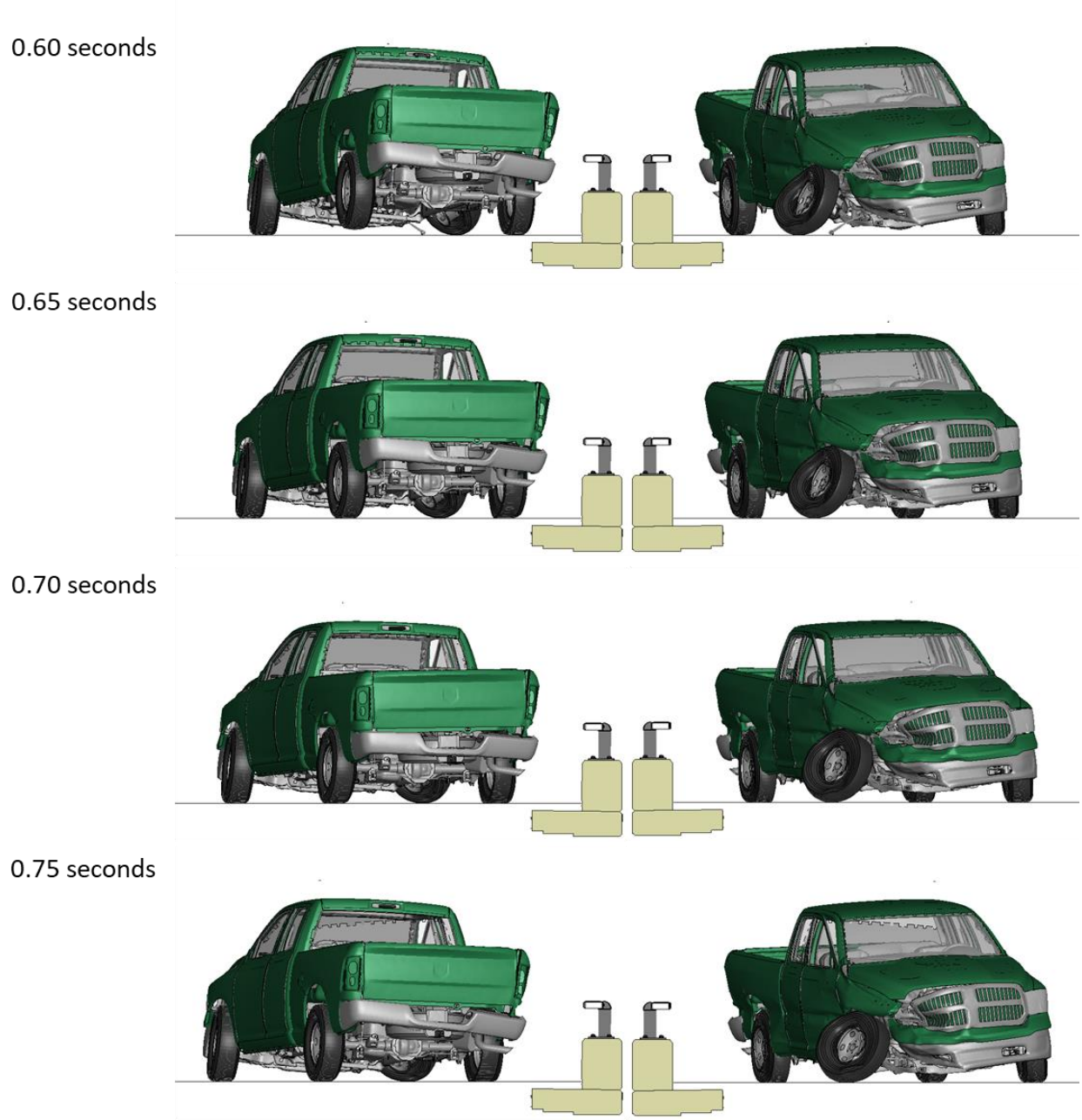

Figure 3 [CONTINUED] Sequential views from analysis of MASH Test 3-11 for CIP relative to Post from a front and rear viewpoint.